MECHANISMS AND DYNAMICS OF REGULATORY T CELL FUNCTION

A Dissertation

Presented to the Faculty of the Weill Cornell Graduate School

of Medical Science

In Partial Fulfillment of the Requirements for the Degree of

Doctor of Philosophy

by

Andrew G Levine

January 2017

MECHANISMS AND DYNAMICS OF REGULATORY T CELL FUNCTION

Andrew G Levine, Ph. D.

Cornell University 2017

Regulatory T (Treg) cells, a subset of $CD4^+$ T cells whose development and function is specified by the transcription factor Foxp3, are essential for maintenance of immune homeostasis at steady state as well as during inflammatory and infections conditions. Congenital deficiency of Treg cells in mice and humans as well as inducible ablation of Treg cells in adult mice results in rapid and lethal spontaneous T-cell driven autoimmunity. The mechanisms by which Treg cells function, however, remain relatively unknown. Here, we have attempted to elucidate some of these mechanisms and to provide a framework for understanding how suppressor function may be divided amongst distinct subpopulations of Treg cells. We demonstrate that—in addition to its essential role in Treg cell differentiation in the thymus—T cell receptor (TCR) expression in Treg cells is required for the Treg cell transition from a naïve to an effector state that occurs in the periphery and for continuous maintenance of suppressor function. We further show—as a proof of principal—through generation of mice harboring a monoclonal population of Treg cells that TCR-dependent Treg cell function can be uncoupled to some extent from antigenic specificity and repertoire diversity. Lastly, we explore how antigen-experienced effector Treg cells that have undergone an additional differentiation marked by stable expression of high amounts of the transcription factor T-bet selectively suppress T_H1 autoimmunity and participate in T_H1 responses to pathogenic challenge. Together, these studies

provide insight into how Treg cell function is elaborated and organized for optimal maintenance of immune tolerance.

BIOGRAPHICAL SKETCH

Andrew Levine completed his undergraduate degree in English literature at Yale University in 2004. After completing further study and research in biology at Yale University 2007, he worked for two years as a Research Assistant at The Rockefeller University studying squamous cell carcinoma in a mouse model. In 2009 Andrew enrolled in the Tri-Institutional MD-PhD Program of Cornell/Rockefeller/Sloan Kettering. Following two years of medical school, Andrew joined the lab of Alexander Rudensky in the Immunology and Microbial Pathogenesis PhD program at the Weill Cornell Graduate School.

This dissertation is dedicated to my colleagues and friends in the Rudensky lab and to my mentor Sasha Rudensky, who have all supported and taught me—with enthusiasm, humor, generosity, and intelligence—how to pursue a life in science. This work is equally dedicated to my family and friends who through painstaking questions and great love have come to know, generally, that something vaguely called a T regulator cell exists and does something important for something.

ACKNOWLEDGEMENTS

This work would not have been possible without the many contributions to the field of regulatory T cell biology, made by my predecessors as well as colleagues in and outside of the Rudensky lab, ranging from the realm of ideas to the generation of mouse models I have been privileged to use during my time in the lab. In particular, I would like to acknowledge Saskia Hemmers, Bruno Moltedo, and Nick Arpaia in the Rudensky lab for our many discussions; my thesis committee members Ming Li, Eric Pamer, Sasha Tarakhovsky, and Dan Littman for their support and advice; and the Tri-Institutional MD-PhD office. I would also like to thank Sasha Rudensky for his mentorship over the past five years, for his thoughtful enthusiasm for our projects, his offhand suggestions that often led to surprising and novel insights, and his friendship. I was supported in this work by the Tri-Institutional MD-PhD program MSTP grant (T32GM07739) and the Frank Lappin Horsfall Jr. Student Fellowship.

TABLE OF CONTENTS

LIST OF FIGURES

LIST OF ABBREVIATIONS

APC	Antigen presenting cell
ABX	Antibiotics
BAC	Bacterial artificial chromosome
DT	Diptheria toxin
DTR	Diptheria toxin receptor
eGFP	Enhanced green fluorescent protein
ERT2	mutated human estrogen receptor ligand binding domain
FACS	Flow assisted cell sorting
Foxp3	Forkhead box p3
IFNγ	Interferon gamma
IL-#	Interleukin-#
IPEX	Immunodysregulation, polyendocrinopathy, and enteropathy X-linked
KO	Knock out
LCMV	*Lymphocytic choriomeningitis virus*
Lm	*Listeria monocytogenes*
LN	Lymph node
MACS	Magnetic assisted cell sorting
MHCII	Major histocompatibility complex class II
Nb	*Nippostrongylus brasiliensis*
PBS	Phosphate buffered saline
R26Y	Rosa26-lox-stop-lox-YFP
RAG	Recombination-activating gene
RFP	Red fluorescent protein
TCR	T cell receptor
tdTomato	Tandem dimer Tomato
Tg	Transgene
TH1	T helper type 1
TH2	T helper type 2
TH17	T helper type 17
Treg	Regulatory T cell
YFP	Yellow fluorescent protein
WT	Wild type

CHAPTER 1
INTRODUCTION

Biology of regulatory T cells

The mammalian immune system constitutes the host's defense against invading pathogens. Upon infection, innate immune cells detect conserved components of bacteria, viruses, fungi, and multicellular parasites through an array of pattern recognition receptors (PRRs) and initiate the immune response through elaboration of cytokines and other effector molecules. The adaptive arm of the immune system, coordinated in large part by $CD4^+$ T cells that possess a vast array of randomly rearranged T cell receptors (TCRs) capable of recognizing non-conserved foreign proteins, amplifies the initial response, promotes pathogen clearance, and drives the rapid memory response that occurs upon secondary challenge (Zhu and Paul, 2010).

$CD4^+$ T cell development in the thymus—through a process termed negative selection which forms the basis for "central" tolerance—ensures that the TCR repertoire is largely purged of frank self recognition in order to protect the host from unwanted T cell-driven autoimmune activation (Kappler et al., 1987). However, studies involving autoimmunity secondary to neonatal thymectomy together with the discovery of a subset of $CD4^+$ T cells constitutively expressing the high affinity IL-2 receptor α-chain (CD25) that actively suppressed autoimmunity driven by $CD4^+CD25^-$ cells indicated that another form of tolerance—peripheral, or dominant tolerance—also exists (Ohki et al., 1987; Sakaguchi et al., 1995). Subsequent identification of mutations in the X-chromosome encoded *Foxp3* gene in human

immunodysregulation, polyendocrinopathy, and enteropathy X-linked syondrome (IPEX) patients and scurfy mice that develop early onset lethal autoimmunity suggested Foxp3 to be the transcription factor responsible for coordinating the development and function of these immunosuppressive $CD4^+CD25^+$ regulatory T (Treg) cells (Bennett et al., 2001; Brunkow et al., 2001; Wildin et al., 2001). Genetic deletion of the *Foxp3* gene has confirmed that Foxp3 is essential both for Treg cell development and for suppressive function in mature Treg cells, and genetic ablation of $Foxp3^+$ Treg cells in adult mice demonstrated that Treg cells are continuously required throughout life for prevention of spontaneous autoimmunity (Gavin et al., 2007; Kim et al., 2007; Lin et al., 2007; Williams and Rudensky, 2007).

Distinct from conventional $CD4^+$ T cells and consistent with their activated phenotype at steady state, Treg cells were shown to possess a TCR repertoire skewed towards self-recognition (Hsieh et al., 2004; Jordan et al., 2001). Indeed, TCR-mediated high affinity engagement with self in the thymus is critical for initiation of the Treg cell developmental program and for *Foxp3* induction (Gavin et al., 2007; Ohkura et al., 2012). As compared to effector $CD4^+$ T cells, Treg cells in secondary lymphoid organs express higher levels of TCR-induced genes, are more proliferative, and are enriched for effector-like $CD44^{hi}CD62^{Lo}$ cells (Fisson et al., 2003). TCR engagement in the periphery is important for Treg cell homeostasis and has been suggested to play a role in immunosuppressive function (Kim et al., 2009; Thornton and Shevach, 1998). However, whether TCR expression and specifically high affinity interactions with a diverse array of self antigens is (akin to Foxp3 expression) continuously required for Treg cell function remains to be resolved.

Precisely how Treg cells suppress effector T cell activation and maintain immunological tolerance at steady state and during immune challenge is unknown. It is notable, however, that Treg cells do not appear to utilize a unique suite of anti-inflammatory effector mechanisms but rather employ inhibitory factors—in an exaggerated manner—that are normally expressed by effector $CD4^+$ T cell as part of their intrinsic activation-inhibition feedback loops. This propensity to express anti-inflammatory factors (e.g., IL-10, CTLA-4, CD25, CD73, CD39) is initiated in the thymus as part of a TCR stimulation- and cytokine-dependent developmental program that is subsequently solidified and maintained by Foxp3 (Gavin et al., 2007; Lin et al., 2007; Ohkura et al., 2012).

It has also been noted that some activated Treg cells at steady state and during infectious challenge, in addition to Foxp3 can express the T_H1, T_H2, and T_H17 $CD4^+$ T cell master transcription factors T-bet, GATA-3, and RORγt, respectively, and it has been suggested that expression of these factors endows Treg cells with capacities to suppress and regulate distinct types of autoimmune and immune responses (Koch et al., 2009; Ohnmacht et al., 2015; Rudra et al., 2012; Sefik et al., 2015; Wohlfert et al., 2011). It remains unknown whether Treg cells further stably differentiate into T_H1-, T_H2-, and T_H17-like subsets that each suppress a limited range of responses, or whether given that Treg cells already stably express their own master transcription factor Foxp3, expression of additional factors is transient and reversible, with any given Treg cell able to suppress any given type of immune response in a context-dependent manner.

Overview of dissertation

This dissertation focuses on two questions outlined briefly above: the role of the TCR in Treg cell function, and the degree of compartmentalization of function within the TCR-activated Treg cell population.

First, we address the question of whether following TCR-dependent induction in the thymus, Treg cells continue to require their TCRs for suppressor function *in vivo* (Chapter 2). We demonstrate that TCR expression by Treg cells is indispensable for their activation and function in the periphery, as mice constitutively lacking TCR expression on Treg cells phenocopy *Foxp3*^{KO} mice lacking Treg cells. Moreover, we show that inducible ablation of the TCR on mature Treg cells also results in Treg cell dysfunction that resembles inducible ablation of Treg cells. TCR expression maintained the expression of a subset of genes comprising 25% of the activated Treg cell transcriptional signature. These results reveal a profound and continuous role for the TCR in the suppressor capacity of Treg cells.

Next, we describe our studies on the role of TCR repertoire specificity and diversity in TCR-dependent Treg cell function (Chapter 3). Although in studies described in Chapter 2 we were able to demonstrate that TCR expression by Treg cells was continuously required for function, it remained unclear whether the same diverse TCR-mediated interactions between Treg cells and their cognate antigens which drove Treg cell induction in the thymus were also strictly required in the periphery for suppressor function (Bautista et al., 2009; Leung et al., 2009). By generating mice harboring a monoclonal Treg cell population expressing a single Treg cell TCR recognizing an endogenous amount of antigen, we demonstrate that Treg cell function can to an extent be uncoupled from specificity and diversity, as replacement of the naturally diverse Treg cell TCR repertoire with this single TCR suppressed the

lethal autoimmunity that occurs in the absence of TCR on Treg cells. The monoclonal Treg cell pool exhibited essentially a complete spectrum of TCR-dependent gene expression, suggesting that TCR-dependent activation in the absence of appropriate specificity can still provide significant immunosuppressive function.

In studies described in Chapter 4 we explore features of TCR-activated effector Treg cells that express the T_H1 master transcription factor, T-bet (Koch et al., 2009). We assessed whether expression of this factor in Treg cells would be stable and indicative of a functionally distinct Treg cell subset, and thus reflect an essential Treg cell heterogeneity, or whether instead T-bet expression would be readily reversible, indicative of a more homogenous and labile effector Treg cell population. We demonstrate that T-bet expression in Treg cells, induced at steady state and following infection, is highly stable even under non-T_H1 inflammatory conditions and marks a discrete subset of Treg cells. Although expression of T-bet itself in Treg cells was dispensable for their function, wholesale elimination of T-bet-expressing Treg cells resulted in severe T_H1-type autoimmunity, demonstrating a major non-redundant immunosuppressive function carried out by a distinct subset of stably differentiated Treg cells.

In total, our studies contribute to understanding of some of the key mechanisms Treg cells employ and some of the features they adopt in order to mediate their essential immunosuppressive function. Insights offered by our studies, directly or indirectly, may also facilitate future development of clinical Treg cell-based therapies for autoimmunity and inflammatory diseases.

References

Bautista, J.L., Lio, C.W., Lathrop, S.K., Forbush, K., Liang, Y., Luo, J., Rudensky, A.Y., and Hsieh, C.S. (2009). Intraclonal competition limits the fate determination of regulatory T cells in the thymus. Nature immunology *10*, 610-617.

Bennett, C.L., Christie, J., Ramsdell, F., Brunkow, M.E., Ferguson, P.J., Whitesell, L., Kelly, T.E., Saulsbury, F.T., Chance, P.F., and Ochs, H.D. (2001). The immune dysregulation, polyendocrinopathy, enteropathy, X-linked syndrome (IPEX) is caused by mutations of FOXP3. Nature genetics *27*, 20-21.

Brunkow, M.E., Jeffery, E.W., Hjerrild, K.A., Paeper, B., Clark, L.B., Yasayko, S.A., Wilkinson, J.E., Galas, D., Ziegler, S.F., and Ramsdell, F. (2001). Disruption of a new forkhead/winged-helix protein, scurfin, results in the fatal lymphoproliferative disorder of the scurfy mouse. Nature genetics *27*, 68-73.

Fisson, S., Darrasse-Jeze, G., Litvinova, E., Septier, F., Klatzmann, D., Liblau, R., and Salomon, B.L. (2003). Continuous activation of autoreactive CD4+ CD25+ regulatory T cells in the steady state. The Journal of experimental medicine *198*, 737-746.

Gavin, M.A., Rasmussen, J.P., Fontenot, J.D., Vasta, V., Manganiello, V.C., Beavo, J.A., and Rudensky, A.Y. (2007). Foxp3-dependent programme of regulatory T-cell differentiation. Nature *445*, 771-775.

Hsieh, C.S., Liang, Y., Tyznik, A.J., Self, S.G., Liggitt, D., and Rudensky, A.Y. (2004). Recognition of the peripheral self by naturally arising CD25+ CD4+ T cell receptors. Immunity *21*, 267-277.

Jordan, M.S., Boesteanu, A., Reed, A.J., Petrone, A.L., Holenbeck, A.E., Lerman, M.A., Naji, A., and Caton, A.J. (2001). Thymic selection of CD4+CD25+ regulatory T cells induced by an agonist self-peptide. Nature immunology *2*, 301-306.

Kappler, J.W., Roehm, N., and Marrack, P. (1987). T cell tolerance by clonal elimination in the thymus. Cell *49*, 273-280.

Kim, J.K., Klinger, M., Benjamin, J., Xiao, Y., Erle, D.J., Littman, D.R., and Killeen, N. (2009). Impact of the TCR signal on regulatory T cell homeostasis, function, and trafficking. PloS one *4*, e6580.

Kim, J.M., Rasmussen, J.P., and Rudensky, A.Y. (2007). Regulatory T cells prevent catastrophic autoimmunity throughout the lifespan of mice. Nature immunology *8*, 191-197.

Koch, M.A., Tucker-Heard, G., Perdue, N.R., Killebrew, J.R., Urdahl, K.B., and Campbell, D.J. (2009). The transcription factor T-bet controls regulatory T cell homeostasis and function during type 1 inflammation. Nature immunology *10*, 595-602.

Leung, M.W., Shen, S., and Lafaille, J.J. (2009). TCR-dependent differentiation of thymic Foxp3+ cells is limited to small clonal sizes. The Journal of experimental medicine *206*, 2121-2130.

Lin, W., Haribhai, D., Relland, L.M., Truong, N., Carlson, M.R., Williams, C.B., and Chatila, T.A. (2007). Regulatory T cell development in the absence of functional Foxp3. Nature immunology *8*, 359-368.

Ohki, H., Martin, C., Corbel, C., Coltey, M., and Le Douarin, N.M. (1987). Tolerance induced by thymic epithelial grafts in birds. Science *237*, 1032-1035.

Ohkura, N., Hamaguchi, M., Morikawa, H., Sugimura, K., Tanaka, A., Ito, Y., Osaki, M., Tanaka, Y., Yamashita, R., Nakano, N.*, et al.* (2012). T cell receptor stimulation-induced epigenetic changes and Foxp3 expression are independent and complementary events required for Treg cell development. Immunity *37*, 785-799.

Ohnmacht, C., Park, J.H., Cording, S., Wing, J.B., Atarashi, K., Obata, Y., Gaboriau-Routhiau, V., Marques, R., Dulauroy, S., Fedoseeva, M.*, et al.* (2015). MUCOSAL IMMUNOLOGY. The microbiota regulates type 2 immunity through RORgammat(+) T cells. Science *349*, 989-993.

Rudra, D., deRoos, P., Chaudhry, A., Niec, R.E., Arvey, A., Samstein, R.M., Leslie, C., Shaffer, S.A., Goodlett, D.R., and Rudensky, A.Y. (2012). Transcription factor Foxp3 and its protein partners form a complex regulatory network. Nature immunology *13*, 1010-1019.

Sakaguchi, S., Sakaguchi, N., Asano, M., Itoh, M., and Toda, M. (1995). Immunologic self-tolerance maintained by activated T cells expressing IL-2 receptor alpha-chains (CD25). Breakdown of a single mechanism of self-tolerance causes various autoimmune diseases. Journal of immunology *155*, 1151-1164.

Sefik, E., Geva-Zatorsky, N., Oh, S., Konnikova, L., Zemmour, D., McGuire, A.M., Burzyn, D., Ortiz-Lopez, A., Lobera, M., Yang, J.*, et al.* (2015). MUCOSAL IMMUNOLOGY. Individual intestinal symbionts induce a distinct population of RORgamma(+) regulatory T cells. Science *349*, 993-997.

Thornton, A.M., and Shevach, E.M. (1998). CD4+CD25+ immunoregulatory T cells suppress polyclonal T cell activation in vitro by inhibiting interleukin 2 production. The Journal of experimental medicine *188*, 287-296.

Wildin, R.S., Ramsdell, F., Peake, J., Faravelli, F., Casanova, J.L., Buist, N., Levy-Lahad, E., Mazzella, M., Goulet, O., Perroni, L.*, et al.* (2001). X-linked neonatal diabetes mellitus, enteropathy and endocrinopathy syndrome is the human equivalent of mouse scurfy. Nature genetics *27*, 18-20.

Williams, L.M., and Rudensky, A.Y. (2007). Maintenance of the Foxp3-dependent developmental program in mature regulatory T cells requires continued expression of Foxp3. Nature immunology *8*, 277-284.

Wohlfert, E.A., Grainger, J.R., Bouladoux, N., Konkel, J.E., Oldenhove, G., Ribeiro, C.H., Hall, J.A., Yagi, R., Naik, S., Bhairavabhotla, R.*, et al.* (2011). GATA3 controls Foxp3(+) regulatory T cell fate during inflammation in mice. The Journal of clinical investigation *121*, 4503-4515.

Zhu, J., and Paul, W.E. (2010). Peripheral CD4+ T-cell differentiation regulated by networks of cytokines and transcription factors. Immunological reviews *238*, 247-262.

CHAPTER 2

CONTINUOUS REQUIREMENT FOR THE TCR IN REGULATORY T CELL FUNCTION[•]

Abstract

Foxp3$^+$ regulatory T cells (Treg cells) maintain immunological tolerance, and their deficiency results in fatal multiorgan autoimmunity. Although heightened signaling via the T cell antigen receptor (TCR) is critical for the differentiation of Treg cells, the role of TCR signaling in Treg cell function remains largely unknown. Here we demonstrated that inducible ablation of the TCR resulted in Treg cell dysfunction that could not be attributed to impaired expression of the transcription factor Foxp3, decreased expression of Treg cell signature genes or altered ability to sense and consume interleukin 2 (IL-2). Instead, TCR signaling was required for maintaining the expression of a limited subset of genes comprising 25% of the activated Treg cell transcriptional signature. Our results reveal a critical role for the TCR in the suppressor capacity of Treg cells.

Introduction

Regulatory CD4$^+$ T cells that express the transcription factor Foxp3 have an essential role in maintaining immune tolerance (Josefowicz et al., 2012). In the thymus, increased affinity for engagement of the T cell antigen receptor (TCR) by immature CD4$^+$ single-positive thymocytes is required for the initiation of a program for the differentiation of regulatory T cells (Treg cells) and induction of

[•] Adapted from Levine, A.G., Arvey, A., Jin, W., and Rudensky, A.Y. (2014). Continuous requirement for the TCR in regulatory T cell function. Nat. Immunol. *15*, 1070-1078.

Foxp3 expression (Lee et al., 2012). As a consequence, Treg cells exported to the periphery exhibit a TCR repertoire skewed toward self-recognition (Hsieh et al., 2004; Hsieh et al., 2006). However, it remains unclear whether TCR signaling is needed to mediate the suppressive function of Treg cells in the periphery.

Treg cells exhibit impaired calcium flux, activation of the kinase Akt and phosphorylation of the kinase Erk upon TCR stimulation relative to that of conventional $CD4^+$ T cells, and Foxp3 is known to potently repress at least some TCR-induced genes, as well as some genes encoding molecules involved in the TCR signaling pathway (Au-Yeung et al., 2010; Gavin et al., 2002; Marson et al., 2007; Ouyang et al., 2012). At the same time, $Foxp3^+$ Treg cells have high basal expression of several cell surface molecules that are known to contribute to Treg cell function (such as CD25, CD39 and CTLA-4), and the expression of these molecules in conventional $CD4^+$ T cells is dependent upon TCR stimulation (Borsellino et al., 2007; Gavin et al., 2007; Lin et al., 2007; Pandiyan et al., 2007; Williams and Rudensky, 2007; Wing et al., 2008). It is not known whether high-affinity interactions of the TCR with complexes of self peptide and major histocompatibility complex (MHC) class II contribute to constitutive expression of these genes and, consequently, to Treg cell function.

Treg cells, despite their intrinsically dampened response to TCR stimulation, acquire an activated phenotype and expand their populations in response to their cognate antigens in settings of activation of the immune system, such as infection and autoimmunity (Rosenblum et al., 2011; Shafiani et al., 2013). These observations indicate that recognition of self antigen helps maintain Treg cells of particular specificities and may potentiate their

suppressive ability during immunological challenge (Samy et al., 2005). Nevertheless, strict reliance on TCR expression for Treg cell activation, rather than 'preferential' activation of antigen-specific Treg cells, has not been demonstrated, nor has engagement of the TCR *in vivo* been shown to be required for Treg cell function in any context.

We used inducible genetic ablation of cell-surface TCR complexes to directly address the requirement for TCR expression in the immunosuppressive ability of Treg cells. Notably, the TCR was largely dispensable for Foxp3 expression, for lineage stability and for high expression of many signature genes in Treg cells. Nevertheless, these features were not sufficient to preserve Treg cell function or to prevent activation of the immune system. Loss of suppressor capacity in the absence of the TCR was not due to an impaired ability of Treg cells to gain access to interleukin 2 (IL-2) and, accordingly, administration of exogenous IL-2 failed to 'rescue' systemic autoimmunity. Instead, TCR expression was essential for the activation of Treg cells and for Treg cells to maintain expression of a limited set of genes found to be expressed almost exclusively in activated Treg cells. Among those genes, expression of the transcription factor IRF4 contributed to the optimal function and homeostasis of Treg cells. Our results demonstrate an essential role for the TCR in eliciting the suppressor function of differentiated Treg cells.

Results

Maintenance of Treg cell identity in the absence of the TCR

To investigate the role of TCR signaling in Treg cell function, we crossed *Trac*^{FL} mice (which have a *lox*P-flanked allele encoding the TCR α-chain constant region (Cα or TCRα)) with *Foxp3*$^{eGFP\text{-}Cre\text{-}ERT2}$ mice (with expression of

enhanced green fluorescent protein (eGFP) fused to a Cre recombinase–estrogen-receptor-ligand-binding-domain protein from the 3′ untranslated region of *Foxp3*; called '*Foxp3*$^{\text{Cre-ERT2}}$' here) to achieve tamoxifen-inducible deletion of *Trac* specifically in Treg cells (Polic et al., 2001; Rubtsov et al., 2010). In this model, Cre-induced loss of the conditional *Trac* allele upon tamoxifen administration eliminates TCRα expression, which prevents formation of heterodimers of TCRα and TCRβ (TCRαβ) at the cell surface. We administered tamoxifen via oral gavage on days 0 and 1 and analyzed mice on day 9. Allelic exclusion at the *Trac* locus in heterozygous *Trac*$^{FL/WT}$*Foxp3*$^{Cre-ERT2}$ mice yielded a small population (25%) of TCR-deficient (as assessed by flow cytometry (TCRβ^{-}; called 'TCR^{-}' here)) Treg cells (~25%), whereas in homozygous *Trac*$^{FL/FL}$*Foxp3*$^{Cre-ERT2}$ mice, the majority of Treg cells (~60–70%) lacked cell surface TCRβ (Figure 2.1A). Although we cannot definitively exclude the possibility that few residual TCR complexes were present in minute amounts (below the detection limit of flow cytometric analyses), functional *in vitro* analyses confirmed loss of TCR crosslinking–dependent activation of TCR^{-} Treg cells (Figure 2.2A-D).

Because binding sites for the transcription factors NFAT and c-Rel have been identified in the *Foxp3* locus, and because TCR engagement–driven signaling via the transcription factor NF-κB is critical for induction of Foxp3 expression, we speculated that the TCR might be essential for maintaining Foxp3 expression (Hsieh et al., 2012; Ruan et al., 2009; Zheng et al., 2010). However, Foxp3 expression was reduced only marginally in TCR^{-} Treg cells in *Trac*$^{FL/WT}$*Foxp3*$^{Cre-ERT2}$ mice and was not reduced at all in TCR^{-} Treg cells in *Trac*$^{FL/FL}$*Foxp3*$^{Cre-ERT2}$ mice, relative to its expression in TCR-expressing (as assessed by flow cytometry (TCRβ^{+}; called 'TCR^{+}' here)) Treg cells in the

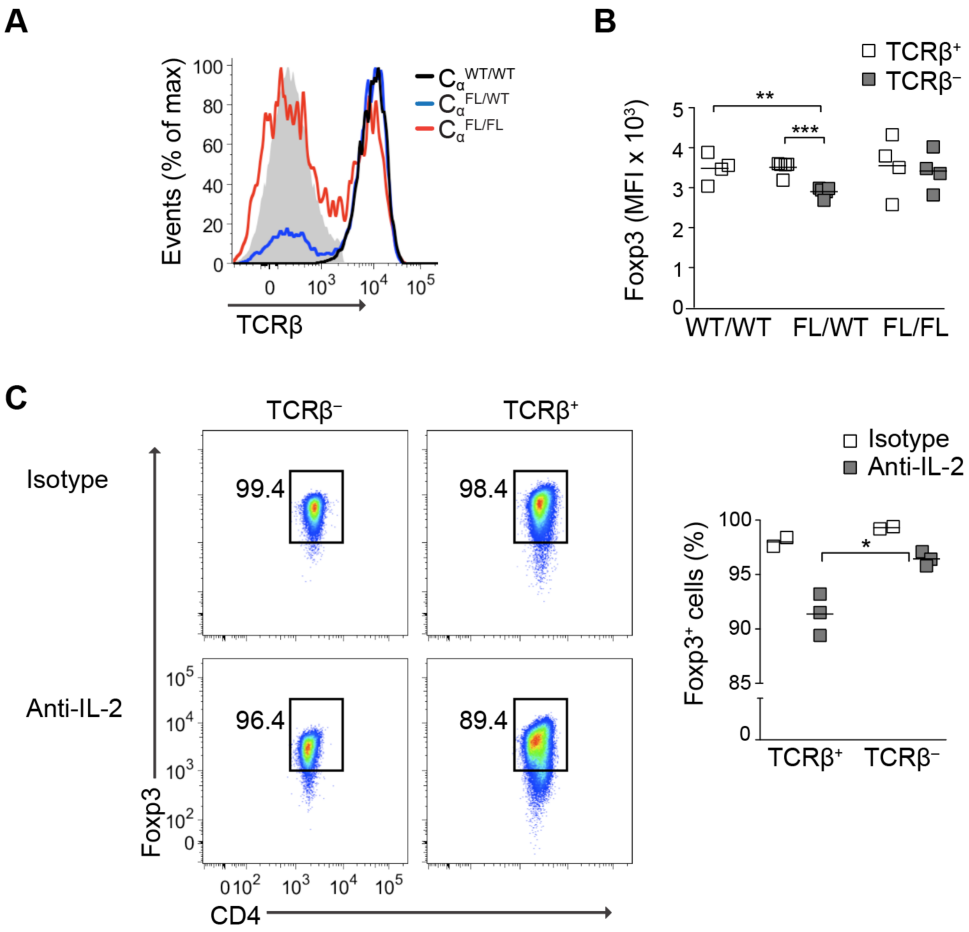

Figure 2.1: Maintenance of Treg cell identity in the absence of the TCR. (**A**,**B**) Expression of TCRß (**A**) and median fluorescence intensity (MFI) of Foxp3 (**B**) in CD4$^+$Foxp3$^+$ lymph node cells from 8- to 10-week-old *Trac*$^{WT/WT}$*Foxp3*$^{Cre\text{-}ERT2}$ mice (WT/WT), *Trac*$^{FL/WT}$*Foxp3*$^{Cre\text{-}ERT2}$ mice (FL/WT) and *Trac*$^{FL/FL}$*Foxp3*$^{Cre\text{-}ERT2}$ mice (FL/FL) treated with tamoxifen by gavage on days 0 and 1 and analyzed on day 9. Gray shading (**A**), TCRß staining on CD4$^-$TCRß$^-$ cells. (**C**) Flow cytometry of Foxp3$^+$ T cells among CD4$^+$YFP$^+$ cells sorted to >99% purity from the spleens and lymph nodes of *Trac*$^{FL/WT}$*Foxp3*$^{Cre\text{-}ERT2}$*Rosa26*^{YFP} mice on day 13 following treatment with tamoxifen on days 0 and 1 and intraperitoneal injection of IL-2-neutralizing antibody (Anti-IL-2) or isotype-matched control antibody (Isotype) on days 4 and 8. Numbers adjacent to outlined areas (left) indicate percent Foxp3$^+$ cells among TCRß$^+$ cells (right) or TCRß$^-$ cells (left). Each symbol (**B**,**C** (right)) represents an individual mouse; small horizontal lines indicate the mean. *$P <$ 0.05. **$P < 0.01$ and ***$P < 0.001$ (two-tailed unpaired *t*-test). Data are representative of two independent experiments with four or more (**A**,**B**) or two or more (**C**) mice per group in each.

Figure 2.2. Treg cell surface phenotype and proliferative capacity in the absence of a functional TCR.
(**A**) $CD4^+$ $eGFP^+$ $TCR\beta^+$ and $TCR\beta^-$ cells were sorted from $Trac^{FL/WT}Foxp3^{Cre\text{-}ERT2}$ mice 9 days after tamoxifen treatment on days 0 and 1 (**A**), labeled with CellTrace Violet and plated in 96-well plates coated with anti-CD3ε (clone 2C11) (**B**), anti-TCRβ (clone H57-597) (**C**) or PMA and Ionomycin (**D**) in the presence of 25U/mL IL-2 for 84 hours before analysis. All conditions were performed in triplicate wells with similar results. (**E**) Expression of Treg cell markers on $TCR\beta^+$ and $TCR\beta^-$ $CD4^+Foxp3^+$ cells in lymph nodes of $Trac^{WT/WT}Foxp3^{Cre\text{-}ERT2}$ (WT/WT), $Trac^{FL/WT}Foxp3^{Cre\text{-}ERT2}$ (FL/WT) and $Trac^{FL/FL}Foxp3^{Cre\text{-}ERT2}$ (FL/FL) mice. Gray histograms are gated on $CD4^+Foxp3^-$ cells in $Trac^{WT/WT}Foxp3^{Cre\text{-}ERT2}$ mice. (**F**) Percentages and absolute numbers of total $Foxp3^+$ among $CD4^+$ cells in spleens and lymph nodes of the indicated mice. (**G**) Gating strategy for analysis of $TCR\beta^+$ and $TCR\beta^-$ cells among $CD4^+Foxp3^+$ lymph node cells. For (**E-G**), mice were analyzed on day 9 following tamoxifen treatment on days 0 and 1. Mice in (**F-H**) are indicated as in (**E**). (**H**) BrdU incorporation vs. TCRβ expression on $CD4^+$ $eGFP^+$ cells sorted to >99% purity from pooled spleens and lymph nodes of the indicated mice on day 9 following tamoxifen treatment on days 0 and 1 and i.p. injection of BrdU on day 8. Data is representative of two experiments with four or more mice per group each (**E-G**) or three experiments with two or more mice per group each (**H**). P-value in (**F**) was calculated using a two-tailed unpaired t-test

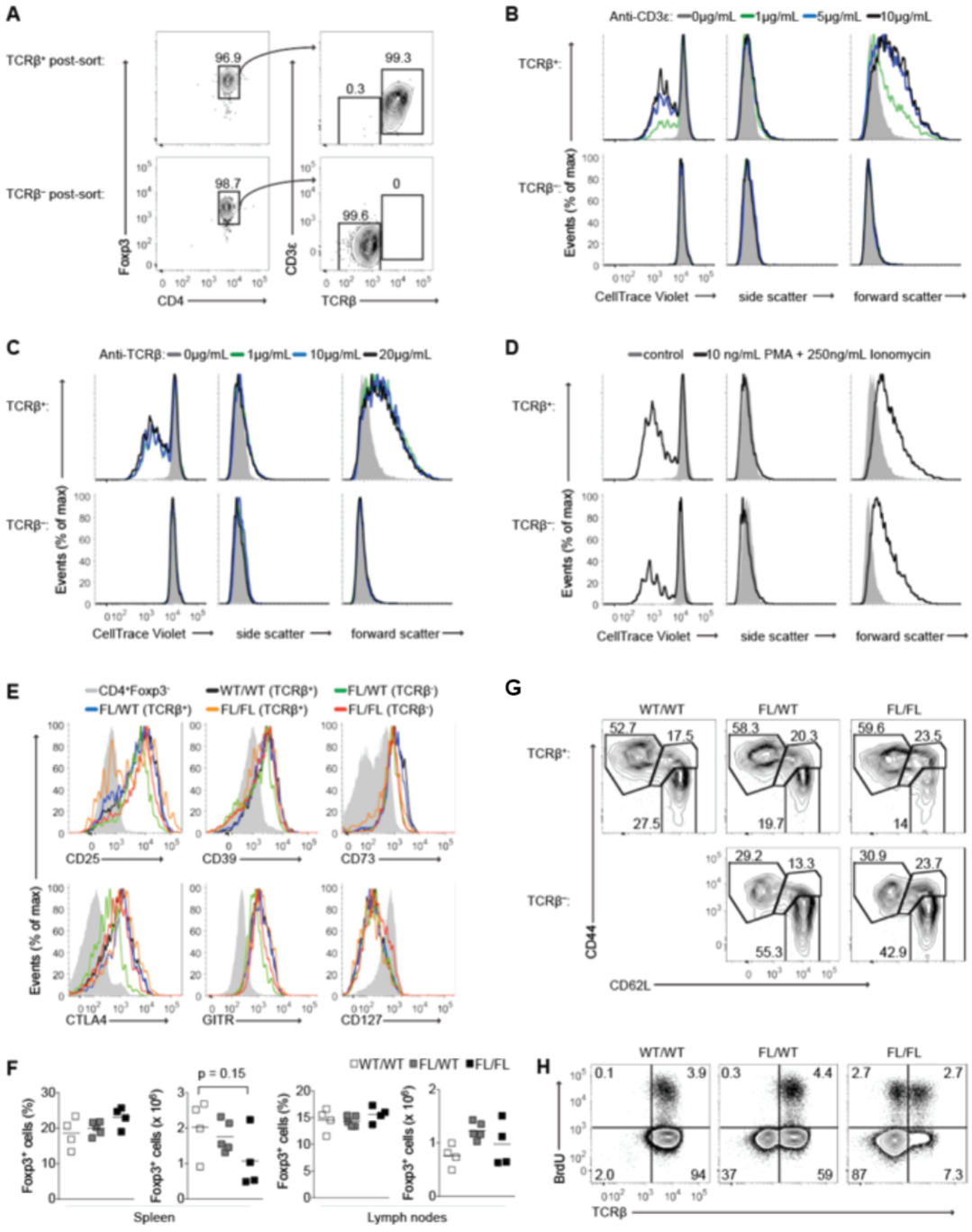
A
TCRβ+ post-sort:
TCRβ- post-sort:
96.9
99.3
0.3
98.7
0
99.6
Foxp3
CD4
CD3ε
TCRβ
B
Anti-CD3ε: 0μg/mL 1μg/mL 5μg/mL 10μg/mL
TCRβ+:
TCRβ-:
Events (% of max)
CellTrace Violet
side scatter
forward scatter
C
Anti-TCRβ: 0μg/mL 1μg/mL 10μg/mL 20μg/mL
TCRβ+:
TCRβ-:
Events (% of max)
CellTrace Violet
side scatter
forward scatter
D
control 10 ng/mL PMA + 250ng/mL Ionomycin
TCRβ+:
TCRβ-:
Events (% of max)
CellTrace Violet
side scatter
forward scatter
E
CD4+Foxp3-
WT/WT (TCRβ+)
FL/WT (TCRβ-)
FL/WT (TCRβ+)
FL/FL (TCRβ+)
FL/FL (TCRβ-)
CD25
CD39
CD73
CTLA4
GITR
CD127
Events (% of max)
F
WT/WT FL/WT FL/FL
p = 0.15
Foxp3+ cells (%)
Foxp3+ cells (x 10^6)
Spleen
Lymph nodes
G
WT/WT
FL/WT
FL/FL
TCRβ+:
TCRβ-:
52.7
17.5
27.5
58.3
20.3
19.7
59.6
23.5
14
29.2
13.3
55.3
30.9
23.7
42.9
CD44
CD62L
H
WT/WT
FL/WT
FL/FL
0.1
3.9
2.0
94
0.3
4.4
37
59
2.7
2.7
87
7.3
BrdU
TCRβ

same mice and in *Trac*$^{WT/WT}$*Foxp3*$^{Cre\text{-}ERT2}$ mice (Figure 2.1B). Similarly, the expression of genes encoding several Treg cell signature molecules, including CD25, GITR, CD39 and CD73, was largely unaffected in TCR^{-} Treg cells from both *Trac*$^{FL/WT}$*Foxp3*$^{Cre\text{-}ERT2}$ and *Trac*$^{FL/FL}$*Foxp3*$^{Cre\text{-}ERT2}$ mice (Figure 2.2E). These results indicated that in the steady state, continuous TCR-mediated recognition of self did not contribute substantially to Foxp3-dependent maintenance of expression of these genes (Wan and Flavell, 2007; Williams and Rudensky, 2007). In contrast, CTLA-4 expression was notably diminished in TCR^{-} Treg cells in *Trac*$^{FL/WT}$*Foxp3*$^{Cre\text{-}ERT2}$ mice, but not in TCR^{-} Treg cells in *Trac*$^{FL/FL}$*Foxp3*$^{Cre\text{-}ERT2}$ mice, relative to its expression in TCR^{+} Treg cells in *Trac*$^{WT/WT}$*Foxp3*$^{Cre\text{-}ERT2}$ mice (Figure 2.2E).

The frequency and absolute number of Foxp3^{+} cells in the spleens and lymph nodes of *Trac*$^{FL/WT}$*Foxp3*$^{Cre\text{-}ERT2}$ and *Trac*$^{FL/FL}$*Foxp3*$^{Cre\text{-}ERT2}$ mice were unaltered compared with that in *Trac*$^{WT/WT}$*Foxp3*$^{Cre\text{-}ERT2}$ mice (Figure 2.2F). However, to address the possibility that a portion of Treg cells completely lost Foxp3 expression upon ablation of the TCR and that these 'former' Treg cells were not accounted for in this experimental setup, we crossed *Trac*$^{FL/WT}$*Foxp3*$^{Cre\text{-}ERT2}$ mice with mice that express the recombination reporter *Rosa26*^{YFP} (with sequence encoding yellow fluorescent protein (YFP) expressed form the ubiquitous *Rosa26* locus). We assessed the expression of TCRβ and Foxp3 in CD4^{+}YFP^{+} cells sorted from the spleens and lymph nodes of *Trac*$^{FL/WT}$*Foxp3*$^{Cre\text{-}ERT2}$*Rosa26*^{YFP} mice on day 9 or 50 following tamoxifen administration on two consecutive days. YFP-expressing CD4^{+}TCRβ^{-} and CD4^{+}TCRβ^{+} cell subsets contained similarly low frequencies of Foxp3^{-} cells at both time points (data not shown). Furthermore, following *in vivo* neutralization of IL-2, a condition known to promote loss of Foxp3 expression (Rubtsov et al.,

2010), in *Trac*$^{FL/WT}$*Foxp3*$^{Cre\text{-}ERT2}$*Rosa26*^{YFP} mice, populations of CD4$^+$YFP$^+$TCRβ$^-$ cells retained a higher percentage of Foxp3$^+$ cells than did populations of CD4$^+$YFP$^+$TCRβ$^+$ cells (Figure 2.1C). Together these data indicated that TCR signaling was dispensable for the maintenance of the Treg cell phenotype and lineage stability and, moreover, that TCR signaling drove the loss of Foxp3 when IL-2 amounts were limiting.

Requirement for the TCR in effector differentiation of Treg cells

Although the Treg cell phenotype was largely preserved upon ablation of the TCR, we observed relative enrichment for naive-like CD44^{lo}CD62L^{hi} cells among TCR$^-$ Treg cells in lymph nodes and spleens of *Trac*$^{FL/WT}$*Foxp3*$^{Cre\text{-}ERT2}$ and *Trac*$^{FL/FL}$*Foxp3*$^{Cre\text{-}ERT2}$ mice (Figure 2.3A and Figure 2.2G). Treg cell proliferation is restricted almost exclusively to the CD44^{hi} subset, and in part the enrichment we observed appeared to be a consequence of severely impaired proliferative capacity of CD44^{hi} Treg cells in the absence of the TCR (Smigiel et al., 2014) (Figure 2.3B). The small population of TCR$^-$ Treg cells in *Trac*$^{FL/WT}$*Foxp3*$^{Cre\text{-}ERT2}$ mice was predominantly nondividing: these cells showed minimal expression of the proliferation marker Ki67, failed to incorporate the thymidine analog BrdU over a 24-hour labeling period and contained the greatest frequency of CD44^{lo}CD62L^{hi} cells among all TCR$^+$ or TCR$^-$ Treg cell populations in *Trac*$^{WT/WT}$*Foxp3*$^{Cre\text{-}ERT2}$, *Trac*$^{FL/WT}$*Foxp3*$^{Cre\text{-}ERT2}$ and *Trac*$^{FL/FL}$*Foxp3*$^{Cre\text{-}ERT2}$ mice (Figure 2.3A,B and Figure 2.2H). In *Trac*$^{FL/FL}$*Foxp3*$^{Cre\text{-}ERT2}$ mice, however, TCR$^-$ Treg cells exhibited considerable proliferative activity, albeit reduced relative to that of TCR$^+$ Treg cells present in the same mouse (Figure 2.3B and Figure 2.2H). Increased Ki67 staining in CD44^{hi} Treg cells was inversely correlated with a lower frequency of

Figure 2.3. Requirement for the TCR in the differentiation and population expansion of Treg cells.
(**A**,**B**) Expression of CD44 and CD62L on TCRβ^{+} or TCRβ^{-} CD4^{+}Foxp3^{+} lymph node cells (**A**) and of Ki67 on CD44^{hi} CD4^{+}Foxp3^{+} lymph node cells (**B**) isolated on day 9 from *Trac*$^{WT/WT}$*Foxp3*$^{Cre\text{-}ERT2}$, *Trac*$^{FL/WT}$*Foxp3*$^{Cre\text{-}ERT2}$ and *Trac*$^{FL/FL}$*Foxp3*$^{Cre\text{-}ERT2}$ mice treated with tamoxifen on days 0 and 1. (**C**) Expression of CD44 and CD62L on TCRβ^{+} or TCRβ^{-} CD4^{+}Foxp3^{+} lymph node cells in 2.5-week-old *Trac*$^{WT/WT}$*Foxp3*$^{YFP\text{-}Cre}$, Trac$^{FL/WT}$Foxp3$^{YFP\text{-}Cre}$ and *Trac*$^{FL/FL}$*Foxp3*$^{YFP\text{-}Cre}$ mice (left), and expression of differentiation markers in those of the *Trac*$^{FL/WT}$*Foxp3*$^{YFP\text{-}Cre}$ mice. Numbers adjacent to outlined areas (left) indicate percent CD44^{hi}CD62L^{lo} cells; numbers in quadrants (right) indicate percent cells in each throughout. (**D**,**E**) Ki67 expression in TCRβ^{+} or TCRβ^{-} CD4^{+}Foxp3^{+} ymph node cells (**D**) and frequency of TCRβ^{+} or TCRβ^{-} CD4^{+}Foxp3^{+} cells among total CD4^{+} cells in the spleen and lymph nodes (LN) (**E**) of mice as in **c**. Each symbol (**A**,**B**,**D**,**E** (right)) represents an individual mouse. *$P < 0.01$ and **$P < 0.001$ (two-tailed unpaired *t*-test). Data are representative of two independent experiments with four or more mice per group in each (**A**,**B**) or three independent experiments with six or more mice per group (**C**) or are pooled from three independent experiments with six or more mice per group (**D**,**E**).

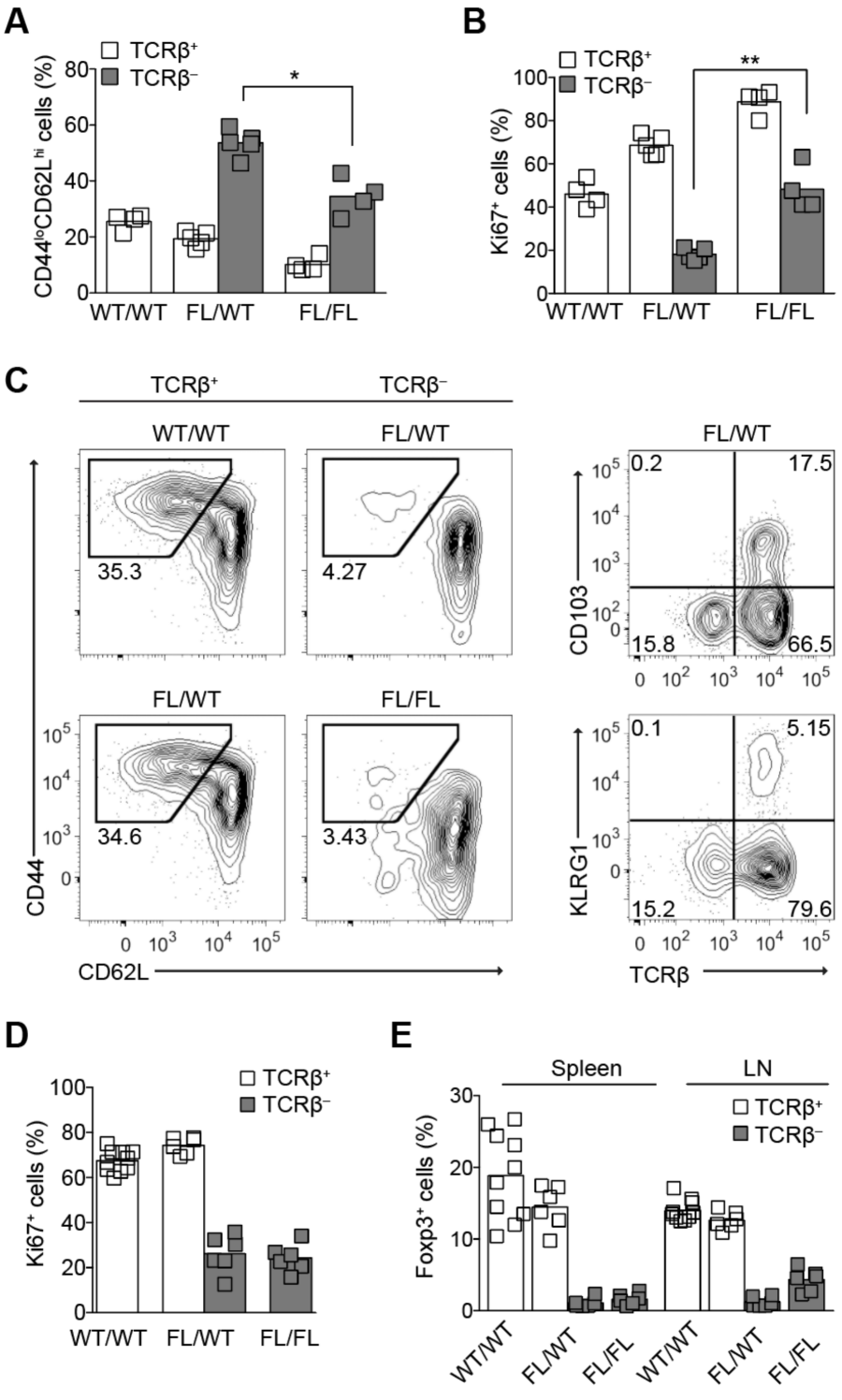
A
TCRβ+
TCRβ−
CD44loCD62Lhi cells (%)
WT/WT
FL/WT
FL/FL
B
Ki67+ cells (%)
C
TCRβ+
TCRβ−
WT/WT
FL/WT
FL/FL
35.3
4.27
34.6
3.43
CD44
CD62L
CD103
KLRG1
TCRβ
0.2
17.5
15.8
66.5
0.1
5.15
15.2
79.6
D
Ki67+ cells (%)
E
Spleen
LN
Foxp3+ cells (%)

$CD44^{lo}CD62L^{hi}$ cells among all TCR^{+} or TCR^{-} Treg cell populations in mice of all three genotypes (Figure 2.3A,B).

To address the possibility that continuous peripheral differentiation of naive-like Treg cells into $CD44^{hi}$ cells was impeded in the absence of TCR expression and that such a differentiation block contributed to the predominantly $CD44^{lo}CD62L^{hi}$ phenotype of TCR^{-} Treg cells, we bred $Trac^{FL}$ mice with $Foxp3^{YFP\text{-}Cre}$ mice (which express a fusion of Cre and YFP from the 3′ untranslated region of *Foxp3*) to induce ablation of the TCR in newly generated, 'naive' Treg cells (Fisson et al., 2003; Rubtsov et al., 2008). We reasoned that if the TCR were critical for the effector differentiation of Treg cells in the periphery, TCR^{-} Treg cells in these mice would retain a $CD44^{lo}CD62L^{hi}$ naive-like phenotype.

Immature HSA^{hi} $CD4^{+}Foxp3^{+}$ cells in the thymi of $Trac^{FL/FL}Foxp3^{YFP\text{-}Cre}$ mice had cell surface expression of TCR complexes similar to that in their wild-type counterparts; more mature $HSA^{lo}CD4^{+}Foxp3^{+}$ thymocytes showed only slightly reduced TCR expression (Figure 2.4A). Among $Foxp3^{+}$ cells present in the spleens and lymph nodes of $Trac^{FL/WT}Foxp3^{YFP\text{-}Cre}$ mice, ~5–15% were $TCR\beta^{-}$, whereas ~80% of $Foxp3^{+}$ cells in $Trac^{FL/FL}Foxp3^{YFP\text{-}Cre}$ mice lacked surface TCRβ expression (Figure 2.3E and Figure 2.4B). We again observed a slight decrease in the amount of Foxp3 protein in the TCR^{-} Treg cells in $Trac^{FL/WT}Foxp3^{YFP\text{-}Cre}$ mice, but not in $Trac^{FL/FL}Foxp3^{YFP\text{-}Cre}$ mice, while expression of Treg cell signature genes was variably affected in the TCR^{-} Treg cell populations in both mouse strains relative to expression in TCR^{+} Treg cells in $Trac^{WT/WT}Foxp3^{YFP\text{-}Cre}$, *TracFL/WTFoxp3*$^{YFP\text{-}Cre}$ and $Trac^{FL/FL}Foxp3^{YFP\text{-}Cre}$ mice (Figure 2.4C,D).

Figure 2.4. Constitutive ablation of the TCR in *Trac*$^{FL/FL}$*Foxp3*$^{YFP\text{-}Cre}$ mice impairs Treg cell population expansion and precipitates early-onset autoimmunity.

(**A-C**) TCRβ expression on CD4$^+$Foxp3$^+$ cells in the thymi (**A**) and lymph nodes (**A**,**B**) of 2.5 wk old mice, and Foxp3 median fluorescence intensity (MFI) in CD4$^+$Foxp3$^+$ lymph node cells (**C**) in 2.5 wk old *Trac*$^{WT/WT}$*Foxp3*$^{YFP\text{-}Cre}$ (WT/WT), *Trac*$^{FL/WT}$*Foxp3*$^{YFP\text{-}Cre}$ (FL/WT) and *Trac*$^{FL/FL}$*Foxp3*$^{YFP\text{-}Cre}$ (FL/FL) mice. (**D**) Representative expression of Treg markers on the indicated TCRβ$^+$ and TCRβ$^-$ populations. Gray histogram is gated on CD4$^+$Foxp3$^-$ cells in *Trac*$^{WT/WT}$*Foxp3*$^{YFP\text{-}Cre}$ mice. (**E**,**F**) Activation status (**E**), spleen and lymph node cell numbers, and percent cytokine producers in the spleen (**F**) of CD4$^+$Foxp3$^-$ and CD8$^+$ cells. (**G**) Absolute numbers of TCRβ$^+$ and TCRβ$^-$ CD4$^+$Foxp3$^+$ cells in 2.5 week old *Trac*$^{WT/WT}$*Foxp3*$^{YFP\text{-}Cre}$ (WT), *Trac*$^{FL/WT}$*Foxp3*$^{YFP\text{-}Cre}$ (Het), and *Trac*$^{FL/FL}$*Foxp3*$^{YFP\text{-}Cre}$ (KO) mice. (**H**) Absolute numbers of CD4$^+$TCRβ$^+$Foxp3$^-$ (left) and TCRβ$^+$ and TCRβ$^-$ CD4$^+$Foxp3$^+$ cells (right) in liver (top) and lungs (bottom) of indicated mice. Data in (**B**-**E**) are representative of three experiments with a total of six or more mice per group. Data in (**F**,**G**) are aggregated from three experiments with a total of six or more mice per group. Data in **(A**) and (**H**) are representative of two experiments with three or more mice per group each. ***, $P < 0.001$; **, $P < 0.01$; *, $P < 0.05$. P-values were calculated using a two-tailed unpaired t-test.

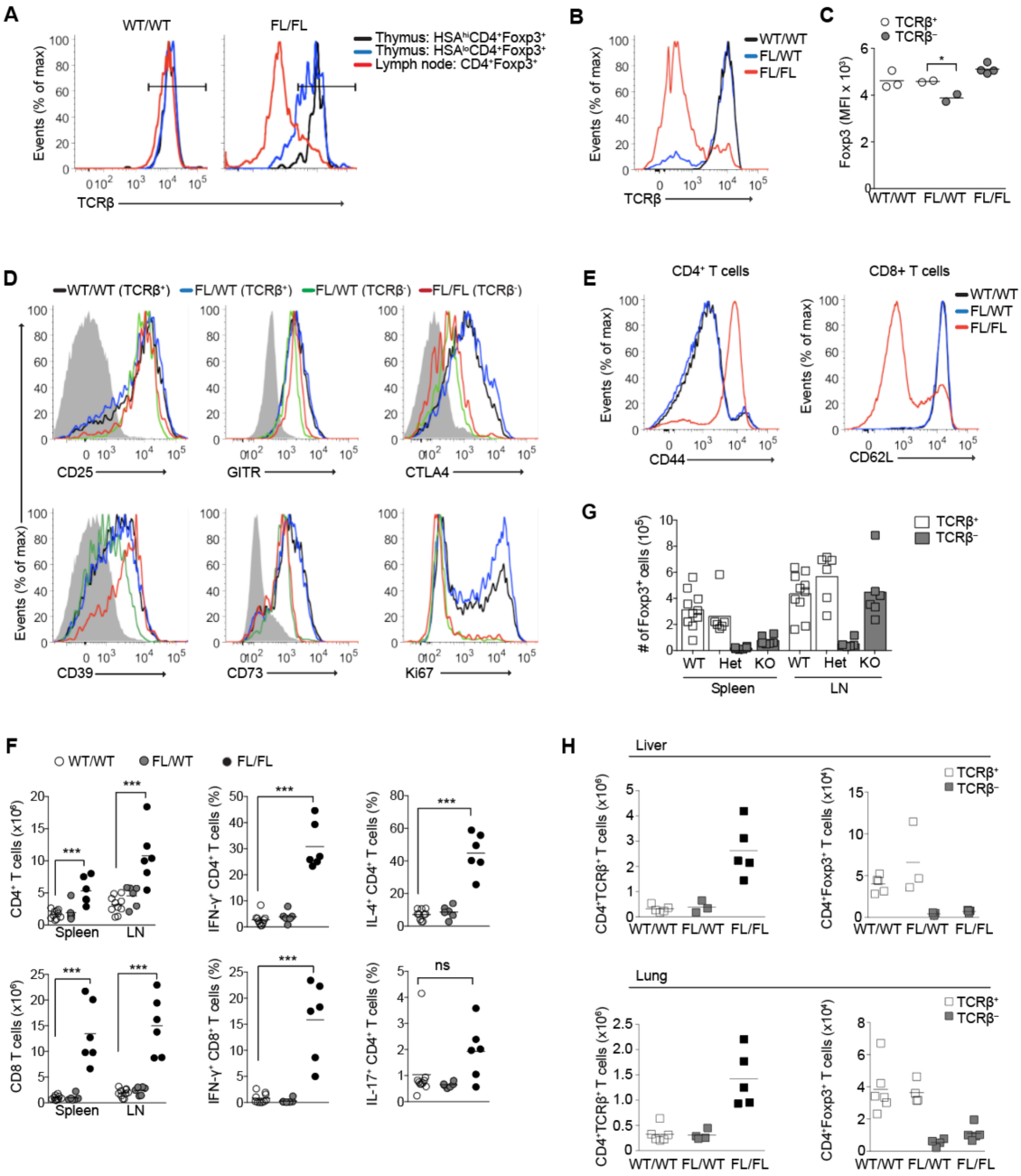
A
WT/WT
FL/FL
Thymus: HSA^hiCD4+Foxp3+
Thymus: HSA^loCD4+Foxp3+
Lymph node: CD4+Foxp3+
Events (% of max)
TCRβ
B
WT/WT
FL/WT
FL/FL
C
TCRβ+
TCRβ-
Foxp3 (MFI x 10^3)
WT/WT FL/WT FL/FL
D
WT/WT (TCRβ+)
FL/WT (TCRβ+)
FL/WT (TCRβ-)
FL/FL (TCRβ-)
CD25
GITR
CTLA4
CD39
CD73
Ki67
E
CD4+ T cells
CD8+ T cells
CD44
CD62L
G
# of Foxp3+ cells (10^5)
WT Het KO WT Het KO
Spleen
LN
F
CD4+ T cells (x10^6)
IFN-γ+ CD4+ T cells (%)
IL-4+ CD4+ T cells (%)
CD8 T cells (x10^6)
IFN-γ+ CD8+ T cells (%)
IL-17+ CD4+ T cells (%)
ns
H
Liver
Lung
CD4+TCRβ+ T cells (x10^6)
CD4+Foxp3+ T cells (x10^4)
WT/WT FL/WT FL/FL

Despite their generally intact Treg cell surface phenotype, nearly all TCR$^-$ Treg cells in healthy *Trac*$^{FL/WT}$*Foxp3*$^{YFP\text{-}Cre}$ mice had a naive-like CD62L^{hi}CD44^{lo} phenotype and lacked expression of all Treg cell differentiation markers tested, including KLRG1, CD103 and CXCR3 (Figure 2.3C and data not shown). Notably, we also observed this pattern under severe inflammatory conditions in *Trac*$^{FL/FL}$*Foxp3*$^{YFP\text{-}Cre}$ mice, which were moribund by 3 weeks of age (Figure 2.3C and Figure 2.4E,F). The lack of CD44^{hi} cells among TCR$^-$ populations in *Trac*$^{FL/WT}$*Foxp3*$^{YFP\text{-}Cre}$ and *Trac*$^{FL/FL}$*Foxp3*$^{YFP\text{-}Cre}$ mice correlated with the decreased proliferation and markedly diminished frequency and number of TCR$^-$ Treg cells relative to that of TCR$^+$ Treg cells in the same mice and in *Trac*$^{WT/WT}$*Foxp3*$^{YFP\text{-}Cre}$ mice; this pattern was evident in lymph nodes and was particularly pronounced in the spleen and other tissues such as the liver and lungs (Figure 2.3D,E and Figure 2.4G,H). Together these data were consistent with an absolute requirement for TCR expression, the loss of which could not be compensated for even in conditions of extreme activation of the immune system, for the peripheral effector differentiation of naive-like Treg cells and acquisition of an activated CD44^{hi} phenotype.

TCR-dependent effector function of mature Treg cells

Foxp3 expression and Treg cell population expansion are facilitated by signaling via the receptor for IL-2 (IL-2R) (Fontenot et al., 2005; Tang et al., 2008; Webster et al., 2009). The increase in Foxp3 protein expression and proliferative activity of TCR$^-$ Treg cells in *Trac*$^{FL/FL}$*Foxp3*$^{Cre\text{-}ERT2}$ mice compared with that in such cells in *Trac*$^{FL/WT}$*Foxp3*$^{Cre\text{-}ERT2}$ mice led us to suspect that ablation of TCR expression, even on mature Treg cells, might precipitate activation of the immune system and elevate the production of IL-2

and other cytokines by activated $CD4^+$ T cells. Indeed, analysis of *Trac*$^{FL/FL}$*Foxp3*$^{Cre\text{-}ERT2}$ mice treated twice with tamoxifen and analyzed on day 9 after treatment revealed increased percentages of $CD44^{hi}$ T cells and increased numbers of IL-2–producing $CD4^+$ T cells compared with that of tamoxifen-treated *Trac*$^{WT/WT}$*Foxp3*$^{Cre\text{-}ERT2}$ and *Trac*$^{FL/WT}$*Foxp3*$^{Cre\text{-}ERT2}$ mice (data not shown).

To more rigorously investigate the role of TCR expression in mature Treg cell function, we administered four doses of tamoxifen to mice (on days 0, 3, 7 and 10) to maximize Cre-ERT2–mediated recombination. On day 13, we noted loss of TCR expression in ~75–80% of Treg cells in *Trac*$^{FL/FL}$*Foxp3*$^{Cre\text{-}ERT2}$ mice and ~25–30% of Treg cells in *Trac*$^{FL/WT}$*Foxp3*$^{Cre\text{-}ERT2}$ mice (Figure 2.5A,B). Despite the normal or even increased frequency of total $Foxp3^+$ cells in the lymph nodes and spleens of *Trac*$^{FL/FL}$*Foxp3*$^{Cre\text{-}ERT2}$ mice, we found elevated numbers of $CD4^+Foxp3^-$ and $CD8^+$ T cells in the lymph nodes of these mice and a higher frequency of $CD44^{hi}CD4^+$ and $CD8^+$ T cells in their lymph nodes and spleens (Figure 2.5C,D). $CD8^+$ T cells from *Trac*$^{FL/FL}$*Foxp3*$^{Cre\text{-}ERT2}$ mice produced more interferon-γ (IFN-γ), and $CD4^+$ T cells from these mice produced more IFN-γ, IL-2, IL-4, IL-13, IL-5 and IL-17, than did T cells from *Trac*$^{WT/WT}$*Foxp3*$^{Cre\text{-}ERT2}$ and *Trac*$^{FL/WT}$*Foxp3*$^{Cre\text{-}ERT2}$ mice (Figure 2.5E and data not shown).

The activation of the immune system in *Trac*$^{FL/FL}$*Foxp3*$^{Cre\text{-}ERT2}$ mice was milder than that resulting from complete depletion of Treg cells in *Foxp3*^{DTR} mice, which express the human diphtheria toxin receptor (DTR) concomitantly with *Foxp3* (Kim et al., 2007). Thus, it was possible that the large number of TCR^- Treg cells in *Trac*$^{FL/FL}$*Foxp3*$^{Cre\text{-}ERT2}$ mice retained measurable TCR-independent suppressor ability and were still capable of immunoregulation.

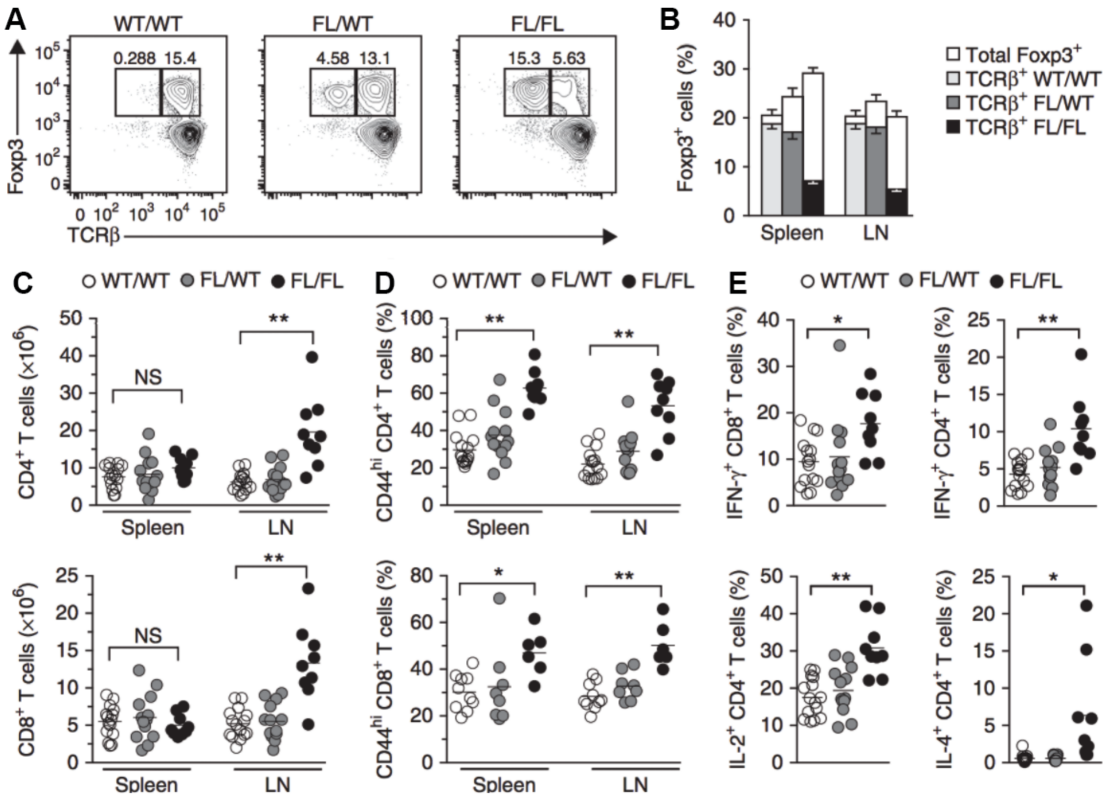

Figure 2.5. TCR-dependent effector function of mature Treg cells in adult mice.

(**A**) Expression of Foxp3 and TCRβ by CD4$^+$ cells in the lymph nodes of *Trac*$^{WT/WT}$*Foxp3*$^{Cre\text{-}ERT2}$, *Trac*$^{FL/WT}$*Foxp3*$^{Cre\text{-}ERT2}$ and *Trac*$^{FL/FL}$*Foxp3*$^{Cre\text{-}ERT2}$ mice on day 13 following tamoxifen treatment on days 0, 3, 7 and 10. Numbers adjacent to outlined areas indicate percent Foxp3$^+$TCRβ$^+$ cells (right) or Foxp3$^+$TCRβ$^-$ cells (left). (**B**) Frequency of TCRβ$^+$ Foxp3$^+$ cells among splenic and lymph node CD4$^+$ cells in *Trac*$^{WT/WT}$*Foxp3*$^{Cre\text{-}ERT2}$, *Trac*$^{FL/WT}$*Foxp3*$^{Cre\text{-}ERT2}$ and *Trac*$^{FL/FL}$*Foxp3*$^{Cre\text{-}ERT2}$ mice, and of total Foxp3$^+$ cells among CD4$^+$ cells for each genotype (Total Foxp3$^+$). (**C**–**E**) Number (**C**), CD44 expression (**D**) and cytokine production (**E**) of CD4$^+$ Foxp3$^-$ or CD8$^+$ T cells in the spleen (**C**–**E**) and lymph nodes (**C**,**D**) of mice as in **A**. Each symbol (**C**–**E**) represents an individual mouse; small horizontal lines indicate the mean. NS, not significant ($P \geq 0.05$); *$P < 0.005$ and **$P \leq 0.0001$ (two-tailed unpaired *t*-test). Data are representative of three experiments with three mice or more per group in each (**A**) or are pooled from three experiments with nine or more per group (**B**–**E**; error bars (**B**), mean ± s.e.m.).

Alternatively, the small population of remaining TCR-sufficient Treg cells in these mice might have limited, to some degree, the activation of effector T cells and the associated autoimmunity. To examine these possibilities, we attempted to reduce the proportion of Treg cells among $CD4^+$ cells in *Foxp3*^{DTR} mice to approximate the frequency of residual TCR-sufficient Treg cells in *Trac*$^{FL/FL}$*Foxp3*$^{Cre\text{-}ERT2}$ mice following four doses of tamoxifen (Tian et al., 2011). We reasoned that if TCR^- Treg cells were capable of substantial suppression, autoimmunity in *Foxp3*^{DTR} mice subjected to only partial depletion of Treg cells would be more severe than that in *Trac*$^{FL/FL}$*Foxp3*$^{Cre\text{-}ERT2}$ mice. Injection of diphtheria toxin depletes mice of Treg cells within 24 h, whereas tamoxifen-induced, Cre-ERT2–mediated recombination progressively increases over a 4-day period (data not shown). Therefore, we treated *Foxp3*^{DTR}, *Trac*$^{WT/WT}$*Foxp3*$^{Cre\text{-}ERT2}$ and *Trac*$^{FL/FL}$*Foxp3*$^{Cre\text{-}ERT2}$ mice with diphtheria toxin 4 d after their first dose of tamoxifen to account for the time needed for complete Cre-ERT2–mediated deletion of *Trac* (we administered both taximofen and diphtheria toxin to all genotypes; Figure 2.6A,B). Partial depletion of the Treg cell compartment in *Foxp3*^{DTR} mice resulted in activation and cytokine production of $CD4^+Foxp3^-$ T cells grossly similar to that observed in *Trac*$^{FL/FL}$*Foxp3*$^{Cre\text{-}ERT2}$ mice with populations of TCR-sufficient Treg cells of a similar or even larger size (Figure 2.6B-D). Together these results demonstrated that Treg cells required continuous TCR expression for the effective elaboration of their suppressor function, and suggested that TCR^- Treg cells, which were abundant in *Trac*$^{FL/FL}$*Foxp3*$^{Cre\text{-}ERT2}$ mice, were largely devoid of detectable suppressor ability.

TCR$^-$ Treg cell dysfunction is not secondary to impaired IL-2R signaling

Figure 2.6. Partial depletion of Treg cells in *Foxp3^{DTR}* mice recapitulates activation of the immune system in *Trac$^{FL/FL}$Foxp3$^{Cre-ERT2}$* mice.
(**A**) Experimental protocol. *Trac$^{WT/WT}$Foxp3$^{Cre-ERT2}$* (*Trac$^{WT/WT}$*), *Trac$^{FL/FL}$Foxp3$^{Cre-ERT2}$* (*Trac$^{FL/FL}$*) and *Foxp3^{DTR}* mice were gavaged with tamoxifen on days 0, 3, 7 and 10. *Foxp3^{DTR}* mice were injected i.p. with PBS, 0.065ug DT, or 0.1ug DT and *Trac$^{WT/WT}$Foxp3$^{Cre-ERT2}$* and *Trac$^{FL/FL}$Foxp3$^{Cre-ERT2}$* mice were injected with 0.065ug DT on days 4, 7 and 10. (**B**) Percent TCRβ^{+}Foxp3^{+} cells among CD4^{+} cells in spleens of *Trac$^{WT/WT}$Foxp3$^{Cre-ERT2}$* and *Trac$^{FL/FL}$Foxp3$^{Cre-ERT2}$* (black squares) and *Foxp3^{DTR}* (gray squares) mice. Total Foxp3^{+} cells among CD4^{+} cells in *Trac$^{FL/FL}$Foxp3$^{Cre-ERT2}$* mice are shown as white squares. (**C**,**D**) Activation of (**C**) and cytokine production by (**D**) splenic CD4^{+}Foxp3^{-} cells. Fold-changes are shown. All data are representative of two experiments with four or more mice per group each. ***, $P < 0.001$; **, $P < 0.01$; *, $P < 0.05$. P-values were calculated using a two-tailed unpaired t-test.

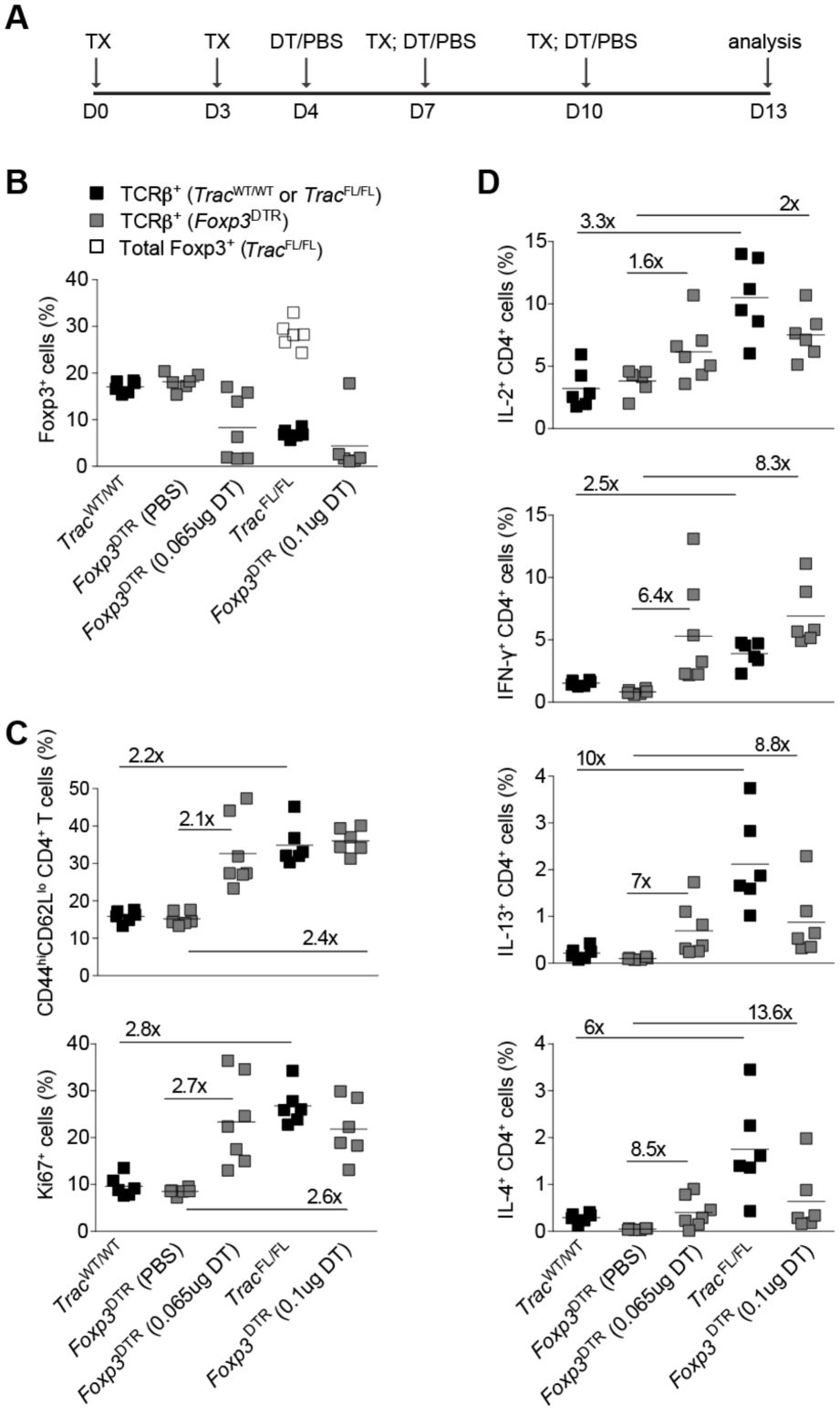
A
TX
TX
DT/PBS
TX; DT/PBS
TX; DT/PBS
analysis
D0
D3
D4
D7
D10
D13
B
TCRβ+ (Trac WT/WT or Trac FL/FL)
TCRβ+ (Foxp3 DTR)
Total Foxp3+ (Trac FL/FL)
Foxp3+ cells (%)
Trac WT/WT
Foxp3 DTR (PBS)
Foxp3 DTR (0.065ug DT)
Trac FL/FL
Foxp3 DTR (0.1ug DT)
C
CD44hiCD62Llo CD4+ T cells (%)
2.2x
2.1x
2.4x
Ki67+ cells (%)
2.8x
2.7x
2.6x
D
IL-2+ CD4+ cells (%)
3.3x
1.6x
2x
IFN-γ+ CD4+ cells (%)
2.5x
6.4x
8.3x
IL-13+ CD4+ cells (%)
10x
7x
8.8x
IL-4+ CD4+ cells (%)
6x
8.5x
13.6x

We considered that the apparent loss of suppressive ability of Treg cells in the absence of the TCR might be an indirect consequence of impaired ability to localize in a TCR- and antigen-dependent manner to sites of $CD4^+$ T cell activation and to thereby acquire IL-2, a cytokine known to be critical for the function and homeostasis of Treg cells. This would explain the decreased expression of Foxp3 and minimal proliferation of TCR^- Treg cells in healthy *Trac*$^{FL/WT}$*Foxp3*$^{Cre\text{-}ERT2}$ mice, in which IL-2 amounts were not elevated and would not be able to partially remedy these defects (Zou et al., 2012).

However, direct *ex vivo* analysis of phosphorylation of the transcription factor STAT5, which occurs downstream of IL-2 signaling in Treg cells, showed that in the spleen and lymph nodes of both Trac$^{FL/WT}$Foxp3^{CreERT2} and Trac$^{FL/FL}$Foxp3$^{Cre\text{-}ERT2}$ mice, the proportion of phosphorylated STAT5 in TCR^- Treg cells was at least equivalent to that in TCR^+ Treg cells (Figure 2.7A and data not shown). In Trac$^{FL/FL}$Foxp3$^{Cre\text{-}ERT2}$ mice, TCR^- Treg cells had more phosphorylated STAT5 than did TCR^+ Treg cells; this mirrored their expression of CD25 and CD62L, which remained high on TCR^- cells but was decreased on the residual activated TCR^+ Treg cells present in these mice (Figure 2.3A and Figure 2.7A and Figure 2.2E,G). These results were consistent with the observation that Treg cells that contain phosphorylated STAT5 are found mainly in the $CD62L^{hi}CD44^{lo}$ (and $CD25^{hi}$) subset of Treg cells; in contrast to the activated $CD44^{hi}CD62L^{lo}$ (and $CD25^{int}$) Treg cell subset, this group of cells has been reported to rely on IL-2R signaling rather than engagement of costimulatory receptors for their maintenance (Smigiel et al., 2014).

In vitro analysis confirmed that lack of TCR expression did not substantially influence the phosphorylation of STAT5 in response to IL-2, nor did it impair the ability of Treg cells to capture and deplete IL-2 from culture

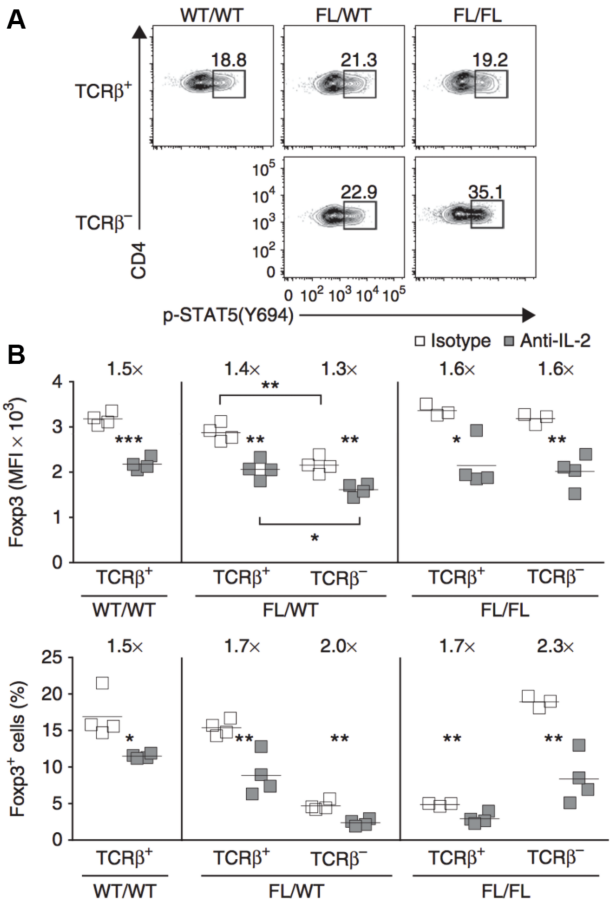

Figure 2.7. TCR expression by Treg cells is dispensable for IL-2R signaling *in vivo*.

(**A**) Phosphorylation of STAT5 at Tyr694 (p-STAT5(Y694)) in TCRβ$^+$ or TCRβ$^-$ CD4$^+$Foxp3$^+$ lymph node cells from *Trac*$^{WT/WT}$*Foxp3*$^{Cre\text{-}ERT2}$, *Trac*$^{FL/WT}$*Foxp3*$^{Cre\text{-}ERT2}$ and *Trac*$^{FL/FL}$*Foxp3*$^{Cre\text{-}ERT2}$ mice on day 9 following tamoxifen administration on days 0 and 1. Numbers adjacent to outlined areas indicate percent CD4$^+$ Foxp3$^+$ cells with phosphorylated STAT5. (**B**) Median fluorescence intensity of Foxp3 in TCRβ$^+$ or TCRβ$^-$ Foxp3$^+$ cells (top) and frequency of TCRβ$^+$ or TCRβ$^-$ Foxp3$^+$ cells among CD4$^+$ cells (bottom) in the lymph nodes of *Trac*$^{WT/WT}$*Foxp3*$^{Cre\text{-}ERT2}$, *Trac*$^{FL/WT}$*Foxp3*$^{Cre\text{-}ERT2}$ and *Trac*$^{FL/FL}$*Foxp3*$^{Cre\text{-}ERT2}$ mice on day 13 following tamoxifen treatment on days 0, 3, 7 and 10 and intraperitoneal injection of IL-2-neutralizing or isotype-matched contol antibody on days 4 and 8. Numbers above plots indicate comparison of results obtained for mice treated with isotype-matched control antibody relative to those for mice treated with anti-IL-2. Each symbol (**B**) represents an individual mouse; small horizontal lines indicate the mean. *$P < 0.05$, **$P < 0.01$ and ***$P < 0.001$ (two-tailed unpaired *t*-test). Data are representative of three experiments involving a total of three or more mice per group (**a**) or of two experiments with two or more mice per group in each (**B**).

media (Figure 2.8A,B), which suggested that in the absence of TCR expression, Treg cell–mediated deprivation of IL-2 might not be an important mechanism of immunosuppression. Furthermore, treatment of *Trac*$^{WT/WT}$*Foxp3*$^{Cre\text{-}ERT2}$, *Trac*$^{FL/WT}$*Foxp3*$^{Cre\text{-}ERT2}$ and *Trac*$^{FL/FL}$*Foxp3*$^{Cre\text{-}ERT2}$ mice with neutralizing antibody to IL-2 (anti-IL-2) or isotype-matched control antibody had a similar effect on TCR^{+} and TCR^{-} Treg cells, reducing Foxp3 expression and lowering the frequency of Foxp3^{+} cells among total CD4^{+} cells (Figure 2.7B). Together these data suggested that TCR^{-} Treg cells efficiently captured IL-2 during activation of the immune system and at steady state. It remains to be determined what signal(s) drove the proliferation of TCR^{-} Treg cells selectively in diseased *Trac*$^{FL/FL}$*Foxp3*$^{Cre\text{-}ERT2}$ mice. However, we observed increased expression of the costimulatory molecules CD80 and CD86 on lymph node dendritic cells (DCs) in *Trac*$^{FL/FL}$*Foxp3*$^{Cre\text{-}ERT2}$ mice, and activated DCs were able to induce limited proliferation of TCR^{-} Treg cells *in vitro* (Figure 2.8C,D).

Finally, the administration of complexes of IL-2 and anti-IL-2 to *Trac*$^{FL/FL}$*Foxp3*$^{Cre\text{-}ERT2}$ mice did not measurably diminish the activation or lymphoproliferation of effector T cells caused by loss of TCR expression in Treg cells (Figure 2.9). Conversely, IL-2 depletion did not further exacerbate autoimmunity (data not shown). Notably, this was the case despite a 1.5-fold population expansion of TCR^{-} Treg cells, but not of TCR^{+} Treg cells, following IL-2 administration (probably a consequence of higher CD25 expression and heightened IL-2 responsiveness in TCR^{-} Treg cells) and a reduction of over twofold in TCR^{-} Treg cells following depletion of IL-2 (Figure 2.7B and Figure 2.9B). These observations further confirmed that TCR^{-} Treg cells, even when present in elevated numbers, had minimal suppressive ability. Together these

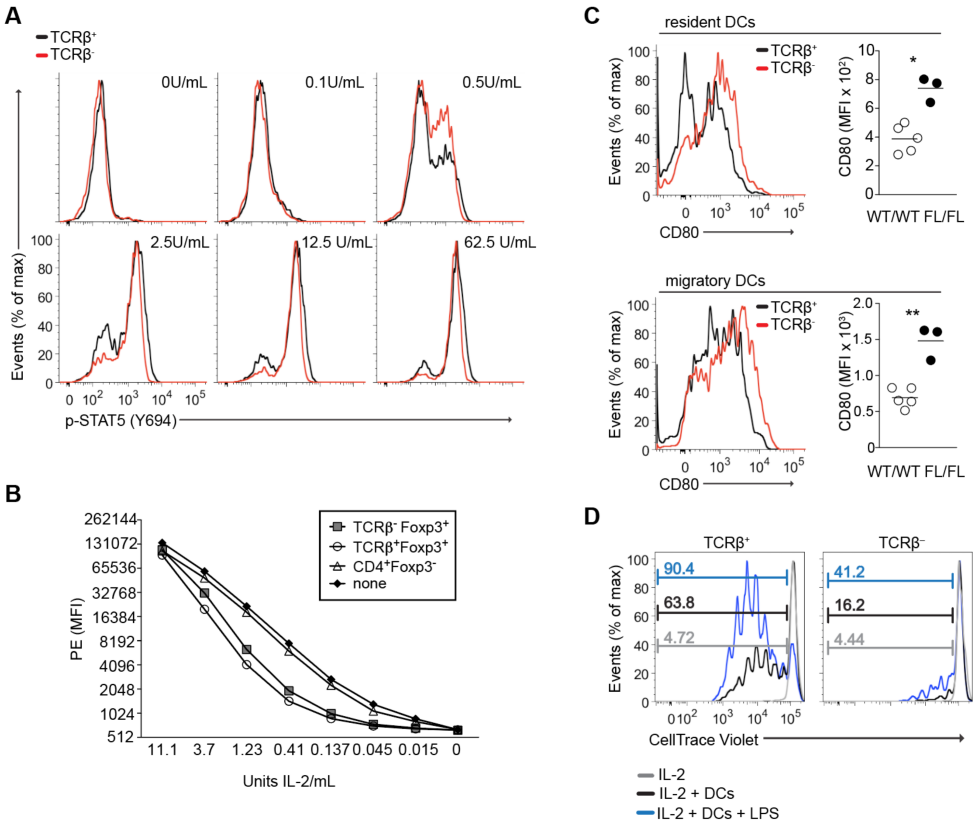

Figure 2.8. Maintenance of TCR-deficient Treg cell responsiveness to IL-2 and proliferation in the presence of activated DCs *in vitro*.
(**A**) p-STAT5 was assessed in eGFP^{+} (Treg) cells among bulk CD4^{+} cells purified on day 9 from *Trac*$^{FL/WT}$*Foxp3*$^{Cre\text{-}ERT2}$ mice treated with tamoxifen on days 0 and 1, stained for CD4 and TCRβ, and cultured with increasing concentrations of IL-2 for 20 minutes before fixation. Data is representative of two experiments with a total of two mice. (**B**) In vitro IL-2 capture assay. *Trac*$^{FL/WT}$*Foxp3*$^{Cre\text{-}ERT2}$ mice were administered tamoxifen on days 0 and 1, and on day 9 CD4^{+} eGFP^{+}TCRβ^{+}, CD4^{+} eGFP^{+}TCRβ^{-}, and CD4^{+}TCRβ^{+} eGFP cells were sorted and cultured in media with increasing concentrations of IL-2. PE median fluorescence intensity (MFI) directly correlates with IL-2 remaining in the media at the time of analysis. (**C**) CD80 expression on DC populations in lymph nodes of *Trac*$^{WT/WT}$*Foxp3*$^{Cre\text{-}ERT2}$ (black lines, left, and white circles, right) and *Trac*$^{FL/FL}$*Foxp3*$^{Cre\text{-}ERT2}$ (red lines, left, and black circles, right) mice on day 13 following tamoxifen administration on days 0, 3, 7 and 10. (**D**) In vitro proliferation of Treg cells was assessed as follows: CD4^{+} eGFP^{+} cells were sorted on day 9 from *Trac*$^{FL/WT}$*Foxp3*$^{Cre\text{-}ERT2}$ mice treated with tamoxifen on days 0 and 1, labeled with CellTrace Violet and cultured for 84 hrs with IL-2 in the presence or absence of DCs with or without LPS. Cells were stained for CD4, TCRβ and Foxp3 for analysis. All conditions were performed in triplicate with similar results. **, $P < 0.001$; *, $P = 0.002$. P-values were calculated using a two-tailed unpaired t-test.

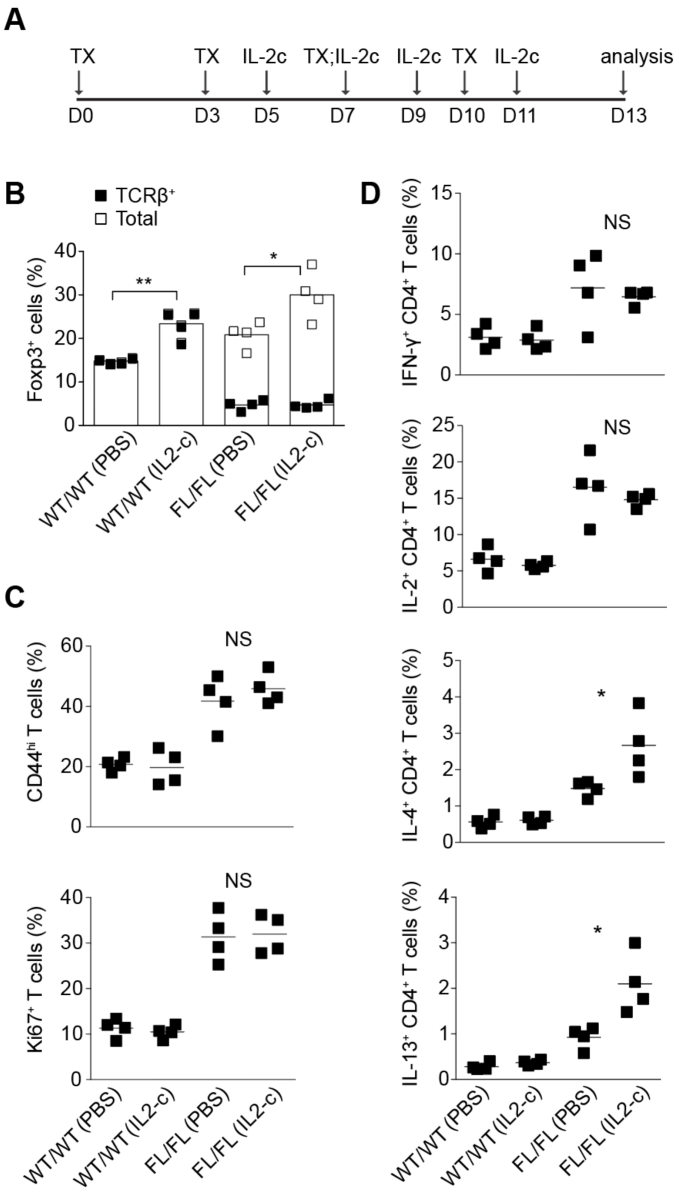

Figure 2.9. IL-2–anti-IL-2 complexes do not 'rescue' autoimmunity in *Trac*$^{FL/FL}$*Foxp3*$^{Cre\text{-}ERT2}$ mice.

(**A**) Schematic of the experimental setup. (**B**) Percent TCRβ$^+$Foxp3$^+$ (black squares) and total Foxp3$^+$ (white squares) cells among CD4$^+$ cells in lymph nodes of *Trac*$^{WT/WT}$*Foxp3*$^{Cre\text{-}ERT2}$ (WT/WT) and *Trac*$^{FL/FL}$*Foxp3*$^{Cre\text{-}ERT2}$ (FL/FL) mice treated with IL-2-anti-IL-2 complexes (IL2-c) or PBS. (**C**,**D**) CD4$^+$ T cell activation (**C**) and cytokine production (**D**) in the spleens of the indicated mice, as in (**B**). NS, not significant ($P \geq 0.05$); **, $P < 0.01$; *, $P < 0.05$. P-values were calculated using a two-tailed unpaired t-test.

results indicated that neither TCR-dependent interactions with antigen-presenting cells nor continuous TCR-mediated localization within lymphoid organs were required for Treg cells to acquire IL-2, and that Treg cell dysfunction in the absence of the TCR could not be attributed to altered IL-2R signaling.

TCR expression promotes Treg cell adhesive properties in vitro

The *in vitro* suppressive ability of Treg cells requires engagement of the TCR (Kim et al., 2009; Thornton and Shevach, 1998). This might involve pathways independent of the catalytic activity of the signaling kinase Zap70, which is essential for the effector function of conventional T cells, but dependent on membrane-proximal inside-out activation of integrins and subsequent enhancement of the interaction of Treg cells with antigen-presenting cells (Au-Yeung et al., 2010). To address this possibility, we cultured TCR^+ or TCR^- Treg cells isolated from $Trac^{WT/WT}Foxp3^{Cre\text{-}ERT2}$, $Trac^{FL/WT}Foxp3^{Cre\text{-}ERT2}$ or $Trac^{FL/FL}Foxp3^{Cre\text{-}ERT2}$ mice with DCs and assessed the formation of DC–Treg cell conjugates. We did not detect any difference in conjugate formation between DCs and TCR^+ or TCR^- Treg cells following 30 min of incubation (data not shown). However, following overnight culture, TCR^- Treg cells isolated from $Trac^{FL/WT}Foxp3^{Cre\text{-}ERT2}$ or $Trac^{FL/FL}Foxp3^{Cre\text{-}ERT2}$ mice were less efficient than were TCR^+ Treg cells at forming conjugates with DCs (3.7% of TCR^- Treg cells compared with 7.5% of TCR^+ Treg cells; Figure 2.10A). Conjugate formation was unaffected by the presence or absence of MHC class II molecules on DCs (Figure 2.10A), which might indicate that the greater adhesion of TCR^+ Treg cells than of TCR^- Treg cells in this assay was not a result of interactions between TCR and MHC class II and might have been a

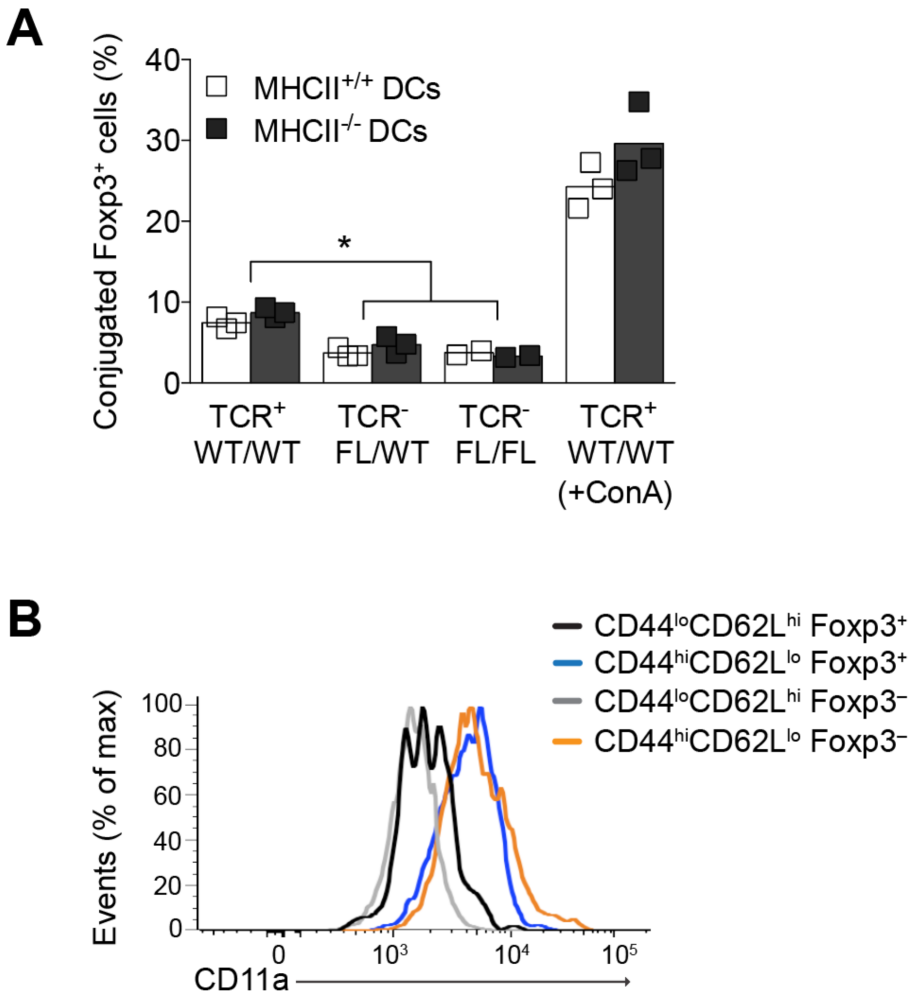

Figure 2.10. Altered *in vitro* conjugate formation between Treg cells and DCs in the absence of the TCR.

(**A**) Conjugate formation was assessed by culturing 6 x10^4 CellTrace Violet-labeled DCs overnight with 10^4 CFSE-labeled TCR^+ or TCR^- Treg cells in the presence of 500 U/mL IL-2. Percent CellTrace $Violet^+$ cells among $CFSE^+$ cells is plotted. TCR^+ cells and DCs were cultured in the presence of 2.5 ug/mL Concanavalin A (ConA) as a positive control. (**B**) Assessment of LFA-1 expression on $CD44^{hi}CD62L^{lo}$ vs. $CD44^{lo}CD62L^{hi}$ $CD4^+Foxp3^+$ and $Foxp3^-$ cells by flow cytometric analysis of CD11a (ITGAL) expression. *, $P < 0.01$. P-value in (**A**) was calculated using a two-tailed unpaired t-test.

consequence of the overall heightened activation status of TCR^+ Treg cells relative to that of TCR^- Treg cells. As expression of the integrin LFA-1 was higher on $CD44^{hi}$ Treg cells than on $CD44^{lo}CD62L^{hi}$ Treg cells (Figure 2.10B), it is possible that greater conjugate formation by TCR^+ Treg cells, which show greater enrichment for $CD44^{hi}$ cells than do TCR^- Treg cells, was due at least in part to increased expression of this integrin. Further work is needed to determine precisely how engagement of the TCR *in vivo* affects signaling pathways to modulate the adhesive properties of Treg cells. However, our results indicated that TCR expression contributed to optimal contact-dependent interactions between Treg cells and antigen-presenting cells, which might support TCR-dependent immunosuppressive function.

TCR modulation of the effector Treg cell transcriptional signature

To explore whether TCR signals, apart from influencing Treg cell adhesion, might drive transcriptional events to 'license' suppressor function *in vivo*, we analyzed the gene expression of TCR^+ and TCR^- Treg cells. Flow cytometry showed that loss of TCR expression had a stronger effect on effector-like $CD44^{hi}CD62L^{lo}$ Treg cells than on naive-like $CD44^{lo}CD62L^{hi}$ Treg cells (data not shown). This prompted us to investigate the gene-expression profiles of these two populations separately in the TCR^+ or TCR^- Treg cell populations isolated from healthy $Trac^{FL/WT}Foxp3^{Cre\text{-}ERT2}$ mice (to avoid confounding effects of activation of the immune system). We found that 155 genes were downregulated by at least twofold and only five genes were upregulated by that amount in effector-like $CD44^{hi}CD62L^{lo}$ TCR^- Treg cells relative to their expression in $CD44^{hi}$CD62Llo TCR^+ Treg cells (Figure 2.11A). 16 genes were downregulated in the naive-like $CD44^{lo}CD62L^{hi}$ TCR^- Treg cells relative to

Figure 2.11. TCR signaling maintains the effector Treg cell transcriptional signature.
(**A**) Genes expressed differently in $CD44^{hi}CD62L^{lo}$ versus $CD44^{lo}CD62L^{hi}$ $TCR\beta^{+}$ Treg cells plotted against those expressed differently in $CD44^{hi}CD62L^{lo}$ $TCR\beta^{-}$ versus $CD44^{hi}CD62L^{lo}$ $TCR\beta^{+}$ T_{reg} cells (top) or $CD44^{lo}CD62L^{hi}$ $TCR\beta^{-}$ versus $CD44^{lo}CD62L^{hi}$ $TCR\beta^{+}$ Treg cells (bottom) among subpopulations sorted by flow cytometry on day 14 from $Trac^{FL/WT}Foxp3^{Cre\text{-}ERT2}$ mice treated with tamoxifen on days 0, 1 and 3; numbers in plots indicate genes up-regulated (blue) or down-regulated (red) by twofold or more in the absence of the TCR ($q < 0.01$). (**B**) Genes down-regulated twofold or more in $CD44^{hi}CD62L^{lo}$ $TCR\beta^{-}$ Treg cells relative to their expression in $CD44^{hi}CD62L^{lo}$ $TCR\beta^{+}$ Treg cells (TCR) among those up-regulated twofold or more in $CD44^{hi}CD62L^{lo}$ T_{reg} cells relative to their expression in $CD44^{lo}CD62L^{hi}$ T_{reg} cells (Up) (left), and genes up-regulated twofold or more in $CD44^{hi}CD62L^{lo}$ Treg cells relative to their expression in $CD44^{lo}CD62L^{hi}$ Treg cells (Up) among those down-regulated twofold or more in $CD44^{hi}CD62L^{lo}$ $TCR\beta^{-}$ T_{reg} cells relative to their expression in $CD44^{hi}CD62L^{lo}$ $TCR\beta^{+}$ Treg cells (TCR) (right). (**C**) Cumulative distribution function plot of TCR-dependent genes plotted against all genes expressed differently in $Foxp3^{GFP\text{-}KO}$ T cells versus $Foxp3^{+}$ $CD4^{+}$ T cells. $P < 10^{-20}$ (two-sample Kolmogorov-Smirnov test). (**D**) Expression patterns of TCR-dependent genes encoding transcription factors, cell surface molecules and secreted molecules in Treg cells. Data are representative of one experiment with two or more replicates with five or more mice per replicate.

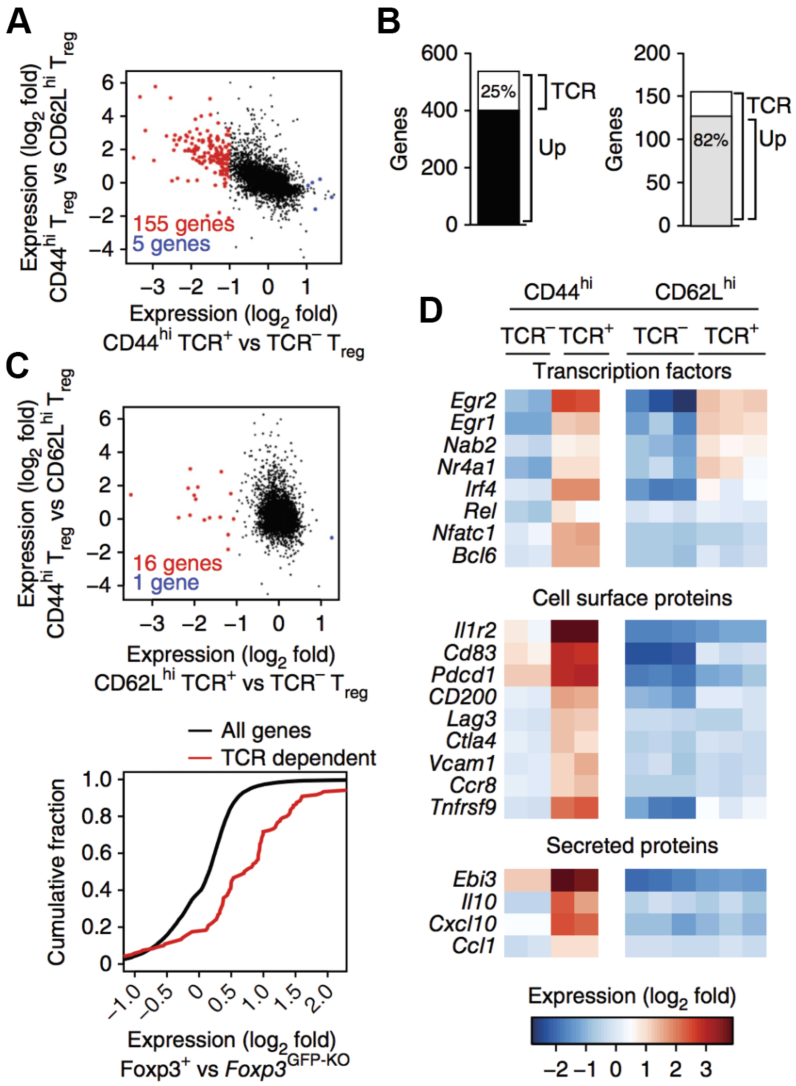
A
Expression (log2 fold) CD44hi Treg vs CD62Lhi Treg
155 genes
5 genes
Expression (log2 fold) CD44hi TCR+ vs TCR− Treg
B
Genes
25%
TCR
Up
82%
C
16 genes
1 gene
Expression (log2 fold) CD62Lhi TCR+ vs TCR− Treg
All genes
TCR dependent
Cumulative fraction
Expression (log2 fold) Foxp3+ vs Foxp3GFP-KO
D
CD44hi
CD62Lhi
TCR− TCR+ TCR− TCR+
Transcription factors
Egr2
Egr1
Nab2
Nr4a1
Irf4
Rel
Nfatc1
Bcl6
Cell surface proteins
Il1r2
Cd83
Pdcd1
CD200
Lag3
Ctla4
Vcam1
Ccr8
Tnfrsf9
Secreted proteins
Ebi3
Il10
Cxcl10
Ccl1
Expression (log2 fold)

their expression in CD44^{lo}CD62L^{hi} TCR^{+} Treg cells (all of these were also downregulated in CD44^{hi}CD62L^{lo} TCR^{-} vs. CD44^{hi}CD62L^{lo} TCR^{+} Treg cells), whereas one gene was upregulated (Figure 2.11A). Some 535 genes showed higher expression (twofold or greater) in effector-like CD44^{hi}CD62L^{lo} TCR^{+} Treg cells than in naive-like CD44^{lo}CD62L^{hi} TCR^{+} Treg cells, and the expression of 136 of these (25%) was TCR dependent (Figure 2.11B). Notably, 127 of the 155 genes (82%) downregulated in the absence of the TCR in CD44^{hi}CD62L^{lo} Treg cells showed at least twofold higher expression in effector-like Treg cells than in naive-like Treg cells (Figure 2.11B).

Foxp3 has been proposed to solidify and amplify a transcriptional program initiated in Treg cell precursors by engagement of the TCR (Gavin et al., 2007; Lin et al., 2007; Ohkura et al., 2012; Samstein et al., 2012). We compared the expression of the 155 genes identified above as being maintained by the TCR in Treg cells (called 'TCR-dependent genes' here) to the expression of Foxp3-dependent genes, identified as being upregulated in wild-type Treg cells relative to their expression in eGFP+ T cells from *Foxp3*$^{GFP\text{-}KO}$ mice, which express eGFP from a *Foxp3*-null allele (Samstein et al., 2012). We found that substantially more of the TCR-dependent genes than all genes were also Foxp3 dependent (Figure 2.11C). These observations suggested that the TCR-driven transcriptional program in Treg cells was enhanced by Foxp3 expression, but that Foxp3 alone was not sufficient to maintain the full transcriptional signature of effector Treg cells.

Examination of the TCR-dependent genes identified several transcription factors that were upregulated in TCR^{+} CD44^{hi}CD62L^{lo} Treg cells relative to their expression in TCR^{-} CD44^{hi}CD62L^{lo}, TCR^{+} CD44^{lo}CD62L^{hi} and TCR^{-} CD44^{lo}CD62L^{hi} Treg cells, including NFATc1, c-Rel, Bcl-6 and IRF4

(Figure 2.11D); published data have shown that Bcl-6 and IRF4 are important for the differentiation and function of effector Treg cells (Cretney et al., 2011; Sawant et al., 2012; Zheng et al., 2009). Of the 155 TCR-dependent genes, we identified only one adhesion molecule–encoding gene (*Vcam1*) whose expression was upregulated in $CD44^{hi}CD62L^{lo}$ Treg cells relative to its expression in $CD44^{lo}CD62L^{hi}$ Treg cells in a manner that depended on TCR expression (Figure 2.11D). Genes encoding several other potential effector molecules were also upregulated in $CD44^{hi}CD62L^{lo}$ Treg cells relative to their expression in $CD44^{lo}CD62L^{hi}$ Treg cells, in a TCR-dependent manner, including those encoding IL-1R2 (a decoy receptor for IL-1); the immunoinhibitory molecules CD83, CD200 and LAG-3; IL-10; and EBI3 (a subunit of the cytokines IL-27 and IL-35) (Collison et al., 2007; Colotta et al., 1993; Hall et al., 2012; Huang et al., 2004; Petermann et al., 2007; Reinwald et al., 2008; Rubtsov et al., 2008). In addition, the chemokine-encoding genes *Cxcl10* and *Ccl1*, as well as *Ccr8* (which encodes the receptor for CCL1), were significantly downregulated in TCR^- Treg cells relative to their expression in TCR^+ Treg cells, which suggested that Treg cells might signal each other through the expression of chemokines and their corresponding receptors or might recruit into close proximity the targets of their suppressive activity (Hoelzinger et al., 2010). Together these data indicated that under physiological conditions, a substantial portion of the effector Treg cell transcriptional program, but not the naive-like Treg cell transcriptional program, characterized by elevated expression of several potential Treg cell effector molecules, was maintained by continuous TCR signaling.

IRF4 expression promotes Treg cell function and homeostasis

To begin to assess the importance of the TCR-dependent transcriptional program for continuous Treg cell function *in vivo*, we focused on IRF4 as a downstream target of the TCR signaling pathway in Treg cells. We confirmed that elevated IRF4 expression in Treg cells was restricted to $CD44^{hi}$ cells and was reduced to basal expression upon ablation of the TCR in both $Trac^{FL/WT}Foxp3^{Cre\text{-}ERT2}$ and $Trac^{FL/FL}Foxp3^{Cre\text{-}ERT2}$ mice (Figure 2.12A). $Irf4^{FL/-}Foxp3^{Cre\text{-}ERT2}$ mice, in which IRF4 is constitutively deleted in Treg cells, have been shown to develop severe autoimmunity dominated by type 2 helper T cell cytokines by 8 weeks of age (Zheng et al., 2009). Treg cells in $Irf4^{-/-}$ mice have been shown to have an almost exclusively naive-like phenotype (Cretney et al., 2011), and we similarly found that Treg cells in $Irf4^{FL/FL}Foxp3^{YFP\text{-}Cre}$ mice were largely $CD44^{lo}CD62L^{hi}$, even in the context of severe inflammation (data not shown), which suggested impaired differentiation, survival and/or population expansion of effector Treg cells.

To determine whether fully differentiated Treg cells require IRF4 expression downstream of TCR engagement for their *in vivo* suppressive function, we administered tamoxifen on days 0, 3, 7 and 10 to $Irf4^{FL/FL}Foxp3^{Cre\text{-}ERT2}$ and $Irf4^{WT/WT}Foxp3^{Cre\text{-}ERT2}$ littermates (Klein et al., 2006). On day 13, we observed slightly but reproducibly lower IRF4 protein expression in $CD44^{hi}$ Treg lymph node cells from $Irf4^{FL/FL}Foxp3^{Cre\text{-}ERT2}$ mice than in cells from $Irf4^{WT/WT}Foxp3^{Cre\text{-}ERT2}$ mice (Figure 2.13A). We also saw higher GFP expression in the Treg cells, measured as a sum of fluorescence from the *Irf4*-deletion GFP reporter (whose expression is switched on in the *Irf4* locus by Cre-mediated deletion of the $Irf4^{FL}$ allele) and from the GFP-Cre-ERT2 fusion protein expressed concomitantly with Foxp3 (Figure 2.12B). Quantitative PCR analysis indicated ~50% lower abundance of *Irf4* mRNA in Treg cells sorted

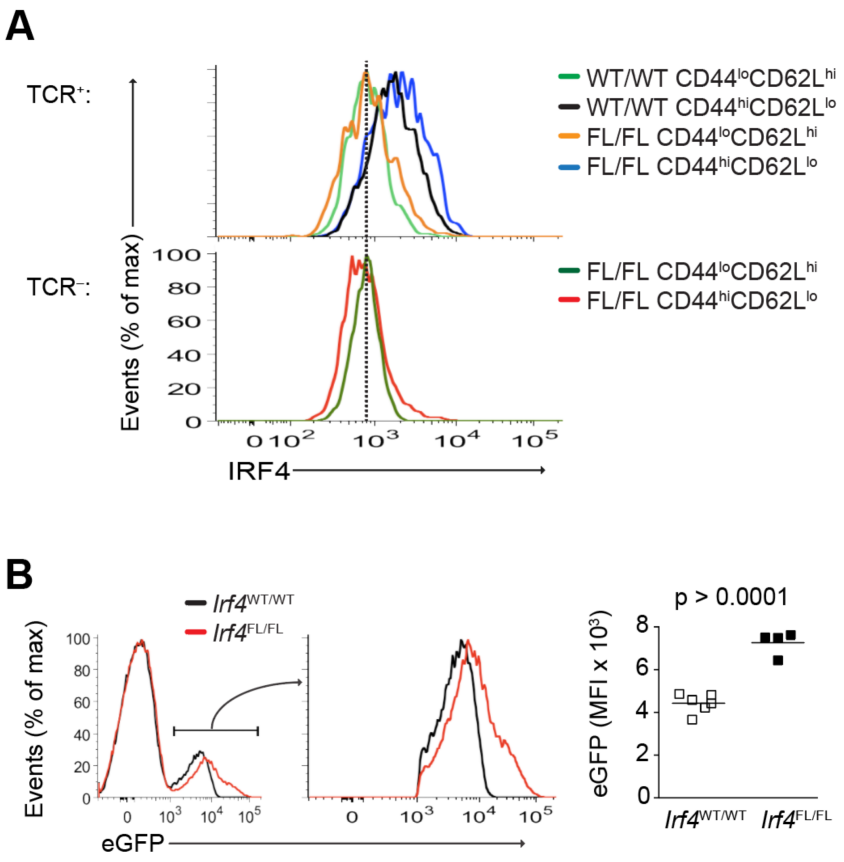

Figure 2.12. IRF4 expression in Treg cells is restricted to CD44^{hi} cells, is TCR dependent and can be inducibly ablated in *Irf4*$^{FL/FL}$*Foxp3*$^{Cre\text{-}ERT2}$ mice.

(**A**) Histograms showing IRF4 protein levels in TCR^{+} Foxp3^{+} cells in *Tcra*$^{WT/WT}$*Foxp3*$^{Cre\text{-}ERT2}$ (WT/WT; CD44^{lo}CD62L^{hi} in green and CD44^{hi}CD62L^{lo} in black) and in *Tcra*$^{FL/FL}$*Foxp3*$^{Cre\text{-}ERT2}$ (FL/FL; CD44^{lo}CD62L^{hi} in orange and CD44^{hi}CD62L^{lo} in blue) mice (above), and in TCR^{-} Foxp3^{+} cells in *Tcra*$^{FL/FL}$*Foxp3*$^{Cre\text{-}ERT2}$ (FL/FL; CD44^{lo}CD62L^{hi} in green and CD44^{hi}CD62L^{lo} in red) mice (below). (**B**) Histograms demonstrating an increase in eGFP median fluorescence intensity (MFI) in eGFP^{+} cells following tamoxifen administration to *Irf4*$^{FL/FL}$*Foxp3*$^{Cre\text{-}ERT2}$ (red line) vs. *Irf4*$^{WT/WT}$*Foxp3*$^{Cre\text{-}ERT2}$ (black line) mice (left); quantitation of eGFP median fluorescence intensity of eGFP^{+} cells in *Irf4*$^{WT/WT}$*Foxp3*$^{Cre\text{-}ERT2}$ (white squares) and *Irf4*$^{FL/FL}$*Foxp3*$^{Cre\text{-}ERT2}$ (black squares) mice (right). Mice were administered tamoxifen on days 0, 3, 7 and 10 and were analyzed on day 13. Data is representative of two experiments with three or more (**A**) or four or more (**B**) mice per group each. Pvalue in (**B**) was calculated using a two-tailed unpaired t-test.

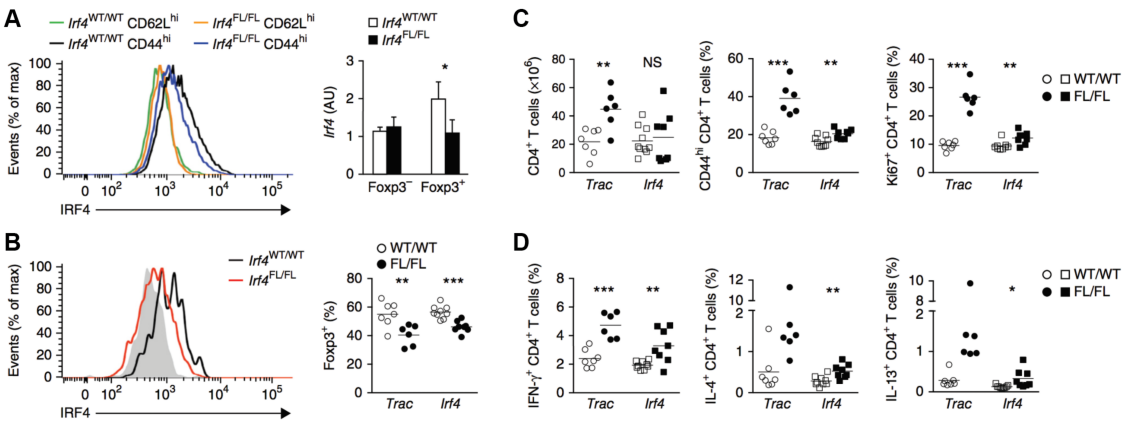

Figure 2.13. IRF4 expression contributes to optimal suppressive ability and homeostasis of Treg cells.

(**A**) IRF4 expression in CD44^{hi}CD62L^{lo} (CD44^{hi}) and CD44^{lo}CD62L^{hi} (CD62L^{hi}) CD4^{+}Foxp3^{+} lymph node cells from *Irf4*$^{WT/WT}$*Foxp3*$^{Cre\text{-}ERT2}$ mice (*Irf4*$^{WT/WT}$) and *Irf4*$^{FL/FL}$*Foxp3*$^{Cre\text{-}ERT2}$ mice (*Irf4*$^{FL/FL}$) analyzed on day 13 following tamoxifen treatment on days 0, 3, 7 and 10 (left), quantitative PCR analysis of *Irf4* mRNA in CD4^{+}eGFP^{-} and CD4^{+}eGFP^{+} cells sorted from pooled spleens and lymph nodes of those mice. AU, arbitrary units. (**B**) IRF4 expression in colonic lamina propria CD4^{+}Foxp3^{+}cells in *Irf4*$^{WT/WT}$*Foxp3*$^{Cre\text{-}ERT2}$ and *Irf4*$^{FL/FL}$*Foxp3*$^{Cre\text{-}ERT2}$ mice (left), and frequency of Foxp3^{+} cells among CD4^{+} cells in the large intestine lamina propria in *Trac*$^{WT/WT}$*Foxp3*$^{Cre\text{-}ERT2}$ or *Irf4*$^{WT/WT}$*Foxp3*$^{Cre\text{-}ERT2}$ mice (open circles) and *Trac*$^{FL/FL}$*Foxp3*$^{Cre\text{-}ERT2}$ or *Irf4*$^{FL/FL}$*Foxp3*$^{Cre\text{-}ERT2}$ mice (filled circles) analyzed on day 13 following tamoxifen treatment on days 0, 3, 7 and 10. Gray shaded curve (left), CD4^{+}Foxp3^{-} cells. (**C**,**D**) Number of cells and frequency of CD44^{hi} or Ki67^{+} cells (**C**) or cytokine-producing cells (**D**) among CD4^{+}Foxp3^{-} T cells in the lymph nodes (**C**) and spleens (**D**) of *Trac*$^{WT/WT}$*Foxp3*$^{Cre\text{-}ERT2}$ mice (open circles), *Irf4*$^{WT/WT}$*Foxp3*$^{Cre\text{-}ERT2}$ mice (open squares), *Trac*$^{FL/FL}$*Foxp3*$^{Cre\text{-}ERT2}$ mice (filled circles) and *Irf4*$^{FL/FL}$*Foxp3*$^{Cre\text{-}ERT2}$ mice (filled squares) analyzed on day 13 following tamoxifen treatment on days 0, 3, 7 and 10. Each symbol (**B**–**D**) represents an individual mouse; small horizontal lines indicate the mean. *$P < 0.05$, **$P < 0.01$ and ***$P < 0.001$ (two-tailed unpaired *t*-test). Data are representative of two experiments with four or more mice per group in each (**A**,**B**, left) or are pooled from two experiments with four or more mice per group in each (**A**,**B**, right, **C**,**D** (error bars (**A**), s.d.).

from pooled spleens and lymph nodes of tamoxifen-treated *Irf4*$^{FL/FL}$*Foxp3*$^{Cre-ERT2}$ mice than in those of *Irf4*$^{WT/WT}$*Foxp3*$^{Cre-ERT2}$ mice (Figure 2.13A).

We hypothesized that the suboptimal ~50% reduction in mRNA transcripts and the only slight reduction in IRF4 protein expression in the spleens and lymph nodes of *Irf4*$^{FL/FL}$*Foxp3*$^{Cre-ERT2}$ mice compared with that of *Irf4*$^{WT/WT}$*Foxp3*$^{Cre-ERT2}$ mice might have resulted from a competitive disadvantage of Treg cells that lack IRF4 protein. Such a disadvantage might lead to 'preferential' population expansion of the IRF4-sufficient Treg cells remaining in the *Irf4*$^{FL/FL}$*Foxp3*$^{Cre-ERT2}$ mice. This would be consistent with the published observation that the survival and expansion of strongly antigen-stimulated CD8^{+} T cells is greatly impaired in the absence of IRF4 (Man et al., 2013).

To determine whether IRF4 might similarly contribute to the maintenance of Treg cells that have been strongly activated, we assessed the colonic lamina propria, in which nearly all Treg cells were CD44^{hi} and had probably recently experienced engagement of the TCR, given their robust IL-10 production (data not shown). Indeed, we observed a lower frequency of colonic lamina propria Treg cells in *Irf4*$^{FL/FL}$*Foxp3*$^{Cre-ERT2}$ mice than in *Irf4*$^{WT/WT}$*Foxp3*$^{Cre-ERT2}$ mice (Figure 2.13B), similar to lower frequency of Treg cells in the colonic lamina propria of *Trac*$^{FL/FL}$*Foxp3*$^{Cre-ERT2}$ mice than in *Trac*$^{WT/WT}$*Foxp3*$^{Cre-ERT2}$ mice noted above. In contrast to spleen and lymph node Treg cells, and consistent with their lower frequency, colonic lamina propria Treg cells in *Irf4*$^{FL/FL}$*Foxp3*$^{Cre-ERT2}$ mice had much lower expression of IRF4 protein than did those in *Irf4*$^{WT/WT}$*Foxp3*$^{Cre-ERT2}$ mice (Figure 2.13B). We hypothesized that the reportedly low influx of circulating Treg cells into the colonic lamina propria at steady state may have precluded IRF4-sufficient cells

from becoming activated and repopulating to a wild-type frequency the Treg cell niche in this tissue (Smigiel et al., 2014).

Despite the only slightly lower IRF4 expression in Treg cells isolated from the spleens and lymph nodes of *Irf4*$^{FL/FL}$*Foxp3*$^{Cre-ERT2}$ mice than in their counterparts from *Irf4*$^{WT/WT}$*Foxp3*$^{Cre-ERT2}$ mice, we were able to detect a very mild, but statistically significant, increase in the frequency of CD44^{hi} and Ki67^{+} lymph node Foxp3^{-}CD4^{+} T cells, as well as increased production of IFN-γ, IL-4 and IL-13 by splenic Foxp3^{-}CD4^{+} T cells (Figure 2.13C,D). This suggested that IRF4 expression downstream of TCR signaling in Treg cells contributed to the suppressive function of Treg cells. An increase in the production of type 2 helper T cell cytokines was consistent with the phenotype of mice with constitutive ablation of IRF4 in Treg cells, whereas the increased IFN-γ was probably a consequence of the substantial type 1 helper T cell bias in C56B/L6 adult mice before induced *Irf4* deletion (Zheng et al., 2009).

As a control, we confirmed that in the absence of tamoxifen treatment, the expression of CD44, Ki67, IFN-γ, IL-4 and IL-13 in CD4^{+}Foxp3^{-} T cells from *Irf4*$^{FL/FL}$*Foxp3*$^{Cre-ERT2}$ mice was indistinguishable from that in their counterparts from *Irf4*$^{WT/WT}$*Foxp3*$^{Cre-ERT2}$ mice, as was the frequency of Treg cells in the colonic lamina propria (data not shown). This suggested that the modest differences between *Irf4*$^{FL/FL}$*Foxp3*$^{Cre-ERT2}$ and *Irf4*$^{WT/WT}$*Foxp3*$^{Cre-ERT2}$ mice that we observed upon tamoxifen treatment were not a consequence of the *Irf4*^{FL} allele itself. Together these data indicated that even partial loss of IRF4 expression downstream of TCR engagement in Treg cells interfered with optimal suppressive function of these cells.

Discussion

Despite major progress in understanding the molecular mechanisms of TCR engagement–driven differentiation of Treg cells, the role of the TCR in Treg cell function *in vivo* has remained unclear. Here we demonstrated that TCR signaling in differentiated Treg cells was dispensable for the maintenance of Foxp3 expression and for the expression of many characteristic markers of Treg cells. Although the bulk of the Treg cell–specific gene signature was also preserved in the absence of the TCR, suppressor function was critically dependent on the TCR.

Given that antigen-activated $CD4^{+}Foxp3^{-}$ T cells in lymphoid organs are thought to produce IL-2 in a spatially restricted manner, we considered the possibility that Treg cells might analogously require their TCRs to correctly position themselves to gain preferential access to IL-2. This might elicit the suppressive function of Treg cells by stimulating IL-2R. However, our *in vivo* and *in vitro* data suggested that Treg cells acquired and probably effectively depleted IL-2 in a TCR-independent manner. Thus, these cells may instead rely predominantly on expression of the chemokine receptor CCR7 to ensure sufficient IL-2 exposure, as has been proposed (Smigiel et al., 2014).

Our observation that newly generated Treg cells in $Trac^{FL/WT}Foxp3^{YFP\text{-}Cre}$ and $Trac^{FL/FL}Foxp3^{YFP\text{-}Cre}$ mice remained naive-like upon loss of the TCR and did not populate non-lymphoid tissues suggested that effector differentiation and population expansion were processes dependent on the TCR and probably dependent on antigens. This finding may help explain the observation that distinct TCR repertoires are displayed by Treg cell populations in different lymphoid organs and tissues in adult mice (Lathrop et al., 2011; Lathrop et al., 2008). Furthermore, inducible ablation of the TCR resulted in a far greater change in gene expression in the effector-like Treg cell

subset than in the naive-like subset. This suggested that continuous TCR signaling might be selectively driving the homeostasis and suppressor function of effector-like Treg cells. As inducible deletion of the TCR in differentiated Treg cells precipitated autoimmunity, our data may suggest that all or most of the suppressor function of Treg cells *in vivo* is mediated by the $CD44^{hi}$ effector-like Treg cell subset.

We found that partial inducible ablation of *Irf4*, expressed downstream of TCR engagement in $CD44^{hi}$ Treg cells, resulted in a very mild but reproducible activation of the immune system. This result suggested that IRF4 expression was important for TCR-dependent Treg cell function; however, given the suboptimal deletion of *Irf4* and very modest activation of the immune system, it remains to be determined to what extent and in what way TCR-dependent induction of IRF4 in Treg cells contributes to their ability to suppress spontaneous autoimmunity. IRF4 may act mainly to control the maintenance of highly activated Treg cells, which was particularly evident in the colonic lamina propria and which, when altered, may affect the ability of the Treg cell pool to suppress. Alternatively, IRF4 may have a more direct role in promoting the suppressive activity of Treg cells, perhaps by driving the expression of certain Treg cell effector molecules. Although we observed decreased expression of the inducible costimulator ICOS on colonic Treg cells that lacked IRF4 (data not shown), the remaining IRF4-sufficient Treg cells in lymphoid organs of $Irf4^{FL/FL}Foxp3^{Cre\text{-}ERT2}$ mice preclude more rigorous identification of IRF4 targets.

However, we note that even though naive-like Treg cells did not express IRF4 and were overwhelmingly unaffected by TCR deletion on a transcriptional level, this did not necessarily indicate that these cells were

nonfunctional or were not experiencing TCR engagement. Indeed, several genes, including *Egr1*, *Egr2* and *Nr4a1*, were downregulated in this Treg cell subset in the absence of the TCR.

Additional experiments are needed to elucidate the contributions of other individual TCR-dependent genes in Treg cells to the maintenance of immunotolerance in the steady state and to the restraint of immune responses directed against commensal microorganisms, food and environmental antigens and pathogens. In connection with this, we note that although IL-10 production by Treg cells has been linked to the control of inflammatory responses at environmental interfaces such as the gut, lungs and skin, it has also been shown to be dispensable for Treg cell control over systemic autoimmunity (Rubtsov et al., 2008). Likewise, we found that whereas constitutive deletion of calcineurin B1 in $Cnb1^{FL/FL}Foxp3^{YFP\text{-}Cre}$ mice (which eliminated calcineurin-dependent activation of NFAT in Treg cells) resulted in lethal early-onset autoimmunity, highly efficient inducible deletion in adult lymphoreplete $Cnb1^{FL/FL}Foxp3^{Cre\text{-}ERT2}$ mice had no detectable adverse effects on Treg cell function (data not shown). Together these findings suggest that engagement of the TCR on Treg cells may drive a focused transcriptional program, select aspects of which are required in a context-dependent manner for mediation of a broad range of Treg cell immunosuppressive functions.

Acknowledgements

We thank M. Schmidt-Supprian (Technical University Munich) and K. Rajewsky (Max Delbrück Center) for *Trac*FL mice. Supported by the US National Institutes of Health (R37AI034206 to A.Y.R.), the Ludwig Cancer

Center at Memorial Sloan-Kettering Cancer Center (A.Y.R.) and the Howard Hughes Medical Institute (A.Y.R.).

Materials and Methods

Mice

Mice were bred and housed in the pathogen-free animal facility at Memorial Sloan-Kettering Cancer Center and were used in accordance with institutional guidelines. Unless otherwise noted, 8- to 10-week-old male and female sex-matched mice were used for all experiments. *Foxp3*$^{YFP\text{-}Cre}$, *Foxp3*$^{eGFP\text{-}Cre\text{-}ERT2}$, *Rosa26*^{YFP}, *Foxp3*^{DTR} and *Irf4*^{FL} mice have been described (Kim et al., 2007; Klein et al., 2006; Rubtsov et al., 2010; Rubtsov et al., 2008). M. Schmidt-Supprian and K. Rajewsky provided *Trac*^{FL} mice. For tamoxifen administration, 40 mg tamoxifen was dissolved in 100µl ethanol and subsequently in 900 µl olive oil (Sigma-Aldrich) and was sonicated four times for 30 s each in a Bioruptor Twin (Diagenode). Mice were given oral gavage of 200 µl tamoxifen emulsion per treatment. For injection of diphtheria toxin (DT), DT was dissolved in PBS and 200 µl of the appropriate dose was injected intraperitoneally into each mouse. For *in vivo* depletion of IL-2, mice were given tamoxifen by gavage on days 0 and 1 or on days 0, 3, 7 and 10 and were given intraperitoneal injection on days 4 and 8 of a 0.5mg 1:1 mixture of IL-2-neutralizing antibody (JES6-1A12 and S4B6-1; Bio X Cell) or IgG2a isotype-matched control antibody (Bio X Cell). For administration of IL-2–anti-IL2 complexes, 1 µg recombinant mouse IL-2 (R&D Systems) was incubated for 10 min at room temperature with 5 µg JES6-1 (Bio X Cell) and was diluted to a volume of 200 µl in PBS immediately before intraperitoneal injection. Mice were given tamoxifen by gavage on days 0, 3, 7 and 10 and received IL-2–

anti-IL-2 complexes or PBS on days 5, 7, 9 and 11. No animals were excluded from analyses. No statistical method was used to predetermine sample size. The experiments were not randomized. The investigators were not blinded to allocation during experiments or outcome assessment.

Flow cytometry staining and cell isolation

Cells were stained with LIVE/DEAD Fixable Yellow Dead Cell Stain (Molecular Probes) and the following antibodies: anti-CD4 (RM4-5), anti-CD8 (5H10), anti-TCRβ (H57-597); anti-CD44 (IM7), anti-CD62L (MEL-14), anti-CD25 (PC61), anti-CD27 (A7R34), anti-Foxp3 (FJK-16s), anti-CTLA-4 (UC10-4B9), anti-CD39 (24-DMS1), anti-CD73 (TY/11.8), anti-Ki67 (SolA15), anti-CD103 (2E7), anti-KLRG1 (2F1), anti-CCR6 (11A9), anti-CXCR3 (CXCR3-173), anti-GITR (DTA-1), anti-IRF4 (3E4), anti-Egr2 (Erongr2), anti-CD11a (2D7), anti-CD11a (M17/4), anti-IFNγ (XMG1.2), anti-IL4 (11B11), anti-IL13 (eBio13A), anti-IL5 (BD Biosciences), anti-IL2 (JES6-5H4). For BrdU experiments, mice were given intraperitoneal injection of 1 mg BrdU (5-bromodeoxyuridine) in 1 ml PBS and cells were stained with a BD Pharmingen BrdU Flow Kit. An LSR II flow cytometer (BD Bioscience) and FlowJo software (TreeStar) were used for flow cytometry. For cell isolation, $CD4^+$ T cells were purified from pooled spleen and lymph node cell suspensions with magnetic Dynabeads (Invitrogen) and were further sorted with a FACSAria II cell sorter (BD Bioscience). Intracellular staining was performed with eBioscience Fixation Permeabilization buffers. For cytokine staining, lymph node and spleen cells were stimulated for 4–6 h at 37 °C, 5% CO2, with soluble anti-CD3 (5 μg/ml; 2C11; Bio X Cell) and anti-CD28 (5 μg/ml; 37.51; Bio X Cell) in the presence of 1 μg/ml brefeldin A (Sigma).

In vitro proliferation assay

DC populations were expanded *in vivo* by subcutaneous injection of cytokine Flt3L–secreting B16 melanoma cells into the left hind flank of B6 mice. Once tumors were visible, spleens from injected mice were dissociated for 20 min at 37 °C, with shaking, in RPMI-1640 medium containing 1.67 units/ml Liberase TL (Roche) and 50 µg/ml DNase I (Roche). EDTA was added at a final concentration of 5 mM to stop digestion, and the resulting homogenate was processed for isolation of $CD11c^+$ cells with a MACS mouse CD11c (N418) purification kit (Miltenyi Biotec). $CD4^+eGFP^+$ cells purified by flow cytometry from tamoxifen-treated $Trac^{FL/WT}Foxp3^{Cre\text{-}ERT2}$ mice were labeled with CellTrace Violet according to the manufacturer's instructions (Molecular Probes) and were plated in triplicate in 96-well flat-bottomed plates (5×10^4 cells per well) in medium containing 25 U/ml human recombinant IL-2 (PeproTech) with or without equal numbers of DCs and with or without 100 ng/ml LPS (*Escherichia coli* strain 0111:B4, Sigma-Aldrich).

In vitro IL-2 stimulation and detection of phosphorylated STAT5

$Trac^{FL/WT}Foxp3^{Cre\text{-}ERT2}$ mice were treated with tamoxifen on days 0 and 1, and on day 9, $CD4^+$T cells were purified from pooled spleen and lymph node cell suspensions with magnetic Dynabeads (Invitrogen). Cells were stained with anti-CD4 (RM4-5; Tonbo Biosciences) and anti-TCRβ (H57-597; Tonbo Biosciences), then were washed and plated in 96-well V-bottomed plates (1×10^6 cells per well) in RPMI medium containing 10% FBS with or without increasing concentrations of IL-2, followed by incubation for 20 min at 37 °C. Cells were subsequently processed with BD Phosflow Lyse/Fix Buffer and

Perm Buffer III (BD Biosciences) and were stained with antibody to STAT5 phosphorylated at Tyr694 (47/Stat5; BD Biosciences) according to the manufacturer's instructions. Treg cells were identified by eGFP expression. For *ex vivo* staining of phosphorylated STAT5, spleen and lymph nodes were dissociated at 4 °C in PBS (0.5% BSA) containing anti-CD4 and anti-TCRβ (both identified above), were stained for 10 min on ice and were washed twice before fixation.

In vitro depletion of IL-2

Trac$^{FL/WT}$*Foxp3*$^{Cre\text{-}ERT2}$ mice were treated with tamoxifen on days 0 and 1, and on day 9, pooled spleens and lymph nodes were enriched for CD4$^+$ cells and subsequently sorted to a purity of >99% into eGFP$^+$TCRβ$^+$, eGFP$^+$TCRβ$^-$ and eGFP$^-$TCRβ$^+$ populations. Each population was divided among eight wells of a 96-well V-bottomed plate (2.5×10^5 cells/well) in 25 ul RPMI medium (10%) with or without increasing doses of recombinant human IL-2, followed by incubation for 2 h at 37 °C. Depletion of IL-2 from the medium was assessed with the BD Cytometric Bead Array and Human IL-2 Enhanced Sensitivity Flex Set according to the manufacturer's instructions (BD Biosciences).

In vitro conjugation assay

Trac$^{WT/WT}$*Foxp3*$^{Cre\text{-}ERT2}$, *Trac*$^{FL/WT}$*Foxp3*$^{Cre\text{-}ERT2}$ and *Trac*$^{FL/FL}$*Foxp3*$^{Cre\text{-}ERT2}$ mice were treated with tamoxifen on days 0 and 1, and on day 9, CD4$^+$ T cells were isolated from spleen and lymph nodes with the Dynabeads Untouched Mouse CD4 Cells negative selection kit (Invitrogen.) TCR$^+$ Treg cells were sorted from *Trac*$^{WT/WT}$*Foxp3*$^{Cre\text{-}ERT2}$ mice on the basis of eGFP expression alone. TCR$^-$ Treg cells were sorted from *Trac*$^{FL/WT}$*Foxp3*$^{Cre\text{-}ERT2}$ and *Trac*$^{FL/FL}$*Foxp3*$^{Cre\text{-}ERT2}$

mice as eGFP^{+}TCRβ^{-} cells. Treg cells were subsequently labeled with CFSE (carboxyfluorescein diacetate succinimidyl ester), and populations of DCs from mice with no deficiency or homozygous deficiency in MHC class II were expanded *in vivo* with Flt3L-secreting B16 melanoma cells and were labeled with CellTrace Violet. 1×10^4 Treg cells and 6×10^4 DCs were cultured together in a 96-well round-bottomed plate in RPMI medium 10% supplemented with 500 U/ml IL-2. Concanavalin A (C2010; Sigma) was used at a final concentration of 2.5 μg/ml. Following 10 h of culture at 37 °C, cells were gently resuspended before flow cytometry.

Gene-expression analysis

eGFP^{+} TCRβ^{+} and TCRβ^{-} CD44^{hi}CD62L^{lo} cell populations (two replicates) and CD44^{lo}CD62L^{hi} cell populations (three replicates) were sorted from tamoxifen-treated *Trac*$^{FL/WT}$*Foxp3*$^{Cre\text{-}ERT2}$ mice (five or more mice per replicate) with a FACS Aria II flow cytometer. Complementary DNA (cDNA) libraries were amplified and hybridized to Affymetrix 430 2.0 chips. Arrays were normalized by the robust multiarray average method, and genes were considered to have a difference in expression if they had a *q* value of <0.01 after Benjamini-Hochberg false-discovery rate correction. Differences in gene expression in Treg cells from *Foxp3*^{GFPKO} mice and *Foxp3*$^{+}$ mice has been described (Samstein et al., 2012).

References

Au-Yeung, B.B., Levin, S.E., Zhang, C., Hsu, L.Y., Cheng, D.A., Killeen, N., Shokat, K.M., and Weiss, A. (2010). A genetically selective inhibitor demonstrates a function for the kinase Zap70 in regulatory T cells independent of its catalytic activity. Nature immunology *11*, 1085-1092.

Borsellino, G., Kleinewietfeld, M., Di Mitri, D., Sternjak, A., Diamantini, A., Giometto, R., Hopner, S., Centonze, D., Bernardi, G., Dell'Acqua, M.L.*, et al.* (2007). Expression of ectonucleotidase CD39 by Foxp3+ Treg cells: hydrolysis of extracellular ATP and immune suppression. Blood *110*, 1225-1232.

Collison, L.W., Workman, C.J., Kuo, T.T., Boyd, K., Wang, Y., Vignali, K.M., Cross, R., Sehy, D., Blumberg, R.S., and Vignali, D.A. (2007). The inhibitory cytokine IL-35 contributes to regulatory T-cell function. Nature *450*, 566-569.

Colotta, F., Re, F., Muzio, M., Bertini, R., Polentarutti, N., Sironi, M., Giri, J.G., Dower, S.K., Sims, J.E., and Mantovani, A. (1993). Interleukin-1 type II receptor: a decoy target for IL-1 that is regulated by IL-4. Science *261*, 472-475.

Cretney, E., Xin, A., Shi, W., Minnich, M., Masson, F., Miasari, M., Belz, G.T., Smyth, G.K., Busslinger, M., Nutt, S.L., and Kallies, A. (2011). The transcription factors Blimp-1 and IRF4 jointly control the differentiation and function of effector regulatory T cells. Nature immunology *12*, 304-311.

Fisson, S., Darrasse-Jeze, G., Litvinova, E., Septier, F., Klatzmann, D., Liblau, R., and Salomon, B.L. (2003). Continuous activation of autoreactive CD4+ CD25+ regulatory T cells in the steady state. The Journal of experimental medicine *198*, 737-746.

Fontenot, J.D., Rasmussen, J.P., Gavin, M.A., and Rudensky, A.Y. (2005). A function for interleukin 2 in Foxp3-expressing regulatory T cells. Nature immunology *6*, 1142-1151.

Gavin, M.A., Clarke, S.R., Negrou, E., Gallegos, A., and Rudensky, A. (2002). Homeostasis and anergy of CD4(+)CD25(+) suppressor T cells in vivo. Nature immunology *3*, 33-41.

Gavin, M.A., Rasmussen, J.P., Fontenot, J.D., Vasta, V., Manganiello, V.C., Beavo, J.A., and Rudensky, A.Y. (2007). Foxp3-dependent programme of regulatory T-cell differentiation. Nature *445*, 771-775.

Hall, A.O., Beiting, D.P., Tato, C., John, B., Oldenhove, G., Lombana, C.G., Pritchard, G.H., Silver, J.S., Bouladoux, N., Stumhofer, J.S.*, et al.* (2012). The cytokines interleukin 27 and interferon-gamma promote distinct Treg cell populations required to limit infection-induced pathology. Immunity *37*, 511-523.

Hoelzinger, D.B., Smith, S.E., Mirza, N., Dominguez, A.L., Manrique, S.Z., and Lustgarten, J. (2010). Blockade of CCL1 inhibits T regulatory cell suppressive function enhancing tumor immunity without affecting T effector responses. Journal of immunology *184*, 6833-6842.

Hsieh, C.S., Lee, H.M., and Lio, C.W. (2012). Selection of regulatory T cells in the thymus. Nature reviews. Immunology *12*, 157-167.

Hsieh, C.S., Liang, Y., Tyznik, A.J., Self, S.G., Liggitt, D., and Rudensky, A.Y. (2004). Recognition of the peripheral self by naturally arising CD25+ CD4+ T cell receptors. Immunity *21*, 267-277.

Hsieh, C.S., Zheng, Y., Liang, Y., Fontenot, J.D., and Rudensky, A.Y. (2006). An intersection between the self-reactive regulatory and nonregulatory T cell receptor repertoires. Nature immunology *7*, 401-410.

Huang, C.T., Workman, C.J., Flies, D., Pan, X., Marson, A.L., Zhou, G., Hipkiss, E.L., Ravi, S., Kowalski, J., Levitsky, H.I.*, et al.* (2004). Role of LAG-3 in regulatory T cells. Immunity *21*, 503-513.

Josefowicz, S.Z., Lu, L.F., and Rudensky, A.Y. (2012). Regulatory T cells: mechanisms of differentiation and function. Annual review of immunology *30*, 531-564.

Kim, J.K., Klinger, M., Benjamin, J., Xiao, Y., Erle, D.J., Littman, D.R., and Killeen, N. (2009). Impact of the TCR signal on regulatory T cell homeostasis, function, and trafficking. PloS one *4*, e6580.

Kim, J.M., Rasmussen, J.P., and Rudensky, A.Y. (2007). Regulatory T cells prevent catastrophic autoimmunity throughout the lifespan of mice. Nature immunology *8*, 191-197.

Klein, U., Casola, S., Cattoretti, G., Shen, Q., Lia, M., Mo, T., Ludwig, T., Rajewsky, K., and Dalla-Favera, R. (2006). Transcription factor IRF4 controls plasma cell differentiation and class-switch recombination. Nature immunology *7*, 773-782.

Lathrop, S.K., Bloom, S.M., Rao, S.M., Nutsch, K., Lio, C.W., Santacruz, N., Peterson, D.A., Stappenbeck, T.S., and Hsieh, C.S. (2011). Peripheral education of the immune system by colonic commensal microbiota. Nature *478*, 250-254.

Lathrop, S.K., Santacruz, N.A., Pham, D., Luo, J., and Hsieh, C.S. (2008). Antigen-specific peripheral shaping of the natural regulatory T cell population. The Journal of experimental medicine *205*, 3105-3117.

Lee, H.M., Bautista, J.L., Scott-Browne, J., Mohan, J.F., and Hsieh, C.S. (2012). A broad range of self-reactivity drives thymic regulatory T cell selection to limit responses to self. Immunity *37*, 475-486.

Lin, W., Haribhai, D., Relland, L.M., Truong, N., Carlson, M.R., Williams, C.B., and Chatila, T.A. (2007). Regulatory T cell development in the absence of functional Foxp3. Nature immunology *8*, 359-368.

Man, K., Miasari, M., Shi, W., Xin, A., Henstridge, D.C., Preston, S., Pellegrini, M., Belz, G.T., Smyth, G.K., Febbraio, M.A.*, et al.* (2013). The transcription factor IRF4 is essential for TCR affinity-mediated metabolic programming and clonal expansion of T cells. Nature immunology *14*, 1155-1165.

Marson, A., Kretschmer, K., Frampton, G.M., Jacobsen, E.S., Polansky, J.K., MacIsaac, K.D., Levine, S.S., Fraenkel, E., von Boehmer, H., and Young, R.A. (2007). Foxp3 occupancy and regulation of key target genes during T-cell stimulation. Nature *445*, 931-935.

Ohkura, N., Hamaguchi, M., Morikawa, H., Sugimura, K., Tanaka, A., Ito, Y., Osaki, M., Tanaka, Y., Yamashita, R., Nakano, N.*, et al.* (2012). T cell receptor stimulation-induced epigenetic changes and Foxp3 expression are independent and complementary events required for Treg cell development. Immunity *37*, 785-799.

Ouyang, W., Liao, W., Luo, C.T., Yin, N., Huse, M., Kim, M.V., Peng, M., Chan, P., Ma, Q., Mo, Y.*, et al.* (2012). Novel Foxo1-dependent transcriptional programs control T(reg) cell function. Nature *491*, 554-559.

Pandiyan, P., Zheng, L., Ishihara, S., Reed, J., and Lenardo, M.J. (2007). CD4+CD25+Foxp3+ regulatory T cells induce cytokine deprivation-mediated apoptosis of effector CD4+ T cells. Nature immunology *8*, 1353-1362.

Petermann, K.B., Rozenberg, G.I., Zedek, D., Groben, P., McKinnon, K., Buehler, C., Kim, W.Y., Shields, J.M., Penland, S., Bear, J.E.*, et al.* (2007).

CD200 is induced by ERK and is a potential therapeutic target in melanoma. The Journal of clinical investigation *117*, 3922-3929.

Polic, B., Kunkel, D., Scheffold, A., and Rajewsky, K. (2001). How alpha beta T cells deal with induced TCR alpha ablation. Proceedings of the National Academy of Sciences of the United States of America *98*, 8744-8749.

Reinwald, S., Wiethe, C., Westendorf, A.M., Breloer, M., Probst-Kepper, M., Fleischer, B., Steinkasserer, A., Buer, J., and Hansen, W. (2008). CD83 expression in CD4+ T cells modulates inflammation and autoimmunity. Journal of immunology *180*, 5890-5897.

Rosenblum, M.D., Gratz, I.K., Paw, J.S., Lee, K., Marshak-Rothstein, A., and Abbas, A.K. (2011). Response to self antigen imprints regulatory memory in tissues. Nature *480*, 538-542.

Ruan, Q., Kameswaran, V., Tone, Y., Li, L., Liou, H.C., Greene, M.I., Tone, M., and Chen, Y.H. (2009). Development of Foxp3(+) regulatory t cells is driven by the c-Rel enhanceosome. Immunity *31*, 932-940.

Rubtsov, Y.P., Niec, R.E., Josefowicz, S., Li, L., Darce, J., Mathis, D., Benoist, C., and Rudensky, A.Y. (2010). Stability of the regulatory T cell lineage in vivo. Science *329*, 1667-1671.

Rubtsov, Y.P., Rasmussen, J.P., Chi, E.Y., Fontenot, J., Castelli, L., Ye, X., Treuting, P., Siewe, L., Roers, A., Henderson, W.R., Jr.*, et al.* (2008). Regulatory T cell-derived interleukin-10 limits inflammation at environmental interfaces. Immunity *28*, 546-558.

Samstein, R.M., Arvey, A., Josefowicz, S.Z., Peng, X., Reynolds, A., Sandstrom, R., Neph, S., Sabo, P., Kim, J.M., Liao, W.*, et al.* (2012). Foxp3 exploits a pre-existent enhancer landscape for regulatory T cell lineage specification. Cell *151*, 153-166.

Samy, E.T., Parker, L.A., Sharp, C.P., and Tung, K.S. (2005). Continuous control of autoimmune disease by antigen-dependent polyclonal CD4+CD25+ regulatory T cells in the regional lymph node. The Journal of experimental medicine *202*, 771-781.

Sawant, D.V., Sehra, S., Nguyen, E.T., Jadhav, R., Englert, K., Shinnakasu, R., Hangoc, G., Broxmeyer, H.E., Nakayama, T., Perumal, N.B.*, et al.* (2012). Bcl6 controls the Th2 inflammatory activity of regulatory T cells by repressing Gata3 function. Journal of immunology *189*, 4759-4769.

Shafiani, S., Dinh, C., Ertelt, J.M., Moguche, A.O., Siddiqui, I., Smigiel, K.S., Sharma, P., Campbell, D.J., Way, S.S., and Urdahl, K.B. (2013). Pathogen-specific Treg cells expand early during mycobacterium tuberculosis infection but are later eliminated in response to Interleukin-12. Immunity *38*, 1261-1270.

Smigiel, K.S., Richards, E., Srivastava, S., Thomas, K.R., Dudda, J.C., Klonowski, K.D., and Campbell, D.J. (2014). CCR7 provides localized access to IL-2 and defines homeostatically distinct regulatory T cell subsets. The Journal of experimental medicine *211*, 121-136.

Tang, Q., Adams, J.Y., Penaranda, C., Melli, K., Piaggio, E., Sgouroudis, E., Piccirillo, C.A., Salomon, B.L., and Bluestone, J.A. (2008). Central role of defective interleukin-2 production in the triggering of islet autoimmune destruction. Immunity *28*, 687-697.

Thornton, A.M., and Shevach, E.M. (1998). CD4+CD25+ immunoregulatory T cells suppress polyclonal T cell activation in vitro by inhibiting interleukin 2 production. The Journal of experimental medicine *188*, 287-296.

Tian, L., Altin, J.A., Makaroff, L.E., Franckaert, D., Cook, M.C., Goodnow, C.C., Dooley, J., and Liston, A. (2011). Foxp3(+) regulatory T cells exert asymmetric control over murine helper responses by inducing Th2 cell apoptosis. Blood *118*, 1845-1853.

Wan, Y.Y., and Flavell, R.A. (2007). Regulatory T-cell functions are subverted and converted owing to attenuated Foxp3 expression. Nature *445*, 766-770.

Webster, K.E., Walters, S., Kohler, R.E., Mrkvan, T., Boyman, O., Surh, C.D., Grey, S.T., and Sprent, J. (2009). In vivo expansion of T reg cells with IL-2-mAb complexes: induction of resistance to EAE and long-term acceptance of islet allografts without immunosuppression. The Journal of experimental medicine *206*, 751-760.

Williams, L.M., and Rudensky, A.Y. (2007). Maintenance of the Foxp3-dependent developmental program in mature regulatory T cells requires continued expression of Foxp3. Nature immunology *8*, 277-284.

Wing, K., Onishi, Y., Prieto-Martin, P., Yamaguchi, T., Miyara, M., Fehervari, Z., Nomura, T., and Sakaguchi, S. (2008). CTLA-4 control over Foxp3+ regulatory T cell function. Science *322*, 271-275.

Zheng, Y., Chaudhry, A., Kas, A., deRoos, P., Kim, J.M., Chu, T.T., Corcoran, L., Treuting, P., Klein, U., and Rudensky, A.Y. (2009). Regulatory T-cell suppressor program co-opts transcription factor IRF4 to control T(H)2 responses. Nature *458*, 351-356.

Zheng, Y., Josefowicz, S., Chaudhry, A., Peng, X.P., Forbush, K., and Rudensky, A.Y. (2010). Role of conserved non-coding DNA elements in the Foxp3 gene in regulatory T-cell fate. Nature *463*, 808-812.

Zou, T., Satake, A., Corbo-Rodgers, E., Schmidt, A.M., Farrar, M.A., Maltzman, J.S., and Kambayashi, T. (2012). Cutting edge: IL-2 signals determine the degree of TCR signaling necessary to support regulatory T cell proliferation in vivo. Journal of immunology *189*, 28-32.

CHAPTER 3

SUPPRESSION OF LETHAL AUTOIMMUNITY BY REGULATORY T CELLS WITH A SINGLE TCR SPECIFICITY*

Abstract

The regulatory T (Treg) cell T cell receptor (TCR) repertoire is highly diverse and skewed towards recognition of self-antigens. In addition to an essential role of certain high affinity TCR-ligand interactions for Treg cell differentiation, TCR expression by Treg cells is continuously required for maintenance of immune tolerance and for a major part of their characteristic gene expression features; however, it remains unknown to what degree diverse TCR-mediated interactions between Treg cells and their cognate self-antigens are required for these processes. Here, by experimentally switching the developmentally selected TCR repertoire to a single, previously characterized Treg cell TCR we demonstrate that to a significant extent, Treg cell function can be uncoupled from Treg cell specificity and diversity. A monoclonal Treg cell pool exhibited essentially the full spectrum of TCR-dependent gene expression imparted by a diverse Treg cell TCR repertoire and was capable of suppressing lethal autoimmunity and T_H2 and T_H17, but not T_H1, activation that occurs in the absence of TCR on Treg cells. Although mice harboring Treg cells expressing predominantly this single TCR still displayed marked immune cell activation and tissue inflammation, our study suggests that Treg cells can exert

---

* Adapted from Levine, A.G., Hemmers, S., Schizas, M., Faire, M.B., Moltedo, B., Konapacki, K., Treuting, P.M., and Rudensky, A.Y. Suppression of lethal autoimmunity by regulatory T cells with a single TCR specificity. (*submitted*).

significant suppressor functions independently of specific interactions with developmentally selected cognate antigens.

Introduction

Increased thymic generation of regulatory T cells resulting from co-expression of transgene-encoded T cell receptors (TCR) and their cognate ligands provided the first experimental evidence that Treg cell differentiation is dependent upon self-antigen recognition in the thymus (Jordan et al., 2001). Transgene-driven expression of naturally occurring Treg cell-derived TCRs, however, has been found to yield few Treg cells with the majority of transgenic TCR-expressing cells differentiating into conventional CD4 T cells (Bautista et al., 2009; Leung et al., 2009). This feature of Treg cell differentiation, ascribed to a profound intra-clonal competition amongst thymic Treg cell precursors, implies a stringent requirement for TCR diversity during Treg cell differentiation. Antigen presentation in the periphery is thought to mirror the thymus (Anderson et al., 2002), and analogously, limiting amounts of tissue-specific self-antigens presented in draining lymph nodes likely maintain the activation status of small numbers of antigen specific Treg cells (Leventhal et al., 2016; Samy et al., 2005). Nevertheless, it remains unknown whether diverse Treg cell specificities molded through recognition of a wide range of endogenous antigens during the differentiation process, are required for restraining a broad spectrum of autoimmune and inflammatory lesions that Treg cells normally control.

Recently, we and others demonstrated that the Treg cell TCR controls expression of a large number of genes in activated Treg cells and is required for suppressor function such that TCR loss in Foxp3-expressing Treg cells

results in spontaneous immune activation and an early onset, highly aggressive fatal lymphoproliferative disease comparable to that observed in Foxp3-deficient mice lacking Treg cells (Levine et al., 2014; Vahl et al., 2014). However, these previous studies left open a question of which TCR-dependent gene expression features might be exhibited by Treg cells expressing just a few, or even a single TCR specificity, and whether these cells might afford any measure of protection against systemic fatal lymphoproliferative disease and tissue pathology. Alternatively, there may be an absolute requirement for a diverse Treg TCR repertoire comprised of developmentally selected specificities for maintenance of the full spectrum of gene expression and suppressor function.

In this regard, we recently reported that loss of TCRs within a lower affinity range for self-ligands in the developing Treg cell population in the absence of the intronic *Foxp3* enhancer CNS3, had a mild effect on immune activation status without detectable clinical manifestations of autoimmunity suggesting that a reduced Treg cell repertoire with 'holes' was largely sufficient to support the bulk of Treg cell suppressor function (Feng et al., 2015). On the other hand, the severe autoimmunity apparent in mice with a combined deficiency in CNS3 and the autoimmune regulator (*Aire*) gene, which among other functions facilitates elimination of tissue-restricted antigen-specific effector T cells and differentiation of Treg cells of corresponding specificities in the thymus, as well as other observations, suggest an important role for Treg cell TCR specificities in establishing tolerance early in life (Feng et al., 2015; Malchow et al., 2016; Samy et al., 2005; Yang et al., 2015).

Efforts to directly address the role of TCR diversity and specificity for Treg cell function through the use of TCR transgenic mice have been impeded

by an inevitable concomitant severe skewing of the effector CD4 T cell repertoire. Thus, while in some RAG-deficient TCR transgenic mice antigen-specific Treg cells can keep in check effector T cells of the same specificity and prevent pathology (Killebrew et al., 2011; Lin et al., 2016), it is unknown whether a monoclonal Treg cell population can suppress a naturally diverse effector T cell pool. Here, we addressed this question by exploring whether lethal autoimmunity exerted by a diverse effector T cell population upon the loss of Treg cell function can be restrained by Treg cells subjected to inducible skewing of their developmentally selected TCR repertoire to a single endogenous Treg cell-derived TCR. Unexpectedly, in the presence of Treg cells expressing a single TCR we observed lasting, even if incomplete, protection from lethal disease resulting from complete ablation of the TCR in Treg cells, with diminished T cell activation and T_H2 and T_H17 cytokine production in select secondary lymphoid organs. Moreover, expression of this single TCR also rescued essentially the entire gene signature imparted by a diverse Treg cell TCR repertoire. These results indicate that the TCR-dependent suppressor capacity of Treg cells to a considerable degree can be uncoupled from their developmentally established TCR-dependent recognition of diverse endogenous antigens.

Results

Monoclonal G113 TCR$^+$ Treg cells suppress a diverse effector T cell pool

To directly assess the role of Treg cell TCR diversity in driving suppressor function we took advantage of the previously characterized Treg cell-derived $V\beta6^+V\alpha2^+$ G113 TCR. The G113 TCR, originally cloned out the $CD4^+CD25^+$ cell pool in TCli TCRβ-expressing *Tcra*$^{+/-}$ mice, is a typical Treg cell TCR in

that it induces strong signaling as well as proliferation and expansion when expressed in T cells in *in vivo* transfer experiments, but when expressed as a transgene on a RAG-deficient background generates a preponderance of conventional CD4 T cells and few Foxp3^{+} thymocytes (Hsieh et al., 2004; Hsieh et al., 2006; Moran et al., 2011). Expression of the G113Tg on a RAG-sufficient background results in highly efficient allelic exclusion of the endogenous *Tcrb* locus such that ~95% of Treg cells in G113Tg mice exclusively express the transgenic Vβ6^{+} TCRβ-chain. Accordingly, as compared to Treg cells in non-G113Tg-expressing mice, Foxp3^{+} cells in G113Tg mice demonstrated minimal staining for endogenous TCRβ chains expressing Vβ5, Vβ8.1/2, Vβ11, Vβ12, and Vβ13 (Figure 3.1). In contrast, less than half of Treg cells expressed the Vα2^{+} TCRα transgene (see Figure 3.4A). As a result, the majority of Treg cells in these mice are selected by TCRs composed of the transgenic Vβ6^{+} TCRb chain paired with an endogenous TCRα chain. To enable replacement of diverse TCRs resulting from endogenous *Tcra* locus rearrangements with predominantly the single transgenic G113 TCR after Foxp3 induction, i.e. Treg cell lineage commitment, we generated G113Tg*Foxp3*$^{YFP\text{-}Cre}$*Tcra*$^{FL/FL}$ mice on a RAG-sufficient background (Figure 3.1 and Figure 3.2A). In these mice, Foxp3 expression in developing Treg cells resulted in Cre recombinase-mediated ablation of the endogenous *Tcra* locus, leaving only the G113 Vα2^{+} TCRα chain to pair with transgenic TCRβ (Figure 3.1 and Figure 3.2A). Thus, in G113Tg*Foxp3*$^{YFP\text{-}Cre}$*Tcra*$^{FL/FL}$ mice, Treg cells were thymically generated in physiologic numbers via expression of endogenous TCRs that recognize endogenous ligands, while the peripheral Treg cell compartment was overwhelmingly of a single, monoclonal specificity. Unique to this experimental set-up was the retention of

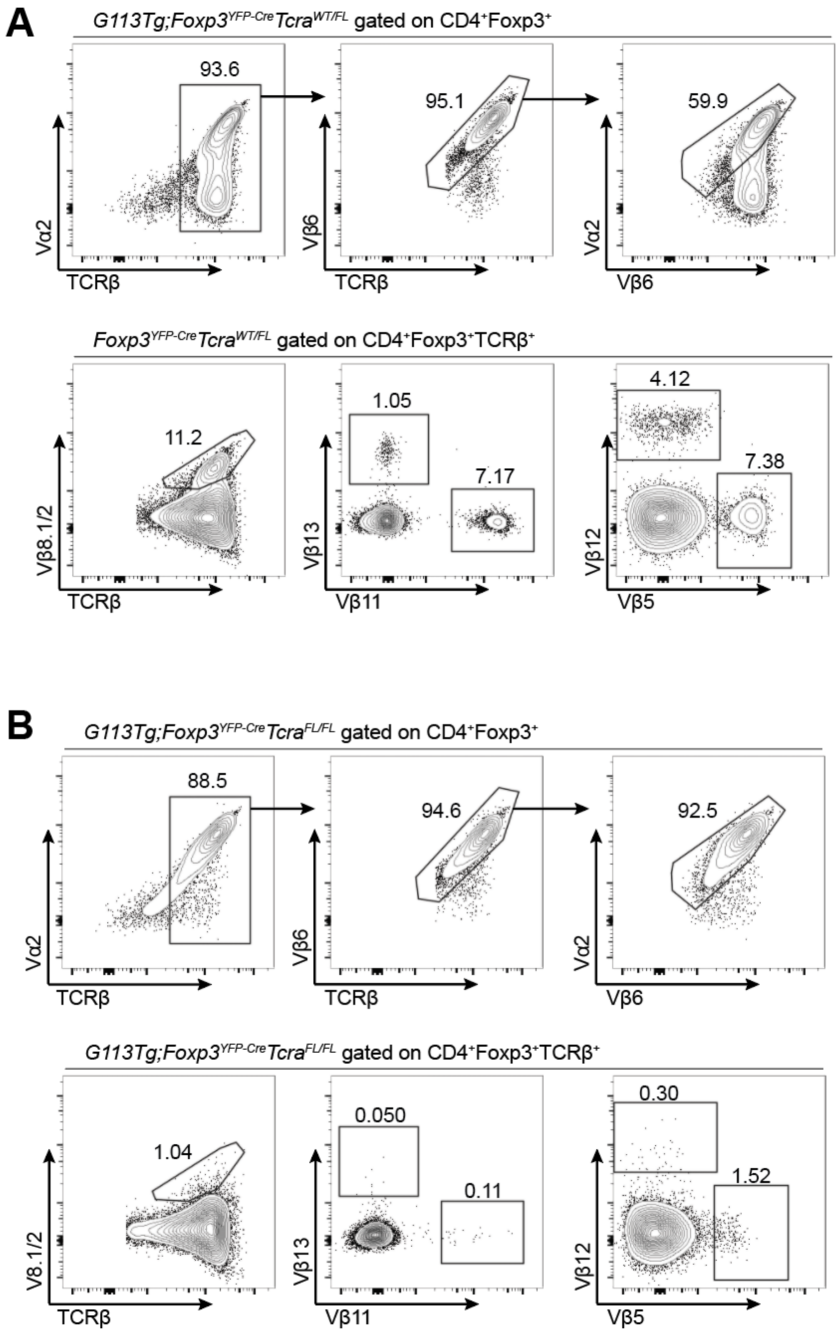

Figure 3.1. Monoclonal expression of the G113 TCR in Treg cells. Mice of the indicated genotypes were analyzed at 2.5 weeks of age. **A-B,** Representative flow cytometry plots of TCR Vα and Vβ usage in $CD4^+Foxp3^+$ (**A**,**B** above) and $CD4^+Foxp3^+TCR\beta^+$ (**A**,**B** below) lymph node cells in the indicated mice. Further gating of indicated cellular subsets is indicated by arrows. Data are representative of several independent experiments.

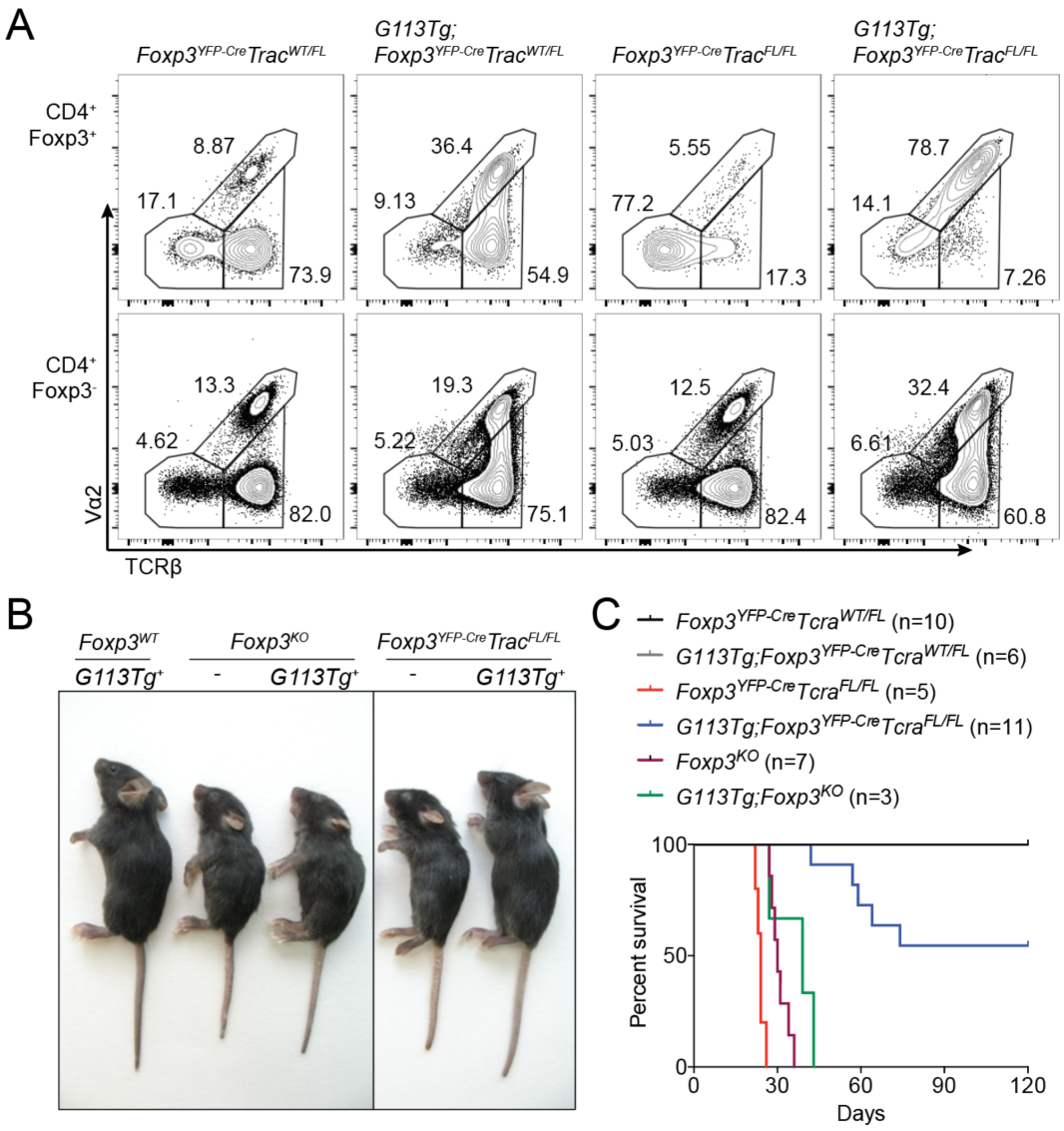

Figure 3.2. Monoclonal G113 TCR expressing Treg cells suppress autoimmune disease mediated by a polyclonal effector T cell population. Mice of the indicated genotypes were analyzed at 2.5 weeks of age. **A**, Representative flow cytometric analysis of lymph node $CD4^+Foxp3^+$ (above) and $CD4^+Foxp3^-$ (below) cells in mice of the indicated genotypes. **B**, Representative mice of the indicated genotypes. **C**, Survival curve for the indicated mice. The data shown represent the combined results of several independent experiments.

significant diversity in the effector T cell population with the majority of effector $CD4^+$ T cells expressing endogenously rearranged TCRα chains (Figure 3.2A).

As we previously reported, all *Foxp3*$^{YFP\text{-}Cre}$*Tcra*$^{FL/FL}$ mice suffered from an early onset lethal autoimmunity characterized by runting and scaly skin, and did not survive past four weeks of age (Figure 3.2B,C) (Levine et al., 2014). Unexpectedly, G113Tg*Foxp3*$^{YFP\text{-}Cre}$*Tcra*$^{FL/FL}$ mice were entirely indistinguishable from control mice bearing normal populations of Treg cells during the first weeks of life (Figure 3.2B). Although by six weeks of age some G113Tg*Foxp3*$^{YFP\text{-}Cre}$*Tcra*$^{FL/FL}$ mice began to show signs of decreased weight gain and variable skin disease and ultimately succumbed to disease, a number of mice continued to show minimal signs of autoimmunity. A striking 50% of mice survived out to 4 months of age—the end point of the experiment—at which point all mice displayed evidence of significant autoimmunity (Figure 3.2C, data not shown).

Consistent with overall increased survival, histological analysis of several tissues demonstrated a widespread but mild diminution of pathology in G113Tg*Foxp3*$^{YFP\text{-}Cre}$*Tcra*$^{FL/FL}$ compared to *Foxp3*$^{YFP\text{-}Cre}$*Tcra*$^{FL/FL}$ mice (data not shown). Critically, these effects did not appear to be the consequence of limited autoreactivity due to G113Tg expression on the effector T cell compartment, as G113Tg*Foxp3*^{KO} mice suffered from lethal autoimmunity largely indistinguishable from that of *Foxp3*^{KO} mice lacking the TCR transgene (Figure 3.2B,C and data not shown) (Fontenot et al., 2003). This result indicates that rescue of disease in G113Tg*Foxp3*$^{YFP\text{-}Cre}$*Tcra*$^{FL/FL}$ mice was due to effects of transgenic TCR expression specifically in the Treg cell compartment.

Indeed, the G113Tg in G113Tg*Foxp3*$^{YFP\text{-}Cre}$*Tcra*$^{FL/FL}$ mice fully rescued percentages and proliferation (as assess by Ki67 staining) of lymph node Treg cells, significantly rescued effector differentiation as assessed by CD44 and CD62L expression, and restored cell surface expression of the receptor IL1R2, among others (Figure 3.3A). Lymph node effector CD4 T cell activation was correspondingly diminished, with decreased percentages of CD44^{hi} and IL-4-, IL-13, and IL-17- but not IFNγ- or IL-2-producing cells (Figure 3.3B). In the spleen, however, where rescue of Treg cell percentages was modest (Figure 3.3C), effector T cell activation was not lessened (data not shown). T cell activation and cytokine production was similar between *Foxp3*^{KO} and G113Tg*Foxp3*^{KO} mice in both spleens and lymph nodes, further ruling out a dominant role for the G113Tg in decreasing T cell activation (data not shown). Thus, the degree of G113Tg-mediated Treg cell rescue correlated with the degree of suppression of effector T cell activation. This further supported an essential role of G113 TCR-expressing Treg cells in down-modulating autoimmunity in G113Tg*Foxp3*$^{YFP\text{-}Cre}$*Tcra*$^{FL/FL}$ mice.

Inducible replacement of the diverse TCR repertoire with the G113 TCR in mature Treg cells

Given that Treg cells undergo TCR-dependent maturation in the periphery we sought to test whether mature Treg cells, which had seeded the spleen and tissues, subjected to inducible replacement of their TCRs with the G113 TCR remained functionally competent or would still be partially impaired in their ability to control immune activation, like Treg cells in *Foxp3*^{CreERT2}*Tcra*$^{FL/FL}$ mice (Levine et al., 2014). Therefore, we generated G113Tg*Foxp3*^{CreERT2}*Tcra*$^{FL/FL}$ mice to enable the switch of endogenous Treg

Figure 3.3. The monoclonal G113 TCR rescues Treg cell activation and suppresses T cell activation in lymph nodes.

Mice of the indicated genotypes were analyzed at 2.5 weeks of age. **A**, Percent Foxp3$^+$ cells among CD4$^+$ cells (top); and percent Ki-67$^+$ (second from top), percent CD44^{hi}CD62L^{lo} (second from bottom) and IL1R2$^+$ (bottom) cells among Foxp3$^+$ cells in the lymph nodes of *Foxp3*$^{YFP\text{-}Cre}$*Tcra*$^{WT/FL}$ (black circles), G113Tg*Foxp3*$^{YFP\text{-}Cre}$*Trac*$^{WT/FL}$ (gray circles), *Foxp3*$^{YFP\text{-}Cre}$*Trac*$^{FL/FL}$ (red circles), and G113Tg*Foxp3*$^{YFP\text{-}Cre}$*Trac*$^{FL/FL}$ (blue circles) mice. **B**, CD4$^+$Foxp3$^-$ T cell activation and cytokine production in lymph nodes of the indicated mice. **C**, The percent Foxp3$^+$ of CD4$^+$ T cells in spleens of the indicated mice. Each circle represents an individual mouse; the horizontal bars represent mean value; *p* values were calculated using Student's *t* test (***, **, and * denotes *p* values <0.001, 0.01, and 0.05, respectively; ns – not significant); the data shown represent the combined results of several independent experiments.

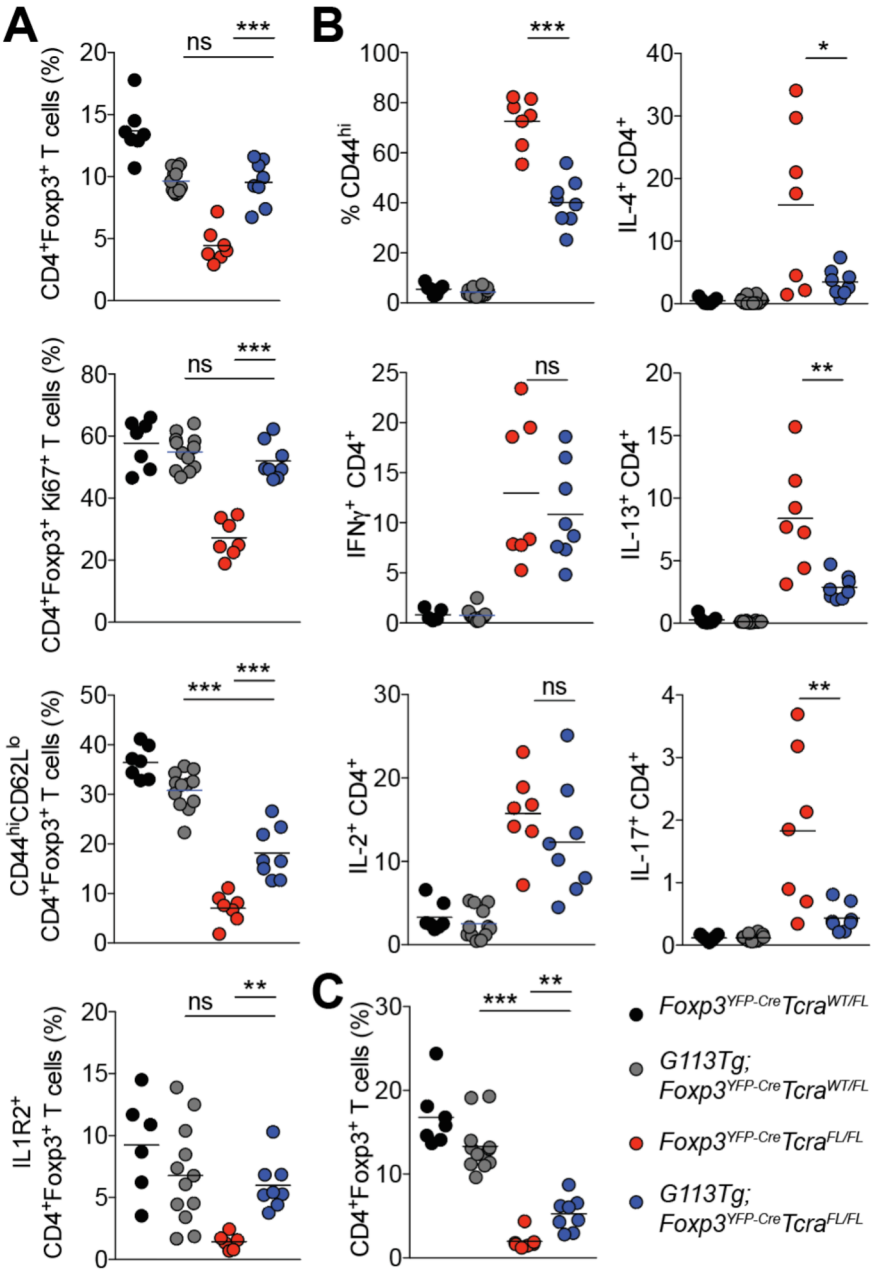
A
B
C
CD4+Foxp3+ T cells (%)
CD4+Foxp3+ Ki67+ T cells (%)
CD44hiCD62Llo CD4+Foxp3+ T cells (%)
IL1R2+ CD4+Foxp3+ T cells (%)
% CD44hi
IFNγ+ CD4+
IL-2+ CD4+
IL-4+ CD4+
IL-13+ CD4+
IL-17+ CD4+
CD4+Foxp3+ T cells (%)
ns
***
**
*
Foxp3YFP-CreTcraWT/FL
G113Tg; Foxp3YFP-CreTcraWT/FL
Foxp3YFP-CreTcraFL/FL
G113Tg; Foxp3YFP-CreTcraFL/FL

cell TCRs in mature Treg cells in adult mice for the G113 TCR in a tamoxifen-inducible manner (Figure 3.4A). Two weeks of tamoxifen administration to G113Tg*Foxp3*^{CreERT2}*Trac*$^{FL/FL}$ mice resulted in clear increases in immune activation compared to control G113Tg*Foxp3*^{CreERT2}*Trac*$^{WT/WT}$ mice (Figure 3.4B-D). This result indicates that the G113 TCR was not sufficient to impart full TCR-dependent Treg cell function in the periphery, even in a normally differentiated and localized Treg cell population.

We turned to an *in vivo* adoptive transfer approach to enable a more stringent assessment for suppressor activity of Treg cells whose diverse TCRs had been inducibly switched to the G113 TCR in comparison to Treg cells expressing diverse TCRs and Treg cells subjected to TCR ablation. We FACS-sorted bulk Treg cells from *Foxp3*^{CreERT2}*Trac*$^{WT/WT}$ mice (control); Vβ6^{+} Treg cells from G113Tg*Foxp3*^{CreERT2}*Trac*$^{WT/WT}$ mice; G113^{+} (Vβ6^{+}Vα2^{+}) Treg cells from G113Tg*Foxp3*^{CreERT2}*Trac*$^{FL/FL}$ mice; and TCR-deficient (TCRβ^{-}) Treg cells from *Foxp3*^{CreERT2}*Trac*$^{FL/FL}$ mice. All groups of mice in these experiments were subjected to identical tamoxifen treatment. Sorted cells were transferred together with pre-activated effector CD4^{+} T cells isolated from Treg cell-depleted CD45.1^{+}*Foxp3*^{DTR} mice into T cell-deficient *Tcrb/Tcrd*^{KO} recipients analyzed four weeks after transfer (Figure 3.5A). In agreement with the markedly diminished disease observed in G113Tg*Foxp3*$^{YFP\text{-}Cre}$*Trac*$^{FL/F}$ mice, co-transfer of G113^{+} Treg cells but not of TCR-deficient Treg cells substantially decreased parameters of immune activation including lymphadenopathy, CD4^{+} T cell numbers, and IFNγ production in lymph nodes but not in spleens of recipient mice (Figure 3.5B,C). These results confirm the capacity of monoclonal G113^{+} Treg cells to exert remarkable, but incomplete suppressor

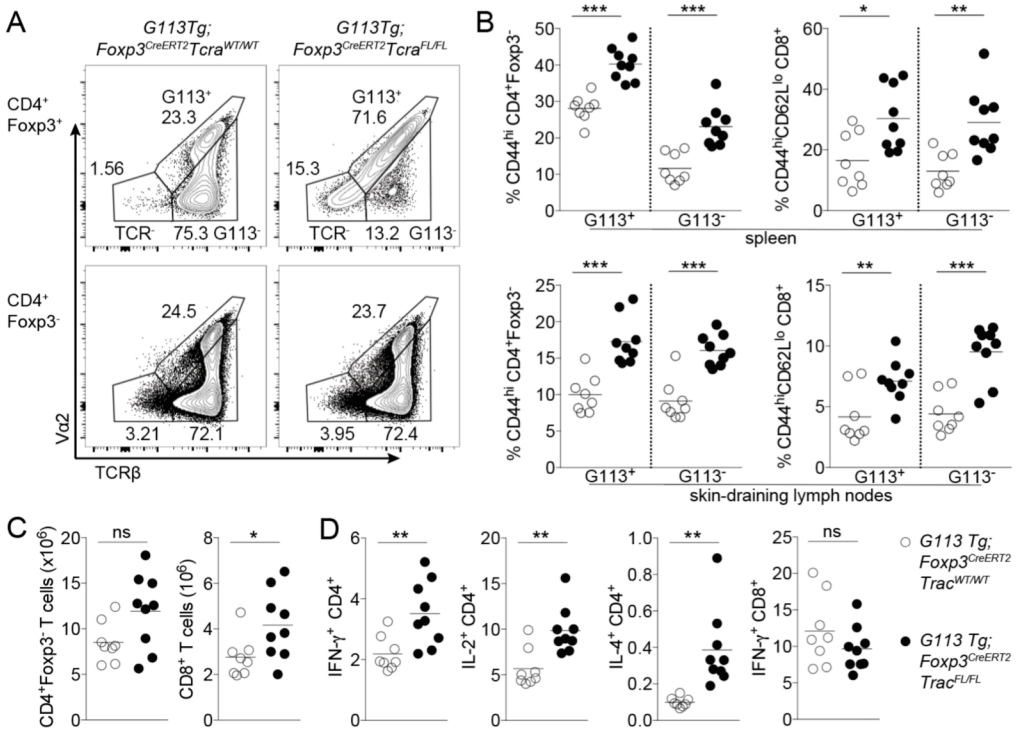

Figure 3.4. Inducible replacement of the diverse TCR repertoire with the G113 TCR in mature Treg cells.
G113Tg*Foxp3*^{CreERT2}*Trac*$^{WT/WT}$ and G113Tg*Foxp3*^{CreERT2}*Trac*$^{FL/FL}$ mice were treated with tamoxifen on days 0, 3, 7, and 10 and analyzed on day 13. **A**, Representative flow cytometric analyses of lymph node CD4$^+$Foxp3$^+$ (above) and CD4$^+$Foxp3$^-$ (below) cells in G113Tg*Foxp3*^{CreERT2}*Trac*$^{WT/WT}$ (left) and G113Tg*Foxp3*^{CreERT2}*Trac*$^{WT/WT}$ (right) mice. **B**, CD4$^+$Foxp3$^-$ (right) and CD8$^+$ (left) T cell activation in spleens (above) and lymph nodes (below) of G113Tg*Foxp3*^{CreERT2}*Trac*$^{WT/WT}$ (white circles) and G113Tg*Foxp3*^{CreERT2}*Trac*$^{WT/WT}$ (black circles) mice. CD4$^+$Foxp3$^-$ and CD8$^+$ cells were further gated as either Vβ6Vα2$^+$ (G113$^+$) or Vβ6Vα2$^-$ (G113$^-$) cells. **C-D**, T cell numbers in lymph nodes (**C**) and cytokine production in spleens (**D**) of mice of the indicated genotypes.

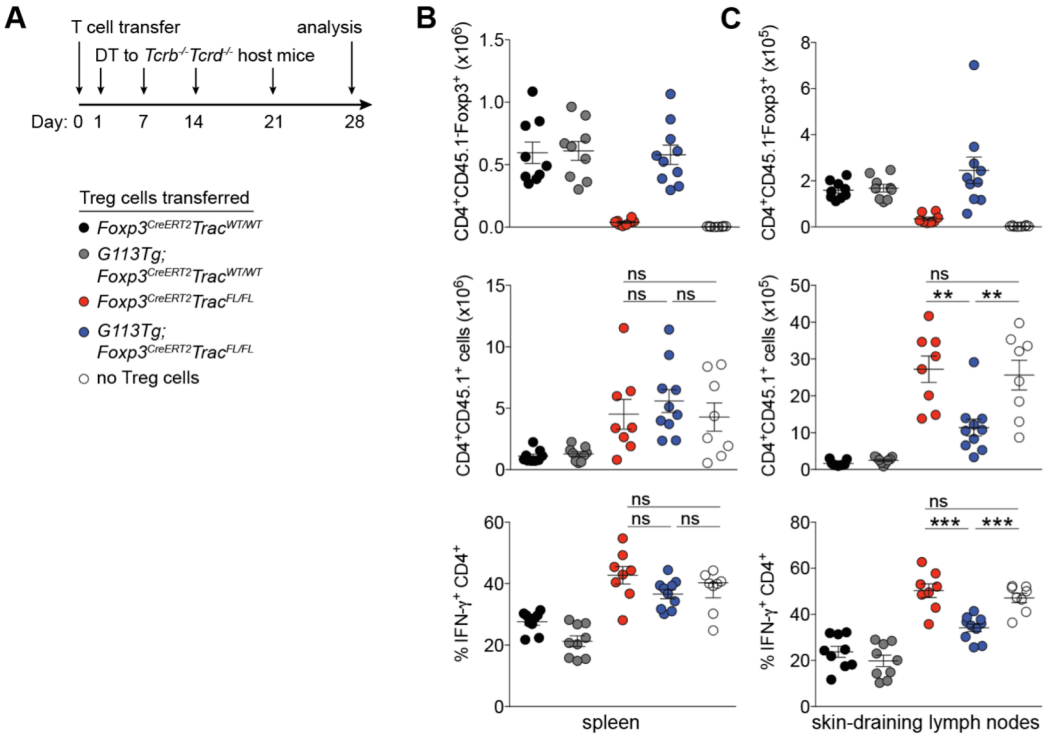

Figure 3.5. Inducible replacement of the diverse TCR repertoire with the G113 TCR in mature Treg cells supports Treg cell function.
A, Schematic of the experiment. Treg cells were sorted from the following mice on day 0 after tamoxifen administration on days -7 and -6: bulk Treg cells from *Foxp3*^{CreERT2}*Tcra*$^{WT/WT}$ mice (black circles), Vβ6^{+} Treg cells from G113Tg*Foxp3*^{CreERT2}*Tcra*$^{WT/WT}$ mice (gray circles), TCRβ^{-} Treg cells from *Foxp3*^{CreERT2}*Tcra*$^{FL/FL}$ mice (red circles), and Vβ6Vα2^{+} Treg cells from G113Tg*Foxp3*^{CreERT2}*Tcra*$^{FL/FL}$ mice (blue circles.) CD4^{+} effector T cells were isolated on day 0 from CD45.1^{+}*Foxp3*^{DTR} mice treated with diptheria toxin on days -5, -4, and -1. On day 0, Treg cells and effector CD4^{+} T cells were transferred into *Tcrb*$^{-/-}$*Tcrd*$^{-/-}$ mice subsequently maintained on weekly doses of diptheria toxin until analysis on day 28. **B-C**, Numbers of CD45.2^{+}CD4^{+}Foxp3^{+} Treg cells (top) and CD45.1^{+}CD4^{+}Foxp3^{-} cells (middle) and percent IFNγ^{+} CD45.1^{+}CD4^{+} cells in spleens (**B**) and skin-draining lymph nodes (**C**) in *Tcrb*$^{-/-}$ *Tcrd*$^{-/-}$ mice transferred with CD45.1^{+}CD4^{+} effector cells and either no Treg cells or Treg cell populations as described in (**A**). Each circle represents an individual mouse; the horizontal bars represent mean value; *p* values were calculated using Student's *t* test (***, **, and * denotes *p* values <0.001, 0.01, and 0.05, respectively; ns – not significant); the data shown represent the combined results of two independent experiments with at least four mice per group each.

activity in comparison to a Treg cell population expressing a diverse TCR repertoire. These observations raised a question of whether the inability of Treg cells expressing a single TCR to fully control immune activation was due to its inability to impart a complete range of TCR-dependent gene expression or rather was due to limiting TCR ligand-driven activation restricted to specific local settings.

Rescue of the Treg cell TCR-dependent gene signature by monoclonal G113 TCR expression

Previously, we used microarray gene expression analysis to identify a set of TCR-dependent genes expressed in effector $CD44^{hi}CD62L^{lo}$ Treg cells (155 genes down- and 5 genes up-regulated with a 2-fold cut-off upon TCR ablation) and in $CD44^{lo}CD62L^{hi}$ naïve Treg cells (16 genes down- and 1 gene up by 2-fold in the absence of TCR) (Levine et al., 2014). In that study, analysis of TCR-sufficient and -deficient Treg cells sorted from healthy, tamoxifen-treated *Foxp3*^{CreERT2}*Trac*$^{FL/WT}$ mice, which due to allelic exclusion at the *Tcra* locus harbored both Treg cell subsets, showed that TCR dependent gene expression accounted for ~25% of the gene signature specific to activated Treg cells. In order to address the major question of whether a single TCR specificity can enable a full or only partial spectrum of Treg cell gene expression, we performed RNA-seq analysis on effector and naïve TCR^{+} and TCR^{-} Treg cells from *Foxp3*^{CreERT2}*Trac*$^{FL/WT}$ mice as well as effector and naïve TCR^{+} and TCR^{-} Treg cells from immune activated *Foxp3*^{CreERT2}*Trac*$^{FL/FL}$ mice. We also performed similar analysis for effector and naïve Treg cells isolated from tamoxifen-treated G113Tg*Foxp3*^{CreERT2}*Trac*$^{WT/WT}$ and G113Tg*Foxp3*^{CreERT2}*Trac*$^{FL/FL}$ mice.

We defined an extensive set of potentially functionally important TCR-dependent genes as all genes significantly under- or over-expressed in effector and naïve TCR-deficient Treg cells from *Foxp3*^{CreERT2}*Trac*$^{FL/FL}$ mice compared to TCR-sufficient Treg cells from healthy *Foxp3*^{CreERT2}*Trac*$^{FL/WT}$ mice. We reasoned that the identified genes encompassed strictly TCR-dependent transcripts, whose expression could not be rescued by TCR-independent inputs resulting from the immune activation and inflammation observed in *Foxp3*^{CreERT2}*Trac*$^{FL/FL}$ mice. Our RNA-seq analysis revealed a comprehensive set of 1,238 genes that were down- and 1,088 genes that were up-regulated in effector Treg cells in the absence of TCR; and 484 genes that were down- and 389 genes that were up-regulated in naïve Treg cells in the absence of TCR. We next determined the extent to which changes in expression of these genes induced upon TCR ablation in effector and naïve Treg cells could be rescued upon expression of the G113 TCR transgene alone in G113Tg*Foxp3*^{CreERT2}*Tcra*$^{FL/FL}$ mice compared to G113 TCR transgene expression in combination with diverse endogenously rearranged TCRs in G113Tg*Foxp3*^{CreERT2}*Tcra*$^{WT/WT}$ mice.

Strikingly, the monoclonal G113 Treg cell-derived TCR was able to support expression of the vast majority of genes whose expression was found to be TCR-dependent in Treg cells expressing a diverse TCR repertoire (Figure 3.6A,B). Of the 1,238 genes we identified as up-regulated in a TCR dependent manner in effector Treg cells, expression of 1008 (81%) was fully rescued by expression of the monoclonal G113 TCR in G113Tg*Foxp3*^{CreERT2}*Tcra*$^{FL/FL}$ when compared to polyclonal Treg cells from

Figure 3.6. Rescue of the polyclonal TCR-dependent gene signature in Treg cells upon expression of the monoclonal G113 TCR.
A-B. *Foxp3*^{CreERT2}*Trac*$^{FL/WT}$, *Foxp3*^{CreERT2}*Trac*$^{FL/FL}$, G113Tg*Foxp3*^{CreERT2}*Trac*$^{WT/WT}$, and G113Tg*Foxp3*^{CreERT2}*Trac*$^{FL/FL}$ mice were treated with tamoxifen on days 0, 1, and 7 and on day 9 the following populations were sorted from the indicated mice: CD44^{hi}CD62L^{lo} and CD44^{lo}CD62L^{hi} TCRβ^{+} and TCRβ^{-} Treg cells from *Foxp3*^{CreERT2}*Trac*$^{FL/WT}$ mice; CD44^{hi}CD62L^{lo} and CD44^{lo}CD62L^{hi} TCRβ^{+} and TCRβ^{-} Treg cells from *Foxp3*^{CreERT2}*Trac*$^{FL/FL}$ mice; CD44^{hi}CD62L^{lo} and CD44^{lo}CD62L^{hi} Vβ6^{+} Treg cells from G113Tg*Foxp3*^{CreERT2}*Trac*$^{WT/WT}$ mice; and CD44^{hi}CD62L^{lo} and CD44^{lo}CD62L^{hi} Vβ6Vα2^{+} Treg cells from G113Tg*Foxp3*^{CreERT2}*Trac*$^{FL/FL}$ mice. **A**, Genes significantly up-regulated (left) or down-regulated (right) in CD44^{hi}CD62L^{lo} (above) and CD44^{lo}CD62L^{hi} (below) TCRβ^{+} Treg cells in *Foxp3*^{CreERT2}*Trac*$^{WT/FL}$ mice compared to TCRβ^{-} Treg cells in *Foxp3*^{CreERT2}*Trac*$^{FL/FL}$ mice were analyze for significantly differential expression in the corresponding Treg cell subsets in G113Tg*Foxp3*^{CreERT2}*Trac*$^{WT/WT}$ compared to G113Tg*Foxp3*^{CreERT2}*Trac*$^{FL/FL}$ mice. Significantly up- (left, red) or down-regulated (right, blue) genes are shown as well as genes not significantly up- (black, left) or down-regulated (black, right). **B**, Cumulative distribution plots showing genes up- (left) and down-regulated (right) in CD44^{hi}CD62L^{lo} (CD44^{hi}, black line) and CD44^{lo}CD62L^{hi} (CD62L^{hi}, dark green line) TCRβ^{+} Treg cells in *Foxp3*^{CreERT2}*Trac*$^{WT/FL}$ vs. TCRβ^{-} Treg cells in *Foxp3*^{CreERT2}*Trac*$^{FL/FL}$ mice. Distribution of the same genes is shown for CD44^{hi}CD62L^{lo} (CD44^{hi}, gray line) and CD44^{lo}CD62L^{hi} (CD62L^{hi}, light green line) Vβ6^{+} Treg cells in G113Tg*Foxp3*^{CreERT2}*Trac*$^{WT/WT}$ vs. Vβ6Vα2^{+} (G113^{+}) Treg cells in G113Tg*Foxp3*^{CreERT2}*Trac*$^{FL/FL}$ mice. Dotted gray and light green lines indicate where gray and light greens lines cross x = 0; numbers indicate fraction of genes below x = 0.

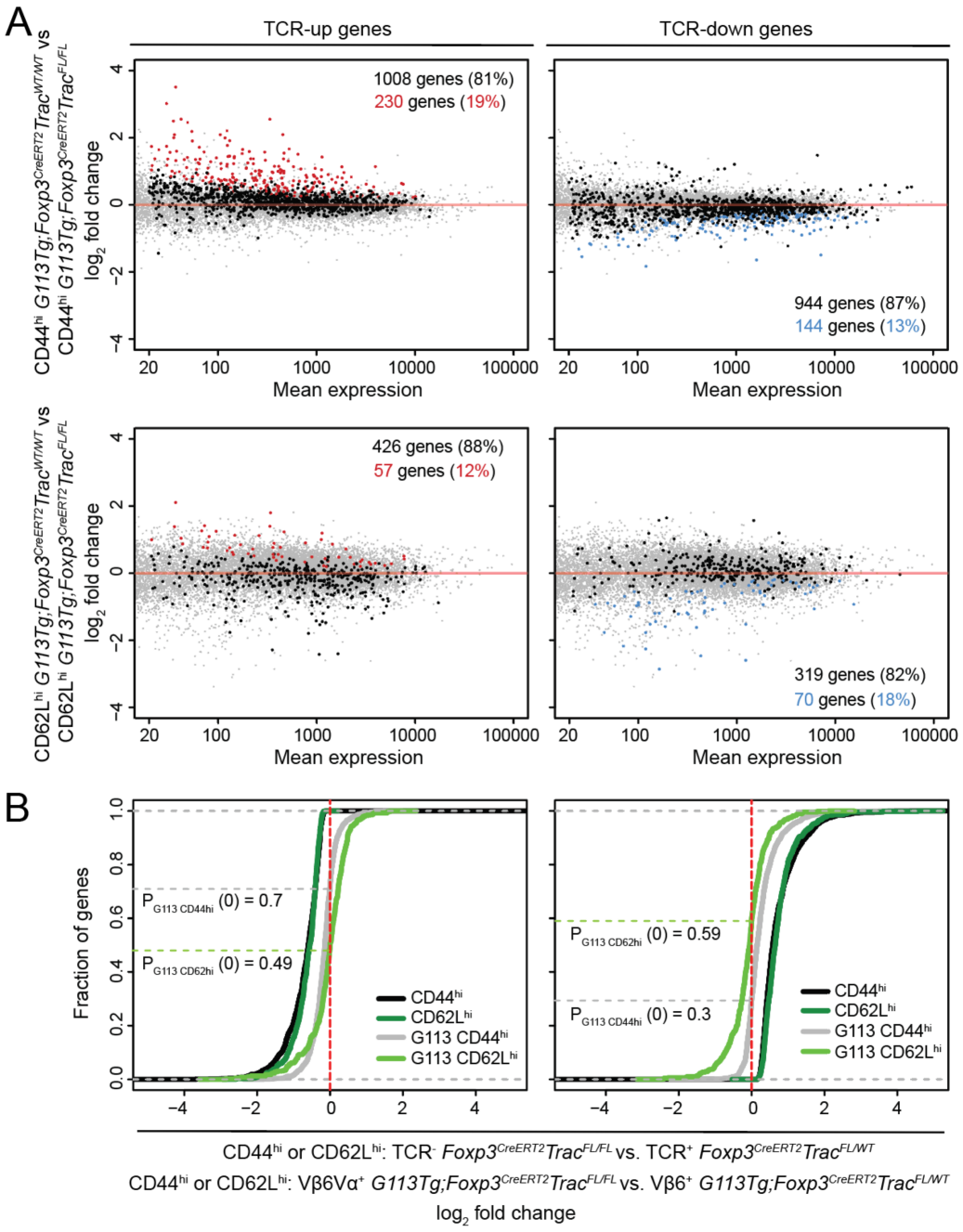
A
TCR-up genes
TCR-down genes
CD44hi G113Tg;Foxp3CreERT2TracWTWT vs CD44hi G113Tg;Foxp3CreERT2TracFL/FL
log2 fold change
1008 genes (81%)
230 genes (19%)
944 genes (87%)
144 genes (13%)
Mean expression
CD62Lhi G113Tg;Foxp3CreERT2TracWTWT vs CD62Lhi G113Tg;Foxp3CreERT2TracFL/FL
426 genes (88%)
57 genes (12%)
319 genes (82%)
70 genes (18%)
B
Fraction of genes
PG113 CD44hi (0) = 0.7
PG113 CD62hi (0) = 0.49
PG113 CD62hi (0) = 0.59
PG113 CD44hi (0) = 0.3
CD44hi
CD62Lhi
G113 CD44hi
G113 CD62Lhi
CD44hi or CD62Lhi: TCR- Foxp3CreERT2TracFL/FL vs. TCR+ Foxp3CreERT2TracFL/WT
CD44hi or CD62Lhi: Vβ6Vα+ G113Tg;Foxp3CreERT2TracFL/FL vs. Vβ6+ G113Tg;Foxp3CreERT2TracFL/WT
log2 fold change

G113Tg*Foxp3*^{CreERT2}*Tcra*$^{WT/WT}$ mice; these included genes coding for putative effectors and regulators of suppressor function *Tigit*, *Fgl2*, *Cxcl10*, *Il10*, *Lag3*, *Icos*, and *Pdcd1*; transcription factors *Irf4*, *Myb*, *Nfatc1*, *Nr4a3*, and *Relb*; and the chemokine receptor *Ccr8*. Furthermore, for 154 of the remaining 230 genes (67%) whose transcript levels were not fully rescued by monoclonal G113 TCR expression, the observed difference in their expression in monoclonal vs. polyclonal Treg cells from G113Tg*Foxp3*^{CreERT2}*Tcra*$^{FL/FL}$ vs. G113Tg*Foxp3*^{CreERT2}*Tcra*$^{FL/FL}$ mice, respectively, was less than that in TCR-deficient vs. –sufficient Treg cells from *Foxp3*^{CreERT2}*Tcra*$^{FL/FL}$ vs. *Foxp3*^{CreERT2}*Tcra*$^{FL/WT}$ mice, respectively. The latter group included typical TCR-dependent genes like *Egr2*, *Egr3*, *Il1r2*, *Penk*, *Cd83*, and *Ebi3*, all of whose difference in expression in non-G113Tg expressing TCR-deficient vs. –sufficient Treg cells was two-fold or more greater than the difference in expression in monoclonal vs. polyclonal G113Tg-expressing Treg cells. Similarly, of the 1,088 genes up in effector Treg cells in the absence of TCR, 944 (87%) were fully rescued. A comparable—if not more profound—rescue of TCR-dependent gene expression was also observed for naïve Treg cells. We found that 426 of 484 (88%) genes up-regulated in a TCR-dependent manner were similarly expressed—or were actually overexpressed—in naïve monoclonal Treg cells in G113Tg*Foxp3*^{CreERT2}*Tcra*$^{FL/FL}$ mice compared to Treg cells in G113Tg*Foxp3*^{CreERT2}*Tcra*$^{WT/WT}$ mice expressing diverse endogenously rearranged TCRs. The latter set included the genes *Egr1*, *Egr2*, *Egr3*, *Cd5*, *Irf4*, *Myb*, *Nab2*, and *Nfatc1*. Likewise, of the 389 genes down-regulated in naïve Treg cells in a polyclonal TCR-dependent manner, 319 (82%) were fully rescued. Together, these data demonstrate that at a population level, G113 TCR expression rescues the vast majority, even if not all, of the TCR-

dependent transcriptional signature in both effector and naïve Treg cell subsets.

Selective activation of G113 TCR-expressing Treg cells in skin-draining lymph nodes

The demonstration of widespread rather than limited rescue of TCR-dependent gene expression in Treg cells by the monoclonal G113 TCR suggested that incomplete protection against autoimmune disease by these cells might be due to activation limited to a particular local setting rather than due to limited TCR-dependent gene expression induced by a given single TCR. Thus, we next used flow cytometric analysis to examine expression of EGR2, as a representative TCR-dependent gene that was somewhat but not fully rescued by the monoclonal G113 TCR. In lymph node effector Treg cells, we observed that compared to polyclonal Treg cells a decreased portion of monoclonal G113^{+} Treg cells were positive for EGR2 (69±0.78% vs 52±5.7%) consistent with restricted engagements with limiting amounts of antigen precluding full activation of the monoclonal G113^{+} Treg cell pool. TCR-deficient Treg cells used as a control showed negligible EGR2 expression (5.0±0.20%.) Conversely, we noted that EGR2 was expressed at higher levels in naïve monoclonal G113^{+} Treg cells in the lymph nodes of G113Tg*Foxp3*^{CreERT2}*Tcra*$^{FL/FL}$ mice than in naïve polyclonal Treg cells from G113Tg*Foxp3*^{CreERT2}*Tcra*$^{WT/WT}$ mice (Figure 3.7A). Even Vβ6^{+}Vα2^{+} G113^{+} Treg cells in G113Tg*Foxp3*^{CreERT2}*Tcra*$^{WT/WT}$ mice expressed more EGR2 than non-G113 Vβ6^{+}Vα2^{-} Treg cells in the same mice (Figure 3.7A). Notably, this was not the case in the splenic Treg cell subset (Figure 3.7A) nor was this true for Treg cells found in intestine-draining mesenteric or lung-draining

Figure 3.7. Selective activation of G113 TCR-expressing Treg cells in skin-draining lymph nodes.

A, Representative flow cytometric analyses of EGR2 expression in naïve TCRβ$^+$ and TCRβ$^-$ Treg cells in skin-draining lymph nodes and spleen in tamoxifen-treated *Foxp3*^{CreERT2}*Trac*$^{WT/WT}$ and *Foxp3*^{CreERT2}*Trac*$^{FL/FL}$ mice, respectively (left); and EGR2 expression in naïve Vβ6$^+$Vα2$^-$ (G113$^-$, black gates and histograms) and Vβ6$^+$Vα2$^+$ (G113$^+$, red gates and histograms) Treg cells in tamoxifen-treated G113Tg*Foxp3*^{CreERT2}*Trac*$^{WT/WT}$ and G113Tg*Foxp3*^{CreERT2}*Trac*$^{FL/FL}$ mice (right). **B**, Flow cytometric analyses of Treg cells in lymph nodes of female *Foxp3*$^{CreERT2/YFP\text{-}Cre}$*Trac*$^{FL/FL}$ (left) and G113Tg*Foxp3*$^{CreERT2/YFP\text{-}Cre}$*Trac*$^{FL/FL}$ (right) mice, gated on CD4$^+$Foxp3$^+$ cells. The percentages YFP-Cre$^+$ and YFP-Cre$^-$ (eGFP$^+$) cells are indicated. **C**, Vα2 and Vβ6 expression in eGFP-CreERT2$^+$ (eGFP$^+$) and YFP-Cre$^+$ CD4$^+$Foxp3$^+$ cell subsets as shown in (**B**, right) in lymph nodes of G113Tg*Foxp3*$^{CreERT2/YFP\text{-}Cre}$*Trac*$^{FL/FL}$ mice. **D**, Representative flow cytometric analyses (left) of CD4$^+$Foxp3$^+$ cells isolated from tissues of G113Tg*Foxp3*$^{CreERT2/YFP\text{-}Cre}$*Trac*$^{FL/FL}$ mice. Quantification of YFP-Cre$^+$ cells within the total Foxp3$^+$ cell population is shown on right.

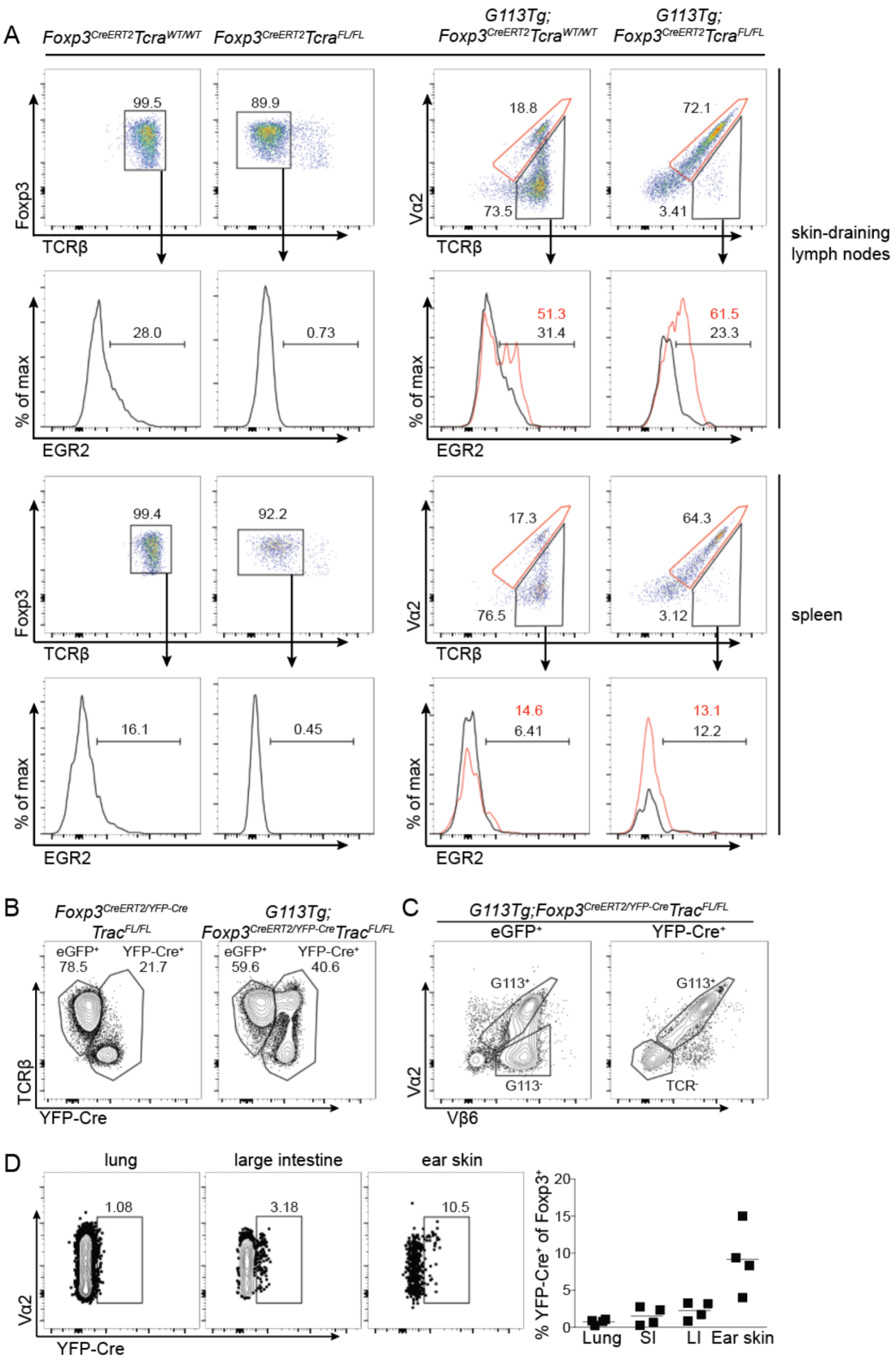
A
Foxp3CreERT2Tcra WT/WT
Foxp3CreERT2Tcra FL/FL
G113Tg; Foxp3CreERT2Tcra WT/WT
G113Tg; Foxp3CreERT2Tcra FL/FL
99.5
89.9
18.8
73.5
72.1
3.41
Foxp3
TCRβ
Vα2
skin-draining lymph nodes
28.0
0.73
51.3
31.4
61.5
23.3
% of max
EGR2
99.4
92.2
17.3
76.5
64.3
3.12
spleen
16.1
0.45
14.6
6.41
13.1
12.2
B
Foxp3CreERT2/YFP-Cre Trac FL/FL
G113Tg; Foxp3CreERT2/YFP-Cre Trac FL/FL
eGFP+ 78.5
YFP-Cre+ 21.7
eGFP+ 59.6
YFP-Cre+ 40.6
TCRβ
YFP-Cre
C
G113Tg;Foxp3CreERT2/YFP-Cre Trac FL/FL
eGFP+
YFP-Cre+
G113+
G113-
TCR-
Vα2
Vβ6
D
lung
large intestine
ear skin
1.08
3.18
10.5
Vα2
YFP-Cre
% YFP-Cre+ of Foxp3+
20
15
10
5
0
Lung
SI
LI
Ear skin

mediastinal lymph nodes (data not shown). Thus, G113 TCR activation was evident only in the skin-draining cervical, axial, brachial, and inguinal lymph nodes. TCR-dependent IRF4 expression assessed at a single cell level showed a pattern similar to that of ERG2 (data not shown). Intriguingly, these data suggested that the G113 TCR might recognize (with an affinity significantly higher than the average naïve Treg cell TCR) antigen predominantly expressed in the skin and consequently presented to naive G113^{+} Treg cells trafficking through skin-draining lymph nodes.

In order to further investigate this possibility, we generated female G113Tg*Foxp3*$^{CreERT2/YFP\text{-}Cre}$*Trac*$^{FL/FL}$ mice in which, due to X-inactivation, half of the Treg cells express eGFP-CreERT2 and half express YFP-Cre (Figure 3.7B). We reasoned that in this setting—in the absence of tamoxifen treatment—where monoclonal G113^{+} YFP-Cre^{+} Treg cells compete with polyclonal eGFP-CreERT2^{+} Treg cells (Figure 3.7C), the tissue expressing highest amounts of antigen recognized by the G113 TCR would enable accumulation and contain the relatively highest proportion of YFP-Cre^{+} G113^{+} Treg cells. Indicative of G113 TCR recognition of a primarily skin-derived antigen, we observed most prominent accumulation of YFP-Cre^{+} cells as a percentage of total Foxp3^{+} cells in skin compared to other tissues (Figure 3.7D). These data suggest that a single Treg cell TCR with an apparent specificity for a yet to be identified antigen, apparently expressed in a tissue-restricted manner, is sufficient to elicit the vast majority of the polyclonal TCR-dependent gene expression signature and life-sparing immunosuppressive function in Treg cells.

Discussion

Our studies provide a nuanced answer to an outstanding question in the field of Treg cell biology, namely, the requirement for a diverse TCR repertoire displayed by Treg cells for their suppressor function *in vivo.* Although a diverse repertoire in mature Treg cells was required for their ability to control T_H1 immune responses and fully restrain tissue inflammation, a single TCR, expressed by Treg cells, unexpectedly endowed them with the capacity to suppress lymphadenopathy and T_H2 responses. It should be noted that when transferred into T cell-deficient hosts, monoclonal Treg cells did suppress T_H1 responses in the lymph nodes; however, in this setting T_H2 cytokines are barely detectable and, accordingly, this experimental set-up may not provide a suitable model for examining specific control of the Th2 responses.

Treg cells expressing the G113 TCR were able to markedly extend the lifespan of mice by restraining fatal early onset autoimmune disease resulting from congenital or induced Treg cell deficiency or from ablation of TCR expression in Treg cells (Fontenot et al., 2003; Kim et al., 2007; Levine et al., 2014). Consistent with functional studies, expression of this single monoclonal Treg cell-derived TCR was able to support the vast majority of gene expression features imparted by a diverse Treg TCR repertoire. These findings suggested that a diverse Treg TCR mosaic was required for activation of Treg cells in specific “geographical” locations, rather than for enabling expression of distinct gene subsets induced in an individual TCR specificity-dependent manner involved either directly or indirectly in elaboration of suppressor function. This notion was supported by the observed preferential stimulation of Treg cells expressing the monoclonal G113 TCR in skin-draining lymph nodes, where they also seem to preferentially exert their suppressor function. An additional and non-mutually exclusive possibility was that

suppression of immune responses in the lymph nodes and, in particular, of T_H2 responses has less stringent requirements for diverse TCR-dependent interactions between Treg cells and their developmentally established cognate antigens as opposed to T_H1 responses, whose suppression by Treg cells may more strictly require diverse and specific Treg cell TCR-ligand interactions. In support of the latter possibility, we found that, similar to inducible G113 TCR expression in mature Treg cells, replacement of a diverse TCR repertoire recognizing developmentally selected ligands for a diverse, but biologically irrelevant TCR repertoire with randomly generated specificities resulted in protection against lymphadenopathy and T_H2, but not T_H1 responses. The latter Treg TCR repertoire switch was accomplished by inducible Cre-mediated expression of the invariant Vα14-Jα18 NKT cell TCRα-chain in place of concomitantly ablated endogenously rearranged diverse TCRα-chains specifically in mature Treg cells *in vivo* (Vahl et al., 2013) (data not shown). T_H1 vs. T_H2 lineage commitment has been linked to TCR signal strength that can be modulated through co-stimulation (van Panhuys et al., 2014). It is possible that a decrease in antigen presenting cell activation in lymph nodes imparted by a largely monoclonal $G113^+$ Treg cell population or aforementioned Treg cells with diverse, but biologically irrelevant TCR specificities, underlies the observed differential suppression of T_H1 and T_H2 responses, although precisely how this may occur is unclear. In any case, our data indicate that once Treg cells have engaged their TCRs (no matter the antigenic specificity) they are able to exert a tolerogenic influence on their surroundings. The observed partial rescue of immune activation and autoimmune disease in mice harboring a largely monoclonal population of $G113^+$ Treg cells gives a measure of both the power and limitations of such

tolerogenic influence in the absence of appropriate repertoire specificity and diversity.

Acknowledgements

We thank members of the Rudensky lab for critical discussions, and A.H. Bravo and S.E. Lee for experimental support. This work was supported by an NIH Medical Scientist Training Program grant T32GM07739 to the Weill Cornell/Rockefeller/Sloan-Kettering Tri-Institutional MD-PhD Program (A.G.L); the Frank Lappin Horsfall Jr. Student Fellowship (A.G.L); NIH grant R37AI034206 (A.Y.R.), the Ludwig Center at Memorial Sloan Kettering Cancer Center, and the Hilton-Ludwig Cancer Prevention Initiative (Conrad N. Hilton Foundation and Ludwig Cancer Research) (A.Y.R.); and the NIH/NCI Cancer Center Support Grant P30 CA008748. A.Y.R. is an investigator with the Howard Hughes Medical Institute.

Materials and Methods

Mice

Foxp3$^{YFP\text{-}Cre}$ *(Rubtsov et al.,* 2008*)*, *Foxp3*$^{eGFP\text{-}CreERT2}$ (Rubtsov et al., 2010), *Tcra*^{FL} (Polic et al., 2001), *Foxp3*^{KO} (Fontenot et al., 2003), G113Tg *(Bautista et al., 2009)*, *Foxp3*^{DTReGFP} (Kim et al., 2007), and *Trac*$^{FL/Vα14i\text{-}StopF}$ (Vahl et al., 2013) mice have been previously described. CD45.1 and *Tcrb*$^{-/-}$*Tcrd*$^{-/-}$ mice were purchased from Jackson Laboratories. Generation and treatments of mice were performed under protocol 08-10-023 approved by the Sloan Kettering Institute (SKI) Institutional Animal Care and Use Committee. All mouse strains were maintained in the SKI animal facility in specific pathogen free (SPF) conditions in accordance with institutional guidelines.

For tamoxifen administration, 40 mg tamoxifen dissolved in 100 µl ethanol and subsequently in 900 mL olive oil (Sigma-Aldrich) were sonicated 4 × 30 seconds in a Bioruptor Twin (Diagenode). Mice were orally gavaged with 200µl tamoxifen emulsion per treatment. For diphtheria toxin (DT) injections, DT (Sigma-Aldrich) was dissolved in PBS and 200 µl of indicated doses were injected i.p per mouse.

Isolation of cells

Spleens and lymph nodes were dissociated using ground glass slides and filtered. Red blood cells in spleens were lysed before analysis. To isolate lymphocytes from tissues, mice were euthanized and immediately perfused with 20 mL PBS. Small and large intestines were removed, flushed with PBS, Peyer's patches were removed, and residual fat and connective tissue was removed. Intestines were opened lengthwise and cut into 0.5 cm-long pieces that were further washed by vortexing in PBS. Samples were incubated in PBS supplemented with 5% fetal calf serum, 1% L-glutamine, 1% penicillin-streptomycin, 10 mM HEPES, 1 mM dithiothreitol, and 1 mM EDTA for 15 minutes to dissociate intraepithelial lymphocytes, which were discarded. Samples were washed and incubated in digest solution (RPMI supplemented with 5% fetal calf serum, 1% L-glutamine, 1% penicillin-streptomycin, 10 mM HEPES, 1 mg/mL collagenase, and 1 U/mL DNase I) for 10 minutes. Cells were collected through a 100-µm strainer, and the residual samples were incubated in digest solution again for 10 minutes before filtering through 100-µm strainers and combining with previously collected cells. Cells were resuspended in 35% Percoll to eliminate debis before resuspension in staining

buffer. To isolate lymphocytes from livers and lungs, tissues were physically dissociated using scissors and incubated for 50-60 minutes in digest solution before being filtered through 100-µm strainers. Lungs samples were resuspended in 35% Percoll to eliminate debris before resuspension in staining buffer. Lymphocytes from liver samples were resuspended in 44% Percoll, underlaid with 67% Percoll, and spun at 1000xg for 7.5 minutes at room temperature. Cells were collected from the interface of the Percoll layers and washed before resuspension in staining buffer.

Cell transfer experiments

For cell transfer experiments, pooled spleens and lymph nodes were enriched for CD4 T cells using the Dynabeads CD4 Positive Isolation Kit. Cells were FACS-sorted on an Aria II cell sorter (BD Bioscience), washed 3 times in PBS, resuspended in 200 μL PBS, and transferred into recipients via retro-orbital injection.

Flow cytometric analysis

Cells were stained with LIVE/DEAD Fixable Yellow Dead Cell Stain (Molecular Probes) and the following antibodies purchased from eBioscience, BioLegend, BD Biosciences, Tonbo, or obtained from the NIH tetramer core facility: anti-CD4 (RM4-5), anti-CD8a (5H10), anti-TCRβ (H57-597), anti-Vβ6 (RR4-7), anti-Vα2 (B20.1), EGR2 (erongr2), IRF4 (E3 4), IL1R2 (4E2), PBS-57-loaded mCD1d tetramer, anti-CD44 (IM7), anti-CD62L (MEL-14), anti-CD25 (PC61), anti-Foxp3 (FJK-16s), anti- IFNγ (XMG1.2), anti-IL-4 (11B11), anti-IL-13 (eBio13A), anti-IL-17A (17B7), and anti-IL-2 (JES6-5H4). Flow cytometric analysis was performed using an LSRII flow cytometer (BD Bioscience) and

FlowJo software (Tree Star). Intracellular staining was performed using eBioscience Fixation Permeabilization buffers. For cytokine staining lymphocytes were stimulated with soluble anti-CD3 clone 2C11 (5µg/ml) and anti-CD28 clone 37.51 (5µg/ml) in the presence of 1µg/mL brefeldin A for 5 hours at 37°C, 5% CO^2.

RNA-seq analysis

Foxp3^{CreERT2}*Trac*$^{FL/WT}$, *Foxp3*^{CreERT2}*Trac*$^{FL/FL}$, *G113Tg;Foxp3*^{CreERT2}*Trac*$^{WT/WT}$, and *G113TgFoxp3*^{CreERT2}*Trac*$^{FL/FL}$ mice were treated with tamoxifen on days 0, 1, and 7 and on day 9—following CD4 T cell enrichment using the Dynabeads CD4 Positive Isolation Kit—the following populations were sorted from the indicated mice and resuspended in Trizol: CD44^{hi}CD62L^{lo} and CD44^{lo}CD62L^{hi} TCRβ$^+$ and TCRβ$^-$ Treg cells from *Foxp3*^{CreERT2}*Trac*$^{FL/WT}$ mice; CD44^{hi}CD62L^{lo} and CD44^{lo}CD62L^{hi} TCRβ$^+$ and TCRβ$^-$ Treg cells from *Foxp3*^{CreERT2}*Trac*$^{FL/FL}$ mice; CD44^{hi}CD62L^{lo} and CD44^{lo}CD62L^{hi} Vβ6$^+$ Treg cells from G113Tg*Foxp3*^{CreERT2}*Trac*$^{WT/WT}$ mice; and CD44^{hi}CD62L^{lo} and CD44^{lo}CD62L^{hi} Vβ6$^+$Vα2$^+$ Treg cells from *Foxp3*^{CreERT2}*Trac*$^{FL/FL}$ mice. Three replicates of each cell subset were generated. RNA-sequencing reads were aligned to the reference mouse genome GRCm38 using the Burrows-Wheeler Aligner (BWA) (Li and Durbin, 2010) and local realignment was performed using the Genome Analysis Toolkit (GATK) (McKenna et al., 2010). For each sample, raw count of reads per gene was measured using R, and DESeq2 R package (Love et al., 2014) was used to perform differential gene expression among different conditions. A cutoff of 0.05 was set on the obtained *p* values (that were adjusted using Benjamini-Hochberg multiple testing correction) to get the significant genes of each comparison.

Statistical analysis

All statistical analyses (excluding RNA-seq analyses, described above) were performed using GraphPad Prism 6 software. Differences between individual groups were analyzed for statistical significance using the unpaired or paired two-tailed Student's t-test. *, $p \geq 0.05$; **, $p \geq 0.01$; ***, $p \geq 0.001$; ns, not significant.

References

Anderson, M.S., Venanzi, E.S., Klein, L., Chen, Z., Berzins, S.P., Turley, S.J., von Boehmer, H., Bronson, R., Dierich, A., Benoist, C., and Mathis, D. (2002). Projection of an immunological self shadow within the thymus by the aire protein. Science *298*, 1395-1401.

Bautista, J.L., Lio, C.W., Lathrop, S.K., Forbush, K., Liang, Y., Luo, J., Rudensky, A.Y., and Hsieh, C.S. (2009). Intraclonal competition limits the fate determination of regulatory T cells in the thymus. Nature immunology *10*, 610-617.

Feng, Y., van der Veeken, J., Shugay, M., Putintseva, E.V., Osmanbeyoglu, H.U., Dikiy, S., Hoyos, B.E., Moltedo, B., Hemmers, S., Treuting, P.*, et al.* (2015). A mechanism for expansion of regulatory T-cell repertoire and its role in self-tolerance. Nature *528*, 132-136.

Fontenot, J.D., Gavin, M.A., and Rudensky, A.Y. (2003). Foxp3 programs the development and function of CD4+CD25+ regulatory T cells. Nature immunology *4*, 330-336.

Hsieh, C.S., Liang, Y., Tyznik, A.J., Self, S.G., Liggitt, D., and Rudensky, A.Y. (2004). Recognition of the peripheral self by naturally arising CD25+ CD4+ T cell receptors. Immunity *21*, 267-277.

Hsieh, C.S., Zheng, Y., Liang, Y., Fontenot, J.D., and Rudensky, A.Y. (2006). An intersection between the self-reactive regulatory and nonregulatory T cell receptor repertoires. Nature immunology *7*, 401-410.

Jordan, M.S., Boesteanu, A., Reed, A.J., Petrone, A.L., Holenbeck, A.E., Lerman, M.A., Naji, A., and Caton, A.J. (2001). Thymic selection of CD4+CD25+ regulatory T cells induced by an agonist self-peptide. Nature immunology *2*, 301-306.

Killebrew, J.R., Perdue, N., Kwan, A., Thornton, A.M., Shevach, E.M., and Campbell, D.J. (2011). A self-reactive TCR drives the development of Foxp3+ regulatory T cells that prevent autoimmune disease. Journal of immunology *187*, 861-869.

Kim, J.M., Rasmussen, J.P., and Rudensky, A.Y. (2007). Regulatory T cells prevent catastrophic autoimmunity throughout the lifespan of mice. Nature immunology *8*, 191-197.

Leung, M.W., Shen, S., and Lafaille, J.J. (2009). TCR-dependent differentiation of thymic Foxp3+ cells is limited to small clonal sizes. The Journal of experimental medicine *206*, 2121-2130.

Leventhal, D.S., Gilmore, D.C., Berger, J.M., Nishi, S., Lee, V., Malchow, S., Kline, D.E., Kline, J., Vander Griend, D.J., Huang, H.*, et al.* (2016). Dendritic Cells Coordinate the Development and Homeostasis of Organ-Specific Regulatory T Cells. Immunity *44*, 847-859.

Levine, A.G., Arvey, A., Jin, W., and Rudensky, A.Y. (2014). Continuous requirement for the TCR in regulatory T cell function. Nature immunology *15*, 1070-1078.

Li, H., and Durbin, R. (2010). Fast and accurate long-read alignment with Burrows-Wheeler transform. Bioinformatics *26*, 589-595.

Lin, J., Yang, L., Silva, H.M., Trzeciak, A., Choi, Y., Schwab, S.R., Dustin, M.L., and Lafaille, J.J. (2016). Increased generation of Foxp3(+) regulatory T cells by manipulating antigen presentation in the thymus. Nature communications *7*, 10562.

Love, M.I., Huber, W., and Anders, S. (2014). Moderated estimation of fold change and dispersion for RNA-seq data with DESeq2. Genome biology *15*, 550.

Malchow, S., Leventhal, D.S., Lee, V., Nishi, S., Socci, N.D., and Savage, P.A. (2016). Aire Enforces Immune Tolerance by Directing Autoreactive T Cells into the Regulatory T Cell Lineage. Immunity *44*, 1102-1113.

McKenna, A., Hanna, M., Banks, E., Sivachenko, A., Cibulskis, K., Kernytsky, A., Garimella, K., Altshuler, D., Gabriel, S., Daly, M., and DePristo, M.A. (2010). The Genome Analysis Toolkit: a MapReduce framework for analyzing next-generation DNA sequencing data. Genome research *20*, 1297-1303.

Moran, A.E., Holzapfel, K.L., Xing, Y., Cunningham, N.R., Maltzman, J.S., Punt, J., and Hogquist, K.A. (2011). T cell receptor signal strength in Treg and iNKT cell development demonstrated by a novel fluorescent reporter mouse. The Journal of experimental medicine *208*, 1279-1289.

Polic, B., Kunkel, D., Scheffold, A., and Rajewsky, K. (2001). How alpha beta T cells deal with induced TCR alpha ablation. Proceedings of the National Academy of Sciences of the United States of America *98*, 8744-8749.

Rubtsov, Y.P., Niec, R.E., Josefowicz, S., Li, L., Darce, J., Mathis, D., Benoist, C., and Rudensky, A.Y. (2010). Stability of the regulatory T cell lineage in vivo. Science *329*, 1667-1671.

Rubtsov, Y.P., Rasmussen, J.P., Chi, E.Y., Fontenot, J., Castelli, L., Ye, X., Treuting, P., Siewe, L., Roers, A., Henderson, W.R., Jr.*, et al.* (2008). Regulatory T cell-derived interleukin-10 limits inflammation at environmental interfaces. Immunity *28*, 546-558.

Samy, E.T., Parker, L.A., Sharp, C.P., and Tung, K.S. (2005). Continuous control of autoimmune disease by antigen-dependent polyclonal CD4+CD25+ regulatory T cells in the regional lymph node. The Journal of experimental medicine *202*, 771-781.

Vahl, J.C., Drees, C., Heger, K., Heink, S., Fischer, J.C., Nedjic, J., Ohkura, N., Morikawa, H., Poeck, H., Schallenberg, S.*, et al.* (2014). Continuous T cell receptor signals maintain a functional regulatory T cell pool. Immunity *41*, 722-736.

Vahl, J.C., Heger, K., Knies, N., Hein, M.Y., Boon, L., Yagita, H., Polic, B., and Schmidt-Supprian, M. (2013). NKT cell-TCR expression activates conventional T cells in vivo, but is largely dispensable for mature NKT cell biology. PLoS biology *11*, e1001589.

van Panhuys, N., Klauschen, F., and Germain, R.N. (2014). T-cell-receptor-dependent signal intensity dominantly controls CD4(+) T cell polarization In Vivo. Immunity *41*, 63-74.

Yang, S., Fujikado, N., Kolodin, D., Benoist, C., and Mathis, D. (2015). Immune tolerance. Regulatory T cells generated early in life play a distinct role in maintaining self-tolerance. Science *348*, 589-594.

CHAPTER 4

STABILITY AND FUNCTION OF REGULATORY T CELLS EXPRESSING THE TRANSCRIPTION FACTOR T-BET*

Abstract

Regulatory T (Treg) cells comprise a distinct anti-inflammatory cell lineage specified by the transcription factor Foxp3. Paradoxically, upon activation Treg cells can express transcription factors specifying pro-inflammatory effector T cell lineages. Whether expression of these factors may indicate stability of Treg cell effector states and reflect essential Treg cell heterogeneity, or readily reversible activation states is unknown. Using genetic fate mapping we demonstrate that in some Treg cells expression of the T_H1-associated transcription factor T-bet, gradually acquired upon Treg cell effector differentiation in the periphery, induced at steady state and following infection is highly stable even under non-permissive conditions. Selective "loss-of-function" or elimination of T-bet-expressing Treg cells—but not of T-bet itself —resulted in a severe and selective T_H1-type autoimmunity, demonstrating a major immunosuppressive function that cannot be compensated for by the remaining T-bet-non-expressing Treg cell pool. These results suggest that Treg cell heterogeneity is a critical feature of immune tolerance.

---

* Adapted from Levine, A.G., Hemmers, H., Moltedo, B., Niec, R.E., Schizas, M., Hoyos, B.E., Putintseva, E.V., Chaudhry, A., Dikiy, S., Chudakov, D.M., Treuting, P.M., and Rudensky, A.Y. Stability and function of regulatory T cells expressing the transcription factor T-bet. (*submitted*).

Introduction

Protective immune responses against different types of pathogens are facilitated by clonal expansion and differentiation of naïve CD4 T cells into functionally distinct subsets of pathogen-specific effector $CD4^+$ T cells, each endowed with specific effector functions tailored to the particular type of pathogens whose antigens they recognize (Zhu et al., 2010). Acquisition of a given effector cell fate, for example, differentiation into the IFNγ-producing T_H1 lineage upon viral or bacterial infection is associated with repression of an alternative cell fate—differentiation into IL-4- or IL-13-producing T_H2 effector cells. The latter, while capable of exerting effective defenses against helminth infection, are ineffective—or even detrimental—for protection against bacterial infection.

This process of effector differentiation and acquisition of effector mechanisms is elicited through activation of particular STAT transcription factor family members and their corresponding key downstream transcription factors, T-bet, RORγt, and GATA3, to specify the appropriate response type in effector CD4 T cells (Zhu et al., 2010). Similar effector mechanisms, however, also underlie misguided responses against "self", commensal microbiota, and dietary antigens associated with a variety of autoimmune and inflammatory diseases.

Regulatory T (Treg) cells express their own X-chromosome encoded lineage defining transcription factor Foxp3, which is continuously required for their suppressor function (Fontenot et al., 2003; Gavin et al., 2007; Hori et al., 2003; Khattri et al., 2003; Williams and Rudensky, 2007). Fate mapping studies have indicated that Treg cells are a distinct cell lineage characterized by heritable maintenance of *Foxp3* gene expression enforced by a dedicated

genetic mechanism (Feng et al., 2014; Rubtsov et al., 2010). However, some activated Treg cells express, in addition to Foxp3, the aforementioned effector CD4 T cell signature transcription factors, which have been suggested to endow Treg cells with enhanced ability to suppress effector responses (Koch et al., 2009; Lee et al., 2015; Ohnmacht et al., 2015; Rudra et al., 2012; Sefik et al., 2015; Wohlfert et al., 2011).

Despite these observations, it remains unclear whether expression of these factors in Treg cells—akin to helper T cells—is indicative of heterogeneity of potentially functionally discrete and/or stable differentiation states. It has been proposed that effector transcription factor expression in Treg cells may be readily reversible, in which case these cells would represent inducible and transitory states within a largely homogeneous activated Treg cell population (Liston and Gray, 2014; Tian et al., 2012). Alternatively, heterogeneity of activated Treg cells—stemming from distinct effector Treg cell differentiation states—may be an essential feature of Treg cell-mediated tolerance, with subpopulations of Treg cells serving particular roles in controlling distinct types of inflammatory responses.

In this regard, several recent studies of the functional implications of expression of T-bet—the T_H1-specifiying transcription factor—in Treg cells failed to reveal defects in tolerance at steady state or in a variety of challenge conditions in mice subjected to Treg cell-specific ablation of this factor (Colbeck et al., 2015; McPherson et al., 2015; Yu et al., 2015). Furthermore, fate mapping experiments utilizing a *Tbx21* (T-bet) BAC transgene-encoded Cre recombinase fused to an estrogen receptor ligand binding domain (CreERT2), in combination with a recombination reporter, suggested that expression of T-bet in Treg cells was transient and reversible (Yu et al., 2015).

This study suggested that, in Treg cells, T-bet expression was functionally interchangeable with GATA3, thus implying a marked degree of Treg cell plasticity.

Here, we explored the question of Treg cell heterogeneity and its functional implications through generation of a novel *Tbx21* fate-mapping knock-in allele. We found that T-bet expression was independently induced in Treg cells at steady state and upon bacterial or viral infection promoting T_H1 immune responses. T-bet expression in Treg cells with high amounts of T-bet (following a gradual up-regulation of T-bet during peripheral effector differentiation) was remarkably stable at both steady state and under T_H2-polarizing conditions induced upon helminthic infection. T-bet expression induced in Treg cells by bacterial infection was also highly stable, persisting in cells following resolution of the primary response as well as during the recall response to secondary challenge. Selective loss-of-function or elimination of T-bet-expressing Treg cells resulted in a severe spontaneous T_H1-type autoimmune inflammation that could not be compensated for by the remaining T-bet-non-expressing Treg cell pool. In contrast, loss of T-bet itself in Treg cells did not impair their ability to prevent disease. These results suggest a particular function differentiated Treg cells expressing T-bet in preventing autoimmunity and suggest an essential role of Treg cell heterogeneity in immunological tolerance.

Results

Stability of T-bet expression in peripheral Treg cells

In order to determine whether T-bet expression was stable or rather was reversible, we generated a *Tbx21*$^{tdTomato\text{-}T2A\text{-}CreERT2}$ knock-in allele containing

sequence encoding tandem dimer (td) Tomato red fluorescent protein (RFP) and CreERT2 separated by a self-cleaving 2A peptide sequence (Figure 4.1A). For fate mapping studies we combined this new allele with the *Foxp3*$^{Thy1.1}$ reporter and the R26Y recombination reporter allele harboring a "floxed" stop cassette followed by YFP coding sequence inserted into the ubiquitously expressed *Rosa26* locus (Liston et al., 2008; Srinivas et al., 2001). The resulting mice, bred to homozygosity at each locus, (referred to hereafter as *Tbx21*$^{RFP\text{-}CreERT2}$ mice) showed a dynamic range of RFP expression and CreERT2 activity corresponding to T-bet protein levels in major lymphocyte subsets including NK and NKT cells, Treg cells, and effector CD4 and CD8 T cells (Fig 4.1B and Figure 4.2A).

To assess stability of T-bet expression in Treg cells under physiologic conditions, *Tbx21*$^{RFP\text{-}CreERT2}$ mice were treated with tamoxifen twice at 2 month of age and analyzed three weeks, three months, and seven months later for RFP and YFP expression (Figure 4.1C and Figure 4.2C). RFP^{+} Treg cells were present in lymphoid organs and all non-lymphoid tissues examined, most prominently the colon; the latter Treg cell population exhibited prevalent co-expression of T-bet and RORγt—as previously reported—but not T-bet and GATA3, confirmed by flow cytometric analysis of *Tbx21*$^{RFP\text{-}CreERT2}$*Rorc*$^{GFP/WT}$ mice (Figure 4.1D,F and Figure 4.21D-G) (Eberl et al., 2004; Sefik et al., 2015). In all tissues, excepting the colon, RFP^{+} cells comprised between 30-40% of CD44^{hi}CD62L^{lo} effector Treg cells, which contain the bulk of RFP^{+} cells (Figure 4.2H); in the colon they comprised 67% (Figure 4.2I). Over time, the percent RFP^{+} cells among Thy1.1^{+} Treg cells increased significantly in spleen and lymph nodes (Figure 4.1F); this was due both to increased percentages of

Figure 4.1. Stable T-bet expression in a subset of peripheral Treg cells. **A**, Targeting strategy for generation of the *Tbx21*$^{RFP\text{-}CreERT2}$ allele. **B**, RFP expression (left) and percent YFP$^+$ cells (right) in indicated splenic cell populations of *Tbx21*$^{RFP\text{-}CreERT2}$ mice 3 weeks following tamoxifen (tx) gavage on days -2 and 0. Numbers on graph (right) indicate the percent YFP$^+$ cells of each cell type. **C**, Schematic of the regimen of tx administration to *Tbx21*$^{RFP\text{-}CreERT2}$ mice in experiments shown in (**D-G)**. **D**, Flow cytometric analysis of TCRβ$^+$ CD4$^+$ cells, which were negative for a-galalctosyl ceramide analogue (PBS-57)- loaded CD1d tetramer staining, 3 weeks post tx gavage. **E**, Flow cytometric analysis of splenic Thy1.1$^+$ (above) and Thy1.1$^-$ (below) cells 3 weeks, 3 months, and 7 months post tx gavage; cells were gated on TCRβ$^+$ PBS-57-CD1d tetramer$^-$ CD4$^+$ cells. **F**, (Above) percent RFP$^+$ (left axis, squares) and YFP$^+$ (right axis, circles) cells of Thy1.1$^+$ cells, and (below) percent RFP$^+$ of Thy1.1$^+$YFP$^+$ cells 3 weeks (white squares), 3 months (gray squares), and 7 months (black squares) post tx gavage. **G**, same as in (**F**) for Thy1.1$^-$ cells. The data shown represent the combined results of 2 independent experiments for each time point with at least 5 mice each.

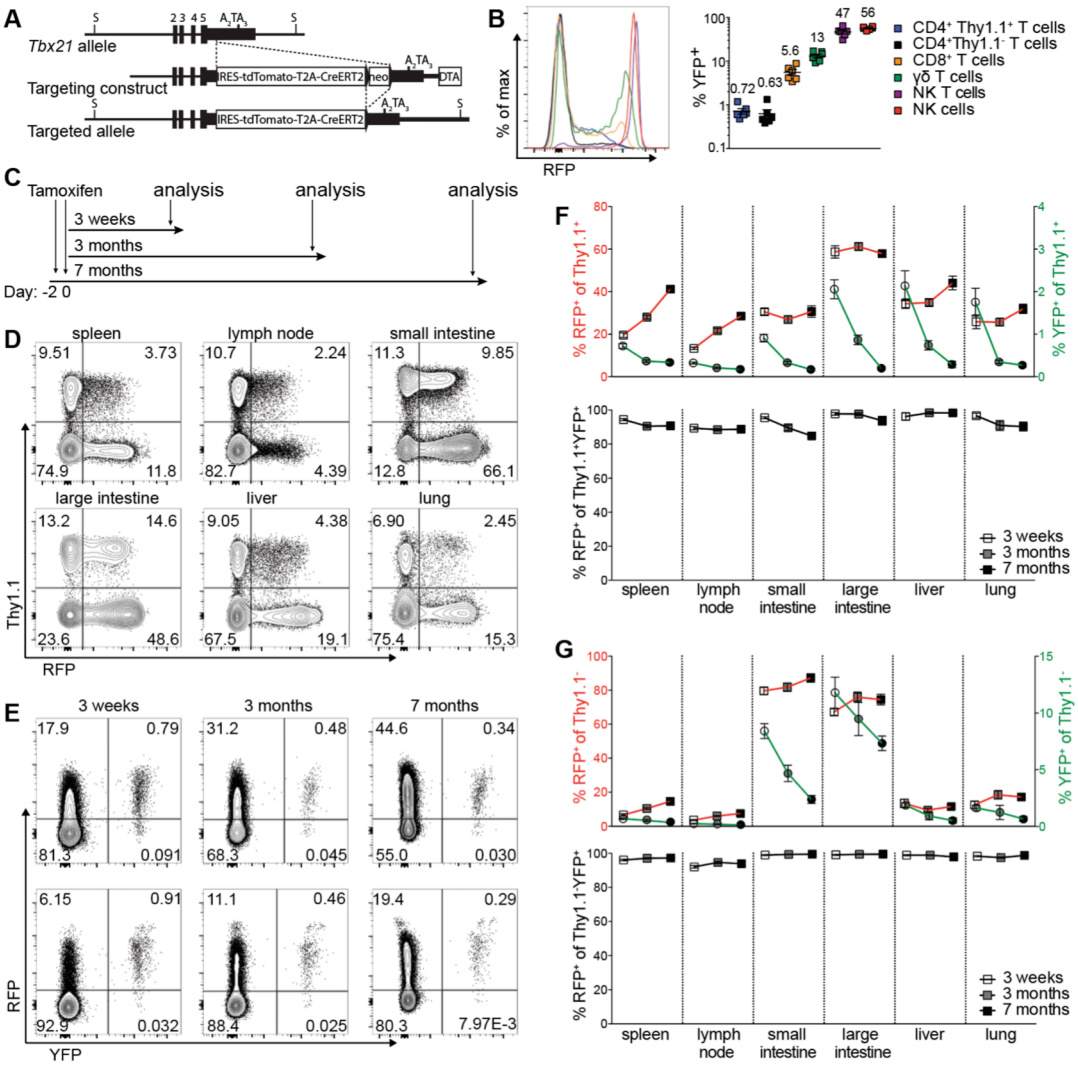
A
Tbx21 allele
Targeting construct
Targeted allele
IRES-tdTomato-T2A-CreERT2
neo
DTA
B
% of max
RFP
% YFP+
CD4+ Thy1.1+ T cells
CD4+Thy1.1- T cells
CD8+ T cells
γδ T cells
NK T cells
NK cells
C
Tamoxifen
analysis
3 weeks
3 months
7 months
Day: -2 0
D
spleen
lymph node
small intestine
large intestine
liver
lung
Thy1.1
RFP
E
3 weeks
3 months
7 months
RFP
YFP
F
% RFP+ of Thy1.1+
% YFP+ of Thy1.1+
% RFP+ of Thy1.1+YFP+
3 weeks
3 months
7 months
spleen
lymph node
small intestine
large intestine
liver
lung
G
% RFP+ of Thy1.1-
% YFP+ of Thy1.1-
% RFP+ of Thy1.1-YFP+

Figure 4.2. Analysis of T-bet$^+$ Treg cells in *Tbx21$^{RFP\text{-}CreERT2}$* reporter mice. **A**, Endogenous T-bet protein levels in select immune cell types in *Tbx21$^{RFP\text{-}CreERT2}$* mice. **B**, *Tbx21$^{RFP\text{-}CreERT2}$* mice were orally gavaged with tamoxifen on days -2 and 0. Three weeks later, splenic cells were fixed and stained for T-bet. Gray shaded histograms show T-bet expression in the bulk indicated cell types; open histograms show T-bet expression in the YFP$^+$ cells of each indicated cell type. **C**, Fate mapping schematic for experiments described in Figure 1. **D**, Representative flow cytometric analysis of T-bet expression in GATA3$^+$ (blue gate, left, and histogram, right) and RORγt$^+$ (black gate, left, and histogram, right) CD4$^+$Foxp3$^+$ cells isolated from the large intestine laminia propria. **E,F**, Quantification of percent RFP$^+$ cells among GFP$^+$ TCRβ$^+$ PBS-57 CD1d tetramer$^-$ CD4$^+$ Thy1.1$^+$ (**E**) and Thy1.1$^-$ (**F**) cells in *Tbx21$^{RFP\text{-}CreERT2}$Rorc$^{GFP/WT}$* mice. **G**, Representative flow cytometric analysis of CD4$^+$Thy1.1$^+$ (above) and Thy1.1$^-$ (below) cells as quantified in (**E-F**). **H**, Representative flow cytometry analysis of splenic CD4$^+$Thy1.1$^+$ cells. **I**, Percent CD44^{hi}CD62L^{lo} among Thy1.1$^+$ cells (above) and the percent RFP$^+$ among CD44^{hi}CD62L^{lo} Thy1.1$^+$ cells (below) in *Tbx21$^{RFP\text{-}CreERT2}$* three weeks (white squares), three months (gray squares), and seven months (black squares) post tx treatment. The data is representative of 2 independent experiments with at least 5 mice each (**A-B,H**); or represent the combined results from two independent experiments with at least 4 mice each (**D-G**).

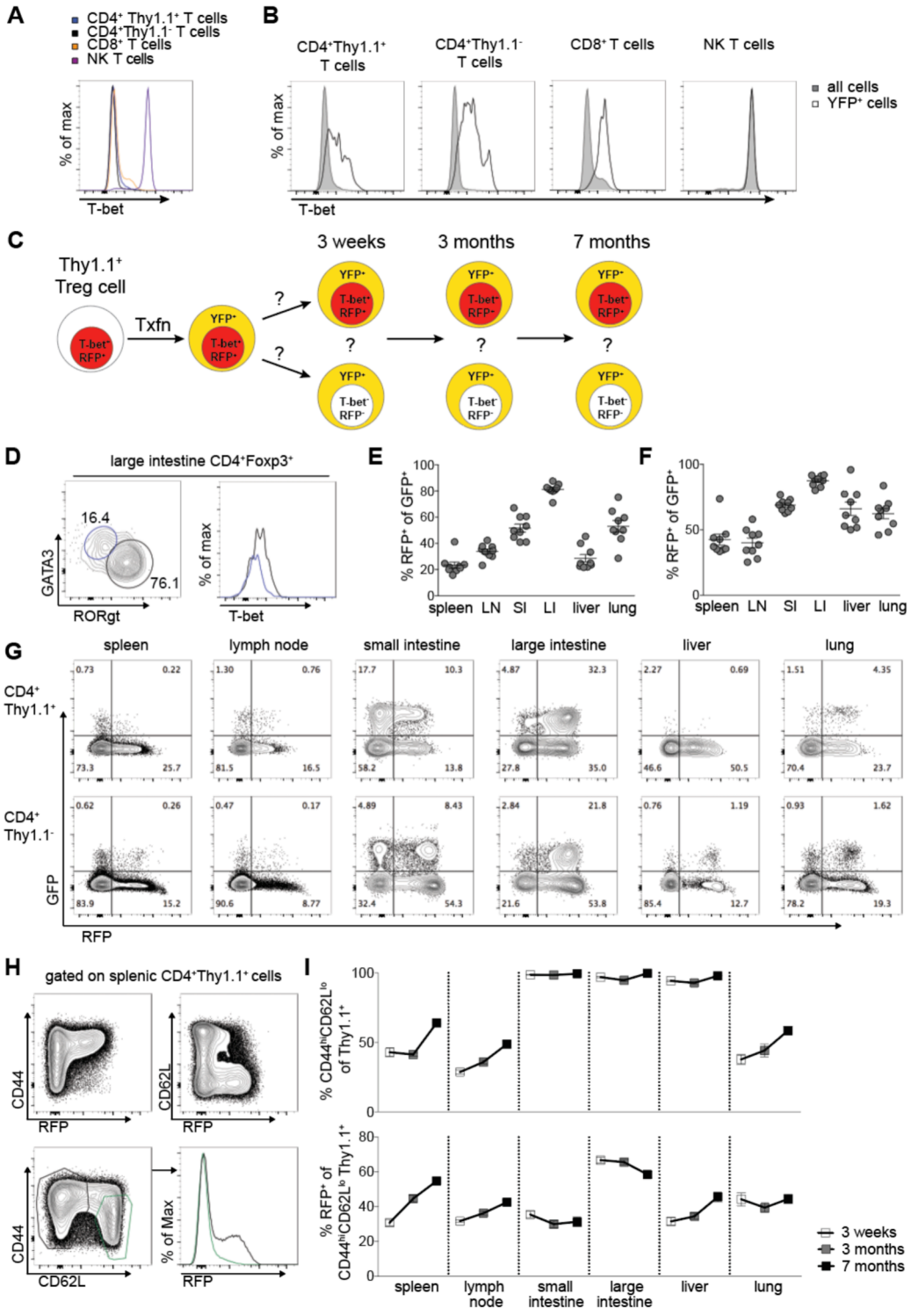
A
CD4+ Thy1.1+ T cells
CD4+Thy1.1- T cells
CD8+ T cells
NK T cells
% of max
T-bet
B
CD4+Thy1.1+ T cells
CD4+Thy1.1- T cells
CD8+ T cells
NK T cells
all cells
YFP+ cells
% of max
T-bet
C
Thy1.1+ Treg cell
Txfn
T-bet+ RFP+
YFP+
3 weeks
3 months
7 months
T-bet- RFP-
D
large intestine CD4+Foxp3+
16.4
76.1
GATA3
RORgt
% of max
T-bet
E
% RFP+ of GFP+
spleen LN SI LI liver lung
F
% RFP+ of GFP+
spleen LN SI LI liver lung
G
spleen
lymph node
small intestine
large intestine
liver
lung
CD4+ Thy1.1+
CD4+ Thy1.1-
GFP
RFP
H
gated on splenic CD4+Thy1.1+ cells
CD44
RFP
CD62L
RFP
CD44
CD62L
% of Max
RFP
I
% CD44hiCD62Llo of Thy1.1+
% RFP+ of CD44hiCD62Llo Thy1.1+
spleen
lymph node
small intestine
large intestine
liver
lung
3 weeks
3 months
7 months

RFP$^+$ cells among CD44^{hi}CD62L^{lo} effectors (Figure 4.2I). In contrast to a previous report, three weeks post tamoxifen administration we found the vast majority of both YFP-labeled Treg cells and effector CD4$^+$ T cells continued to express RFP (Figure 4.1E-G and Figure 4.2B) (Yu et al., 2015). Furthermore, the percentage of YFP$^+$ cells expressing RFP was similarly high at three and seven months post treatment (Figure 4.1E,F). These results indicated T-bet expression in YFP-labeled Treg cells to be remarkably stable as it was in effector CD4 T cells (Figure 4.1G).

At the same time, YFP-tagged Treg cells as a percent of total Treg cells decreased dramatically between the three week and seven month time points, particularly in non-lymphoid tissues even as the relative T-bet-expressing (RFP$^+$) cell population size remained the same (Figure 4.1F). Thus, in contrast to the bulk peripheral Treg cell pool in adult mice, which is largely self-sustaining (Rubtsov et al., 2010), continual Treg cell recruitment into the T-bet$^+$ subset balances out rapid turnover of cells over time.

An unstable T-bet^{lo} intermediate precedes stable T-bet expression in Treg cells

The presence of small percentages of YFP$^+$RFP$^-$ cells lacking T-bet three weeks post gavage (Figure 4.1E,F) suggested that some Treg cells, in which T-bet expression had been induced at the time of, or immediately prior to tamoxifen administration, might have subsequently become T-bet (RFP)$^-$ due to a transient unstable T-bet expression. Such a scenario would reconcile the above result with the aforementioned previously published study, in which highly efficient recombination mediated by a *Tbx21* BAC transgene-encoded CreERT2 revealed considerable instability of T-bet expression in Treg cells

(Yu et al., 2015). Indeed, we observed that the T-bet expressing (RFP^+) Treg cell population in *Tbx21*$^{RFP\text{-}CreERT2}$ mice contained an RFP^{lo} cell subset, which did not express the T-bet-dependent chemokine receptor CXCR3, and $RFP^{hi}CXCR3^+$ cells (Figure 4.3A). Although both populations expressed high levels of CD44, indicating TCR-dependent peripheral activation (Levine et al., 2014; Vahl et al., 2014), CD44 MFI was slightly higher whereas CD62L expression was slightly lower on T-bet^{hi} (RFP^{hi}) $CXCR3^+$ cells suggesting that the latter represented a more differentiated T-bet^+ Treg cell state, whereas T-bet^{lo} (RFP^{lo}) $CXCR3^-$ cells were likely a transient differentiation intermediate (Figure 4.3B,C). Consistent with this possibility, ~40% of FACS-sorted $RFP^{lo}CXCR3^-$ Treg cells lost RFP expression within 14 days following transfer into lymphoreplete hosts, whereas 17% up-regulated T-bet to become $RFP^{hi}CXCR3^+$ (Figure 4.3D, E). In contrast, the vast majority of Tbet^{hi} (RFP^{hi}) $CXCR3^+$ Treg cells retained high T-bet expression. Importantly, the fact that transferred bulk T-bet^{hi} Treg cells behaved the same in terms of stability of T-bet expression as YFP-labeled Treg cells in intact *Tbx21*$^{RFP\text{-}CreERT2}$ mice indicates that YFP-labeled cells accurately represent the T-bet^{hi} population on the whole. Notably, populations of $RFP^{lo}CXCR3^-$ and YFP^+RFP^- cells were also observed within the $CD4^+Thy1.1^-$ non-Treg cell population (Figure 4.3A), suggesting that rather than belying unique instability of T-bet^{lo} Treg cells they instead are indicative of the general, gradual process of peripheral $CD4^+$ T cell effector differentiation, consistent with studies demonstrating up-regulation of both GATA3 and T-bet prior to eventual T_H1 or T_H2 differentiation or RORγt and Foxp3 prior to T_H17 or Treg cell commitment (Hwang et al., 2005; Zhou et al., 2008). Indeed, RNA-seq analysis revealed the characteristic gene expression pattern of $CD44^{hi}RFP^{lo}CXCR3^-$ Treg cells to be intermediate

Figure 4.3. T-bet^{lo} cells likely represent a transient unstable intermediate in the differentiation of stably T-bet^{hi} Treg cells.
A, Representative flow cytometric analysis of the indicated cell subsets, gated on TCRβ^{+} PBS-57-CD1d tetramer^{-} CD4^{+} cells. **B-C**, CD44 median fluorescence intensity (MFI) on (**B**) and percent CD62L^{hi} (**C**) RFP^{-}CXCR3^{-} (gray shaded histogram and squares), RFP^{lo}CXCR3^{-} (open black histogram and squares), and RFP^{hi}CXCR3^{+} (open red histogram and squares) TCRβ^{+} PBS-57-CD1d tetramer^{-} CD4^{+} Thy1.1^{+} splenic cells. **D**, CD62L^{hi}CD44^{lo}RFP^{-}, CD44^{hi}RFP^{-}, CD44^{hi}RFP^{lo}CXCR3^{-}, and CD44^{hi}RFP^{hi}CXCR3^{hi} Thy1.1^{+} cells were FACS-sorted and transferred into lymphoreplete hosts. Flow cytometric analyses show Thy1.1^{+} cells of the indicated sorted subsets (above) from pooled spleens and lymph nodes 14 days after transfer. **E**, Quantification of data in (**D**). *p* values were calculated using Student's *t* test (*** denotes *p* values <0.001). The data is representative of 2 independent experiments with at least 5 mice each (**A-C**) or represent the combined results from two independent experiments with at least 2 mice per group each (**D,E**). **F**, Differential RNA expression between CD44^{hi}RFP^{-} and CD44^{hi}RFP^{hi}CXCR3^{+} Treg cells sorted from pooled spleens and lymph nodes of *Tbx21$^{RFP\text{-}CreERT2}$* mice. All genes significantly up- or down-regulated are indicated in red and blue. The number of genes significantly up (red) or down (blue) in CD44^{hi}RFP^{hi}CXCR3^{+} vs CD44^{hi}RFP^{-} are indicated. **G**, Expression of the 288 genes up ≥ 1.5-fold (left) or 184 genes down ≤ 1.5-fold (right) in CD44^{hi}RFP^{hi}CXCR3^{+} vs. CD44^{hi}RFP^{-} cells. For (**G)**, genes with a mean expression value < 15 were excluded from analysis. *p* values were calculated using paired Student's *t* test.

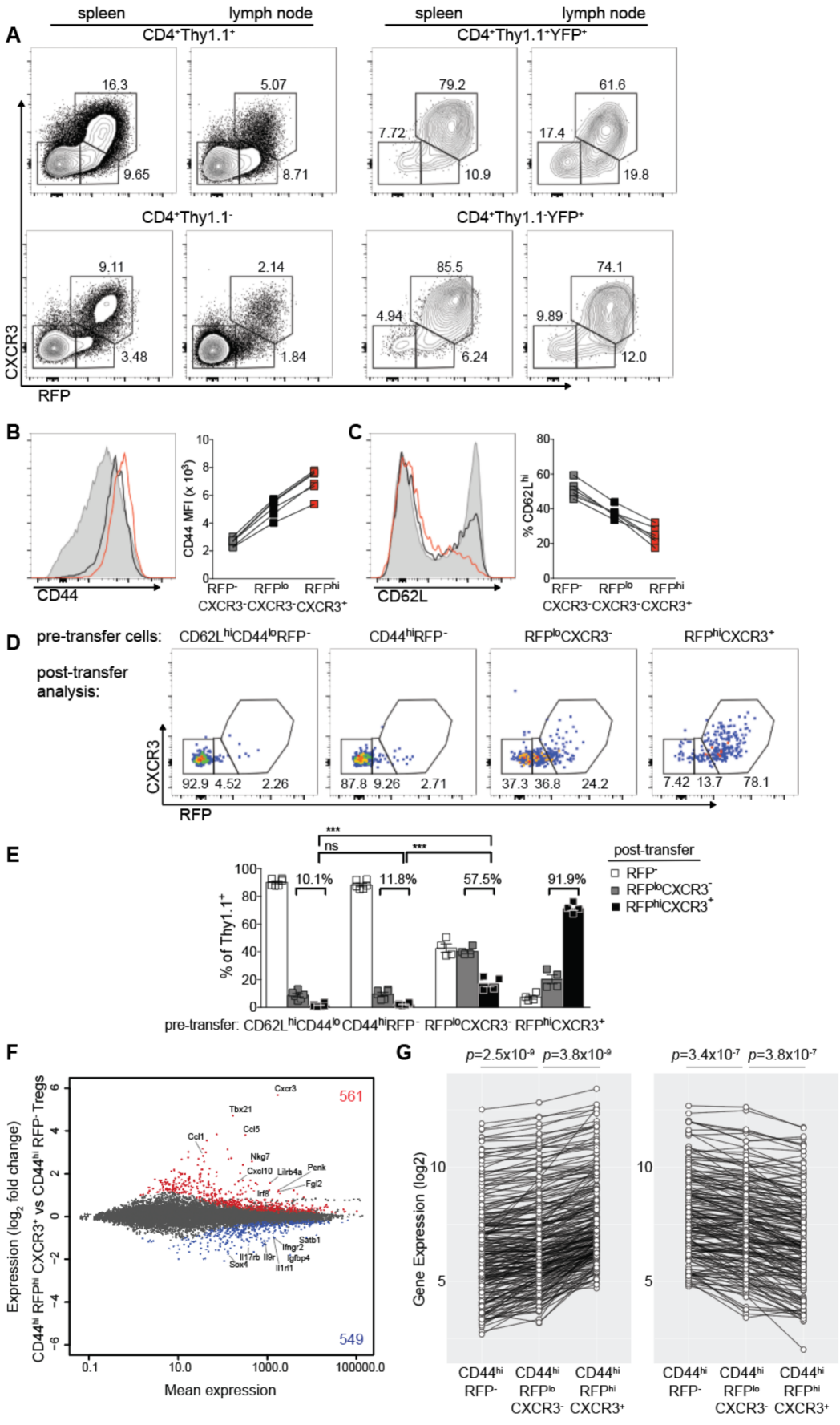
A
spleen
lymph node
CD4+Thy1.1+
CD4+Thy1.1+YFP+
CD4+Thy1.1-
CD4+Thy1.1-YFP+
16.3
9.65
5.07
8.71
79.2
7.72
10.9
61.6
17.4
19.8
9.11
3.48
2.14
1.84
85.5
4.94
6.24
74.1
9.89
12.0
CXCR3
RFP
B
CD44
CD44 MFI (x 10³)
RFP- RFPlo RFPhi
CXCR3- CXCR3- CXCR3+
C
CD62L
% CD62Lhi
RFP- RFPlo RFPhi
CXCR3- CXCR3- CXCR3+
D
pre-transfer cells:
CD62LhiCD44loRFP-
CD44hiRFP-
RFPloCXCR3-
RFPhiCXCR3+
post-transfer analysis:
CXCR3
RFP
92.9 4.52 2.26
87.8 9.26 2.71
37.3 36.8 24.2
7.42 13.7 78.1
E
***
ns
***
post-transfer
RFP-
RFPloCXCR3-
RFPhiCXCR3+
% of Thy1.1+
10.1%
11.8%
57.5%
91.9%
pre-transfer: CD62LhiCD44lo CD44hiRFP- RFPloCXCR3- RFPhiCXCR3+
F
Expression (log2 fold change)
CD44hi RFPhi CXCR3+ vs CD44hi RFP- Tregs
Cxcr3
Tbx21
Ccl5
Ccl1
Nkg7
Cxcl10
Lilrb4a
Penk
Fgl2
Irf8
Satb1
Ifngr2
Il17rb
Il9r
Fgfbp4
Sox4
Il1r1
561
549
0.1
10.0
1000.0
100000.0
Mean expression
G
p=2.5x10-9
p=3.8x10-9
p=3.4x10-7
p=3.8x10-7
Gene Expression (log2)
10
5
CD44hi RFP-
CD44hi RFPlo CXCR3-
CD44hi RFPhi CXCR3+

between that of CD44^{hi}RFP^{-} cells lacking T-bet expression and CD44^{hi}RFP^{hi}CXCR3^{+} cells (Figure 4.3F,G). Together, these studies indicate that following peripheral activation, some Treg cells upregulate T-bet, and after passing through an intermediate state with unstable and relatively low levels of T-bet expression, differentiate into T_H1-like Treg cells characterized by stable and heritable expression of high amounts of T-bet.

Stable T-bet expression in Treg cells during T_H2-polarizing infection

These results raised the question of whether the observed stability of T-bet expression in Treg cells at steady state in mice on a T_H1-prone C57BL/6 genetic background would be maintained under polarizing conditions promoting an alternative effector CD4 T cell fate. To address this question, we performed fate mapping in *Tbx21$^{RFP\text{-}CreERT2}$* mice during *Nippostrongylus brasiliensis* (*Nb*) infection, known to induce a strongly T_H2-polarized systemic and local immune response, and assessed whether T-bet^{+} Treg cells would continue to retain or would instead lose T-bet expression.

Accordingly, we treated *Tbx21$^{RFP\text{-}CreERT2}$* mice with tamoxifen to tag a cohort of T-bet^{+} Treg cells with YFP three weeks prior to infection and analyzed mice at the peak of the T cell response (Figure 4.4A). We reasoned that if pre-existent T-bet^{+} Treg cells were "plastic" and down-regulated T-bet during *Nb* infection, the percent T-bet (RFP)$^{-}$ of YFP^{+} Treg cells would notably increase—while the percent RFP^{+} of YFP-tagged Treg cells would decrease—in infected compared to control uninfected mice. By day 9, robust T cell activation (and production of the T_H2 cytokines IL-4, IL-13, and IL-5) was apparent in spleens and lungs of infected mice, with dramatically increased percentages of CD44^{hi} CD4 T cells that predominantly, as expected, did not

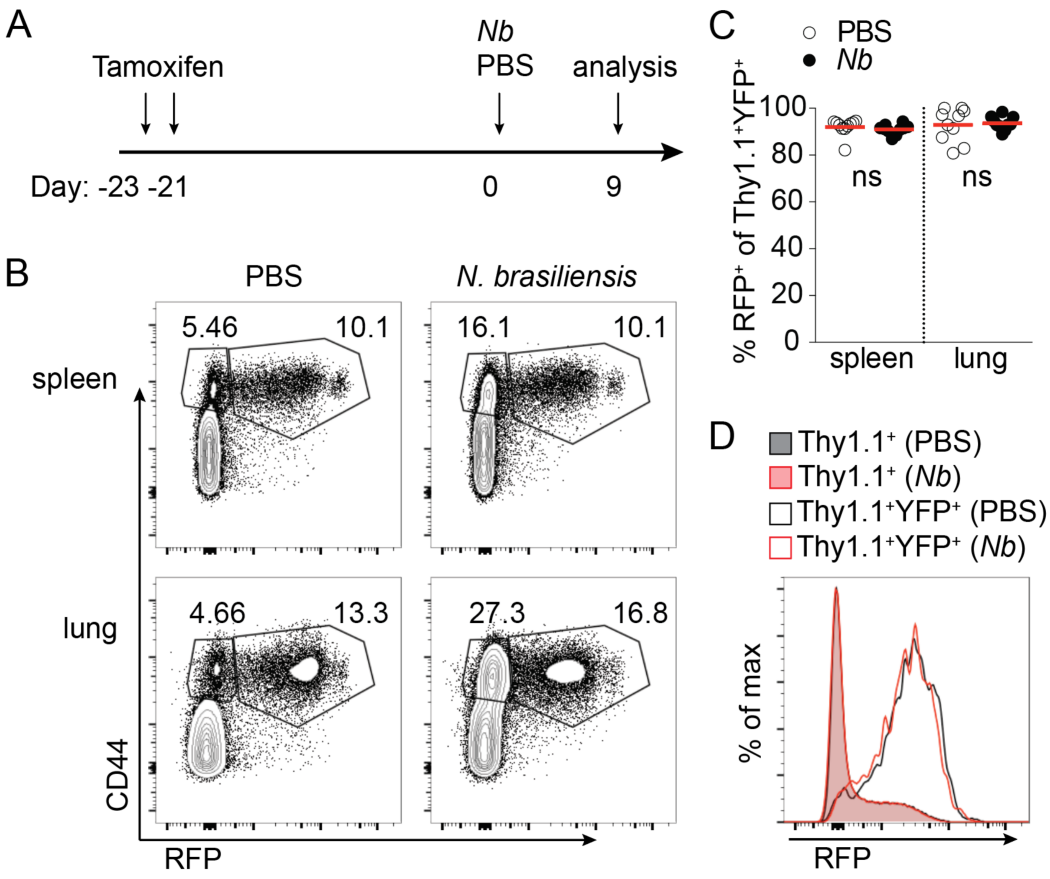

Figure 4.4. Stability of the T_H1-like phenotype during helminthic infection.

A, Schematic of experiments combining tamoxifen treatment with *Nb* infection in *Tbx21*$^{RFP\text{-}CreERT2}$ mice. **B**, Representative flow cytometry of splenic (above) and lung (below) TCRβ$^+$ PBS-57-CD1d tetramer$^-$ CD4$^+$ Thy1.1$^-$ cells of control PBS-treated (left) and *Nb*-infected (right) mice. **C**, Quantification of the percent RFP$^+$ cells among YFP$^+$ TCRβ$^+$ PBS-57-CD1d tetramer$^-$ CD4$^+$ Thy1.1$^+$ cells in control PBS-treated (white circles) and *Nb*-infected (black circles) mice. D, Representative histograms of RFP expression on total TCRβ$^+$ PBS-57-CD1d tetramer$^-$ CD4$^+$ Thy1.1$^+$ (shaded histograms) or Th1.1$^+$YFP$^+$ (open histograms) cells from spleens of *Nb*-infected (red) or PBS-treated control (black) mice. Each circle represents an individual mouse; the horizontal bars represent mean value; *p* values were calculated using Student's *t* test (***, **, and * denotes *p* values <0.001, 0.01, and 0.05, respectively); the data shown represent the combined results of 2 independent experiments with at least 3 mice per group each.

express T-bet (RFP) (Figure 4.4B, data not shown). Strikingly, YFP-labeled Treg cells demonstrated no decrease in RFP expression, either as a percentage of YFP^+ cells or on a per cell basis (Figure 4.4C,D). This was the case despite Treg cell activation in response to infection evidenced by increased percentages of $CD44^{hi}CD62L^{lo}$ Treg cells in *Nb* challenged compared to control mice (data not shown). Similar stability of T-bet expression was observed for effector CD4 T-bet $(RFP)^+$ T cells (data not shown). These data indicate that T-bet expression in Treg cells did not represent a readily reversible activation state. Instead, YFP-marked T-bet-expressing Treg cells exhibited intrinsic stability typical of a differentiated cell state even in face of type 2 inflammation caused by helminthic infection promoting an alternative effector T cell fate.

De novo differentiation of T-bet$^+$ Treg cells upon T_H1-polarizing infection

The idea of peripheral differentiation of steady state T-bet^+ Treg cells in response to "self" was consistent with their numbers in spleens and lymph nodes being unaltered upon antibiotic treatment (see below) and with a recent report that these cells were comparably prominent in the secondary lymphoid organs in germ-free mice on an antigen-free diet and in control mice (Kim et al., 2016). In addition to these steady state cues, infection with intracellular pathogens can also increase numbers of T-bet^+ Treg cells (Hall et al., 2012; Koch et al., 2012; Shafiani et al., 2013). These findings raise the question whether infection-associated increases in the T-bet^+ Treg cell subset represent an expansion of the pre-existent pool or *de novo* differentiation from T-bet-negative Treg precursors, and whether these processes result in a stable or reversible T-bet expression.

To answer these questions we performed fate-mapping studies in *Tbx21*$^{RFP\text{-}CreERT2}$ mice during intracellular bacteria *Listeria monocytogenes* (*Lm*) infection, previously demonstrated to increase numbers of T-bet$^+$ Treg cells which were notably pathogen non-specific (Ertelt et al., 2009; Shafiani et al., 2013). Consistent with previous reports, *Lm* infection increased the proportion and absolute numbers of T-bet (RFP) expressing Treg cells in the spleen and liver (Figure 4.5B,C and data not shown) (Koch et al., 2012). To determine the origin of these *Lm* infection-induced T-bet (RFP)$^+$ cells we treated *Tbx21*$^{RFP\text{-}CreERT2}$ mice with tamoxifen to tag a cohort of T-bet$^+$ Treg cells with YFP three weeks prior to infection and analyzed mice at the peak of the T cell response (Figure 4.5A). We reasoned that if the pre-existent T-bet$^+$ Treg cell pool expanded in response to infection, the percent YFP-tagged Treg cells would increase in parallel to the increase in T-bet (RFP)$^+$ cells; on the other hand, if the percent RFP$^+$ cells increased while the percent YFP$^+$ cells did not, this would imply that infection induced up-regulation of T-bet in previously T-bet$^-$ Treg cells.

Upon *Lm* challenge, splenic and liver subsets of T-bet (RFP)$^+$ Treg cells and effector T-bet (RFP)$^+$ CD4$^+$ T cells increased markedly; however, the proportion of YFP$^+$ cells remained unchanged in both populations (Figure 4.5B-D). This pattern was indicative of *de novo* differentiation of T-bet$^+$ Treg cells from T-bet$^-$ Treg precursors in parallel with the expected differentiation of effector T_H1 cells from naïve T cells. It is important to note that—as opposed to *Nb* infection—T-bet$^+$ Treg cells tagged with YFP prior to *Lm* infection were exposed to, and did sense, T_H1 inflammation as evidenced by increased T-bet and CXCR3 expression on a per cell basis despite the fact that the relative proportion of YFP$^+$ T-bet$^+$ Treg cells did not increase (Figure 4.5E). However,

Figure 4.5. *Listeria monocytogenes* infection drives *de novo* differentiation of T-bet-expressing Treg cells.
A, Schematic of the experiments combining tamoxifen (tx) treatment with *Lm* infection in *Tbx21*$^{RFP\text{-}CreERT2}$ mice. **B**, Representative flow cytometry analysis of splenic TCRβ$^+$ PBS-57-CD1d tetramer$^-$ CD4$^+$ Thy1.1$^+$ (left) and Thy1.1$^-$ (right) cells of control PBS-treated (above) and *Lm*-infected (below) mice. Numbers indicate percent RFP$^+$ and YFP$^+$ cells. **C-D**, Quantification of percent RFP$^+$ (top) and YFP$^+$ (middle) cells and the YFP$^+$/RFP$^+$ ratio (below) for Thy1.1$^+$ (**C**) and Thy1.1$^-$ (**D**) CD4$^+$ cells in spleens and livers of experimental and control mice. **E**, Representative histograms of RFP and CXCR3 expression on total TCRβ$^+$ PBS-57-CD1d tetramer$^-$ CD4$^+$ Thy1.1$^+$ (shaded histograms) or Th1.1$^+$YFP$^+$ (open histograms) cells from spleens of *Lm*-infected (red) or PBS-treated control (black) mice. **F-H**, Analysis of IL-10^{eGFP} expression in *Tbx21*$^{RFP\text{-}CreERT2}$*IL-10*^{eGFP} mice treated with tx and challenged with *Lm* or PBS as in (**A**). **F**, Flow cytometry plots gated on splenic TCRβ$^+$ PBS-57-CD1d tetramer$^-$ CD4$^+$ Thy1.1$^+$ (above) and Thy1.1$^+$YFP$^+$ (below) cells in PBS (left) and *Lm* (right) treated mice. **G**, Percent RFP$^-$eGFP$^+$ and RFP$^+$eGFP$^+$ cells among Thy1.1$^+$ cells, as gated in (**F**, above). **H**, Percent eGFP$^+$ cells among Thy1.1$^+$YFP$^+$ cells, as gated in (**F**, below). **I-J**, T-bet fate mapping during *Lm* infection. **I**, Schematic of experimental setup. CD62L^{hi}CD44^{lo}RFP$^-$, CD44^{hi}RFP$^-$, and CD44^{hi}RFP^{hi}CXCR3^{hi} Thy1.1$^+$ cells were FACS-sorted from pooled spleens and lymph nodes of *Tbx21*$^{RFP\text{-}CreERT2}$ mice and transferred into lymphoreplete hosts one day before i.v. injection of *Lm* or PBS control. **J**, Representative flow cytometry plots of Thy1.1$^+$ cells in spleens of PBS-treated (left) or Lm-infected (right) host mice on day 9. Transferred cell populations are indicated on the left. Each circle or square represents an individual mouse; the horizontal bars represent mean value; *p* values were calculated using Student's *t* test (ns – not significant, denotes *p* value > 0.05); the data shown represent the combined results of 2 independent experiments with at least 5 mice per group each (**B-D**), or 2 experiment with 4 mice per group each (**F-H**), or 2 experiments with at least 2 mice per group each.

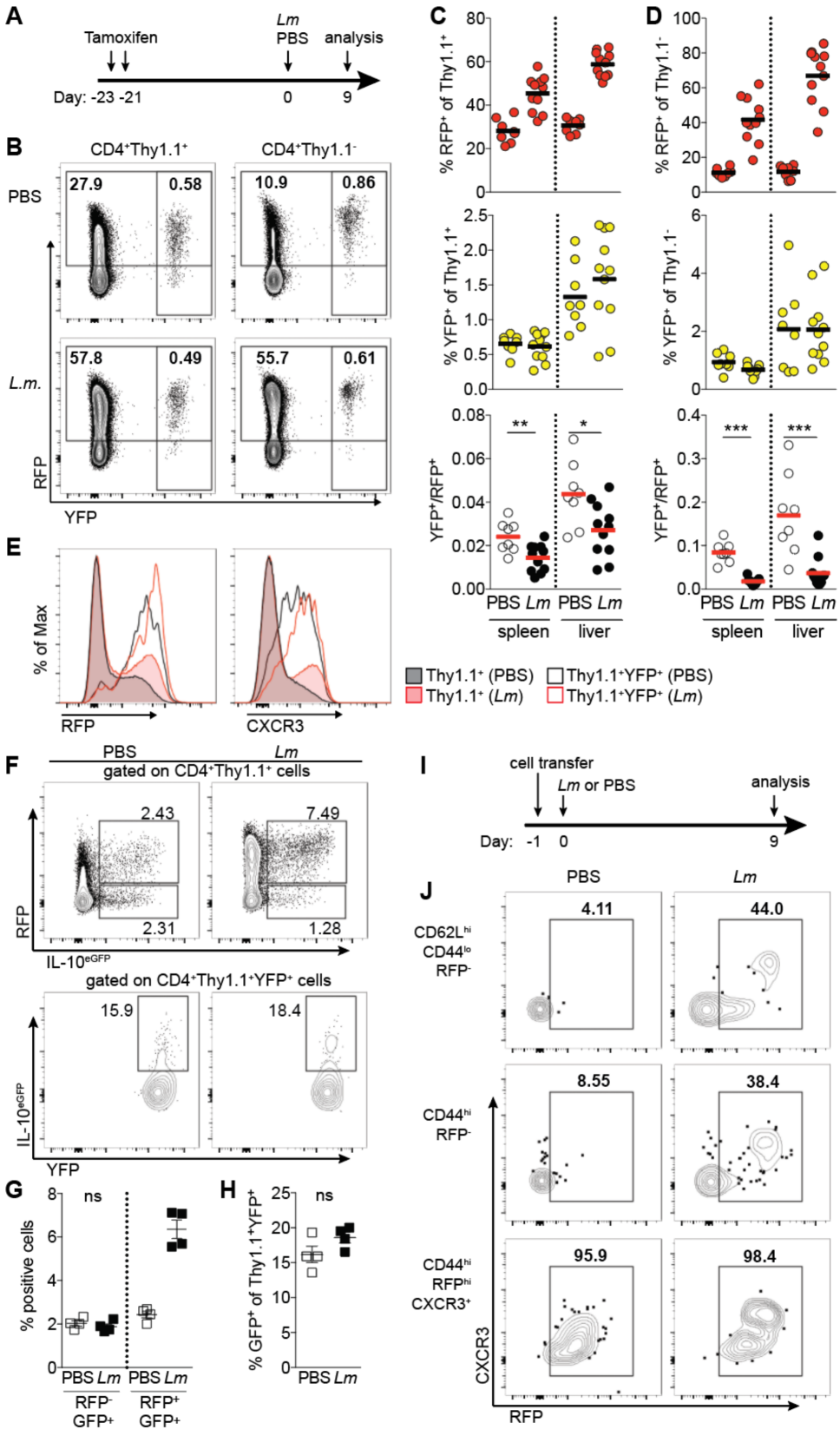
A
Tamoxifen
Lm
PBS
analysis
Day: -23 -21
0
9
B
CD4+Thy1.1+
CD4+Thy1.1-
PBS
L.m.
27.9
0.58
10.9
0.86
57.8
0.49
55.7
0.61
RFP
YFP
C
% RFP+ of Thy1.1+
% YFP+ of Thy1.1+
YFP+/RFP+
D
% RFP+ of Thy1.1-
% YFP+ of Thy1.1-
YFP+/RFP+
**
*
***
***
PBS Lm PBS Lm
spleen
liver
E
% of Max
RFP
CXCR3
Thy1.1+ (PBS)
Thy1.1+ (Lm)
Thy1.1+YFP+ (PBS)
Thy1.1+YFP+ (Lm)
F
PBS
Lm
gated on CD4+Thy1.1+ cells
2.43
7.49
2.31
1.28
RFP
IL-10eGFP
gated on CD4+Thy1.1+YFP+ cells
15.9
18.4
IL-10eGFP
YFP
G
% positive cells
ns
PBS Lm PBS Lm
RFP- GFP+
RFP+ GFP+
H
% GFP+ of Thy1.1+YFP+
ns
PBS Lm
I
cell transfer
Lm or PBS
analysis
Day: -1 0
9
J
PBS
Lm
CD62Lhi CD44lo RFP-
4.11
44.0
CD44hi RFP-
8.55
38.4
CD44hi RFPhi CXCR3+
95.9
98.4
CXCR3
RFP

this increase in T-bet MFI and CXCR3 expression was not associated with obviously increased expression of effectors of suppressor function, as exemplified by the fact that the same fate mapping strategy applied to *Tbx21*$^{RFP\text{-}CreERT2}$*IL-10*$^{eGFP/WT}$ mice expressing previously described eGFP as a transcriptional IL-10 knock-in reporter revealed no increase in IL-10^{eGFP+} cells among pre-labeled Thy1.1^{+}YFP^{+} cells even as total percentages of RFP^{+}IL-10^{eGFP+} Treg cells increased ~3-fold (Figure 4.5F-H)(Kamanaka et al., 2006). Similar results were obtained during lymphocytic choriomeningitis virus (LCMV) infection (data not shown), suggesting this to be a general—rather than *Lm*-specific—phenomenon of Treg cell responsiveness to acute infection with T_H1-polarizing pathogens.

To determine whether "naïve" or activated T-bet (RFP)$^{-}$ Treg cell subsets gave rise to *Lm*-induced RFP^{+} cells, we purified by FACS naïve-like CD44^{lo}CD62L^{hi} T-bet (RFP)$^{-}$ and effector-like CD44^{hi}RFP^{-} Treg cells and transferred them into congenically-marked lymphoreplete hosts one day before *Lm* infection (Figure 4.5I). We found that both CD44^{lo}CD62L^{hi} and CD44^{hi} T-bet (RFP)$^{-}$ Treg cell subsets differentiated into RFP^{+}CXCR3^{+} cells in response to infection (Figure 4.5J). Thus, the increase in T-bet^{+} Treg cells observed following *Lm* infection appears to be the result of both naïve and effector T-bet^{-} Treg cell differentiation into T-bet^{+} Treg cells.

Persistence of Lm-induced T_H1-like Treg cells following resolution of infection

We next assessed whether Treg cells that upregulated T-bet and expanded during *Lm* infection would persist over time following resolution of infection and whether these cells were capable of mounting a recall response upon re-

infection. To address this question, we administered tamoxifen at the peak of the primary response to *Lm* infection (days 7 and 9) to preferentially label infection-induced T-bet$^+$ cells (data not shown) and assessed mice two months later, at which time the percent of splenic and liver Treg cells that were T-bet$^+$ had returned to roughly pre-infection levels (Figure 4.6A,B). As the T-bet$^+$ Treg cell pool is subject to considerable turnover in the course of two months (Figure 4.1), we reasoned that by day 60 post infection YFP$^+$ cells labeled at the peak of infection would be relatively enriched for infection-induced T-bet (RFP)$^+$ Treg cells compared to the bulk RFP$^+$ cell pool.

As expected, reinfection with *Lm* dramatically increased bulk effector T-bet$^+$ CD4 T cells and even more prominently increased the subset of cells tagged with YFP during primary infection, consistent with expansion of memory cells driving secondary increases in T-bet$^+$ cells (Figure 4.6C). Likewise, following secondary challenge we also observed an increase in T-bet$^+$ Treg cells, albeit less pronounced than that of effector CD4 T cells, with a similarly preferential expansion of YFP-tagged cells (Figure 4.6B). Consistent with the idea that secondary infection can cause reactivation of specifically T-bet$^+$ Treg cells, RFP$^+$IL10^{eGFP+} but not RFP$^-$IL10^{eGFP+} cells in *Tbx21*$^{RFP\text{-}CreERT2}$*IL-10*$^{eGFP/WT}$ mice increased upon rechallenge as they did during primary infection (Figure 4.6F,G). These results indicated that infectious episodes, by eliciting differentiation of distinctly responsive T-bet$^+$ Treg cells, further contribute to Treg cell heterogeneity.

To determine whether T-bet expression in these infection-induced T-bet$^+$ Treg cells was a stable feature of differentiation or was a reversible consequence of their activation secondary to infectious challenge conditions, we assessed RFP expression in YFP$^+$ Treg cells that had been labeled at the

Figure 4.6. Stable differentiation of T_H1-like effector Treg cells in response to *L. monocytogenes* infection.
A, A schematic of T-bet fate mapping during *Lm* infection; *Tbx21*$^{RFP\text{-}CreERT2}$ mice were infected i.v. with *Lm* or injected with PBS (control) on day 0, gavaged with tx on days 7 and 9 (**B-D**) or on days 37 and 39 (**E**); mice were re-infected with *Lm* or PBS on day 60, and analyzed on day 65. **B-C**, Percent RFP$^+$ (top) and YFP$^+$ (middle) cells and the YFP$^+$/RFP$^+$ ratio (below) for Thy1.1$^+$ (**B**) and Thy1.1$^-$ (**C**) CD4$^+$ cells in spleens and livers of mice treated with tx on days 7 and 9. **D**, Percent RFP$^+$ of CD4$^+$Thy1.1$^+$YFP$^+$ cells. **E**, Percent RFP$^+$ (top) and YFP$^+$ (middle) cells and the YFP$^+$/RFP$^+$ ratio (below) for Thy1.1$^+$ CD4$^+$ cells in spleens and livers of mice treated with tx on days 37 and 39. **F-G**, *Tbx21*$^{RFP\text{-}CreERT2}$*IL-10*^{eGFP} mice were challenged with *Lm* or PBS on day 0, rechallenged with PBS or *Lm* on day 60 and analyzed on day 65. Representative flow cyotometry plots gated on the indicated populations in *Tbx21*$^{RFP\text{-}CreERT2}$*IL-10*^{eGFP} mice, treated as indicated on the left. **G**, Percent RFP$^-$eGFP$^+$ and RFP$^+$eGFP$^+$ cells among Thy1.1$^+$ cells, as gated in (**F**). Each circle or square represents an individual mouse; the horizontal bars represent mean value; *p* values were calculated using Student's *t* test (***, **, and * denotes *p* values <0.001, 0.01, and 0.05, respectively; ns – not significant). The data represent the combined results from 4 independent experiments with at least 3 mice per group each (**B-D**) or combined results from 2 independent experiments with at least 5 mice per group each (**E**) or 3 mice per group each (**F-G**).

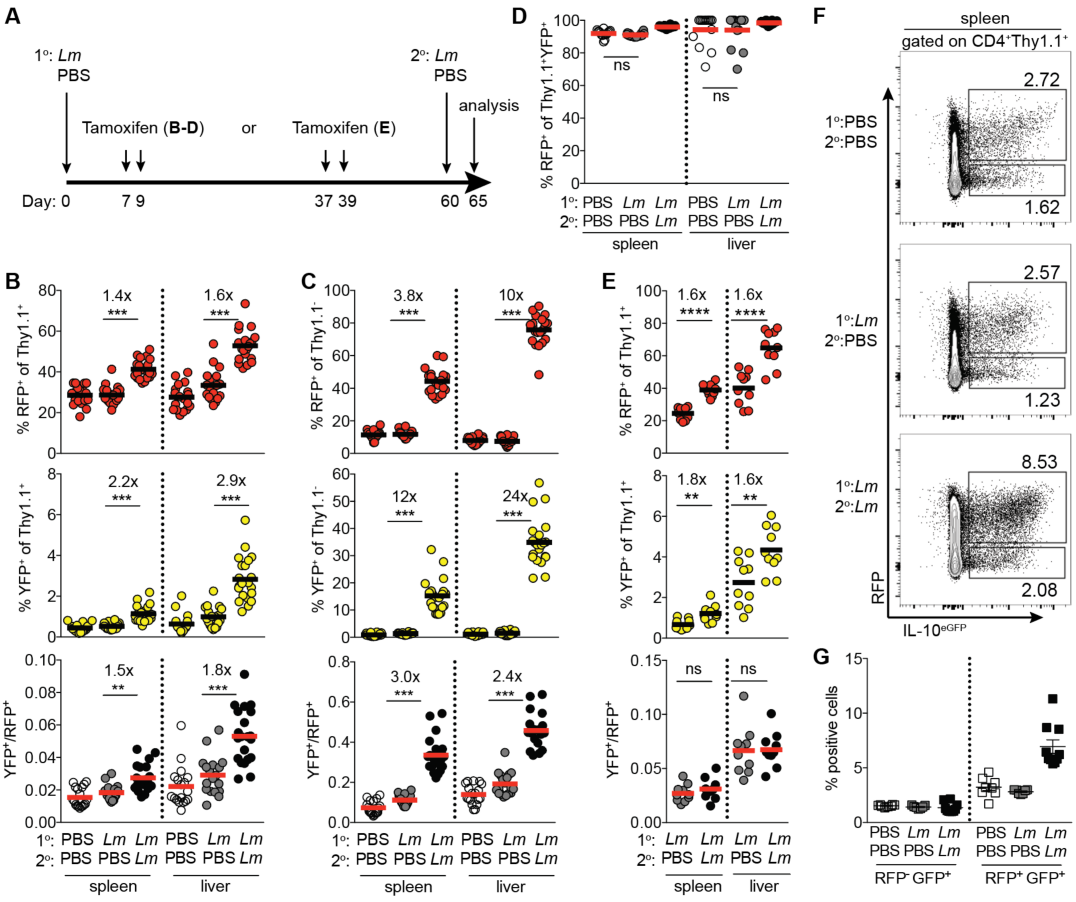
A
1°: Lm
PBS
Tamoxifen (B-D)
or
Tamoxifen (E)
2°: Lm
PBS
analysis
Day: 0
7 9
37 39
60 65
B
C
D
E
F
G
% RFP+ of Thy1.1+
% YFP+ of Thy1.1+
YFP+/RFP+
% RFP+ of Thy1.1+YFP+
1°: PBS Lm Lm PBS Lm Lm
2°: PBS PBS Lm PBS PBS Lm
spleen
liver
ns
1.4x
1.6x
2.2x
2.9x
1.5x
1.8x
3.8x
10x
12x
24x
3.0x
2.4x
1.6x
1.8x
spleen
gated on CD4+Thy1.1+
1°:PBS
2°:PBS
1°:Lm
2°:PBS
1°:Lm
2°:Lm
2.72
1.62
2.57
1.23
8.53
2.08
RFP
IL-10eGFP
% positive cells
RFP- GFP+
RFP+ GFP+

peak of the primary immune response to *Lm*. On day 65 following primary *Lm* infection, 91% and 94% of splenic and liver YFP$^+$ Treg cells continued to express T-bet, respectively, compared to 92% and 94% of splenic and liver YFP$^+$ Treg cells, respectively, in control PBS treated mice (Figure 4.6D). This finding strongly suggested that Treg cells which had become T-bet$^+$ during primary infection had maintained its expression following pathogen clearance and resolution of inflammation. To formally demonstrate this proposition, we infected mice with *Lm* and administered tamoxifen on days 37 and 39 following primary infection, three weeks prior to re-infection (Figure 4.6A). We reasoned that if expansion of T-bet$^+$ cells following secondary challenge was dependent on cells that acquired T-bet expression during primary infection and remained T-bet positive, reinfection would result in a parallel increase in bulk RFP$^+$ and YFP$^+$ Treg cell subsets, which indeed was the case (Figure 4.6E). Together, these studies demonstrate that bacterial infection did not expand a pre-existent, steady-state pool of T-bet$^+$ Treg cells, but caused *de novo* differentiation of T-bet$^-$ Treg cells into stable T-bet-expressing Treg cells uniquely suited for reactivation under conditions that drove their initial acquisition of T-bet. These results suggest that steady state differentiation in response to self-antigens and differentiation during infectious episodes represent two independent sources contributing to the population of T-bet$^+$ Treg cells.

T-bet ablation in Treg cells causes only a mild defect in suppressor function

Continuous peripheral generation of T-bet$^+$ Treg cells at steady state (Figure 4.1F) seemed to imply a particular function for T-bet$^+$ Treg cells in suppression

of spontaneous autoimmunity under physiologic conditions presumably imparted by T-bet itself. However, several studies have failed to identify changes in immune status upon ablation of a conditional *Tbx21* allele in Treg cells at steady state or in response to a variety of challenges (Colbeck et al., 2015; McPherson et al., 2015; Yu et al., 2015). To revisit this issue, we generated and analyzed *Foxp3*$^{YFP\text{-}Cre}$*Tbx21*$^{FL/FL}$ mice (Figure 4.7) (Intlekofer et al., 2008; Rubtsov et al., 2008). Although at 3 months of age these mice were healthy and clinically indistinguishable from littermate controls, they did exhibit mild T_H1 immune activation, with increased CD44^{hi} and CXCR3$^+$ CD4 T cell percentages (from 26% to 41% and 15% to 26%, respectively) and a selective two-fold increase in IFNg-producing CD4$^+$ T cells, whereas IFNg production by CD8$^+$ T cells and IL-2, IL-4, and IL-17 production by CD4$^+$ T cells remained unaffected (Figure 4.7). Thus, in our hands, in contrast to previous reports, T-bet expression moderately potentiates the ability of Treg cells to suppress spontaneous T_H1-type immune activation in unchallenged mice.

T-bet$^+$ Treg cells restrain severe T_H1-dependent autoimmune disease

It remained possible that T-bet deficiency in Treg cells, resulting in a mild increase in T_H1 responses and lacking clinical sequelae, may not fully reflect the functional importance of T_H1-like Treg cells, which may have a broader, but T-bet independent role in maintaining tolerance. We considered the possibility that T-bet$^+$ Treg cells may possess a distinct TCR repertoire that may allow them to suppress particular autoimmune responses even in the absence of T-bet induced gene expression and CXCR3-mediated localization. To test this idea, we sorted CD44^{hi}CXCR3 (T-bet)$^+$ and CD44^{hi}CXCR3 (T-bet)$^-$

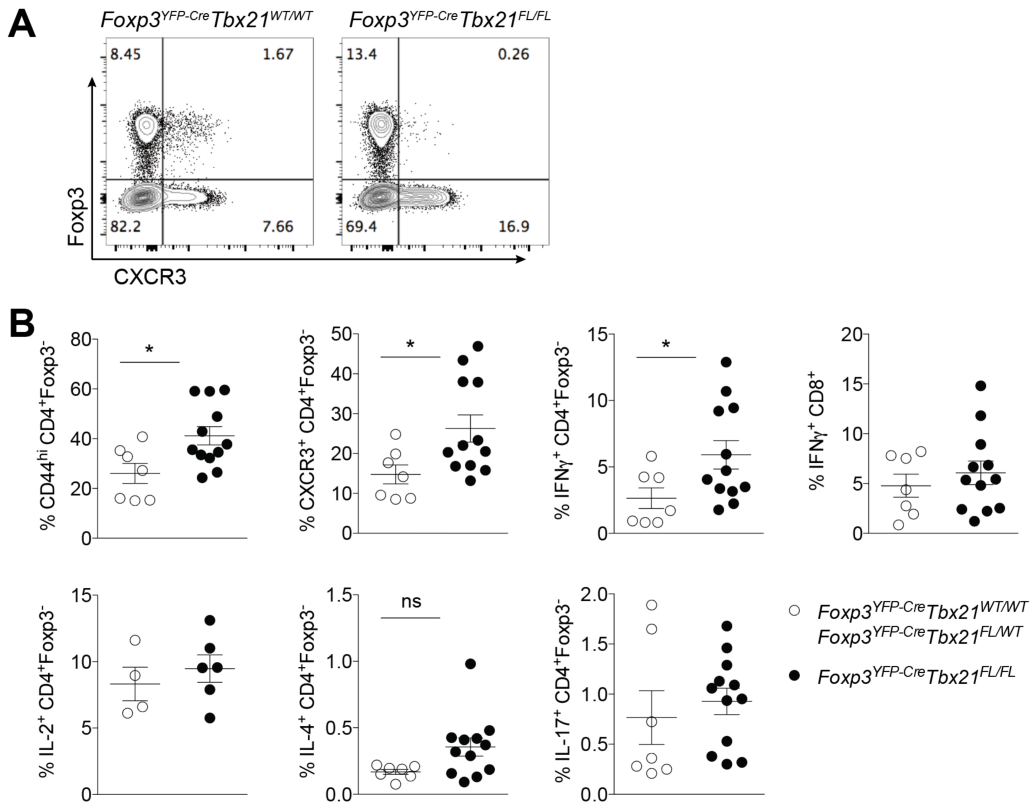

Figure 4.7. Mildly increased T_H1 cytokine production by T cells in mice lacking T-bet expression in Treg cells.

A, Representative flow cytometry plots of $CD4^+$ $TCR\beta^+$ PBS-57-loaded CD1d $tetramer^-$ cells in spleens of the indicated 2-3 month old mice. **B**, T cell activation, CXCR3 expression, and cytokine production in control *Foxp3*$^{YFP\text{-}Cre}$*Tbx21*$^{WT/WT}$ and *Foxp3*$^{YFP\text{-}Cre}$*Tbx21*$^{FL/WT}$ (white circles) and experimental *Foxp3*$^{YFP\text{-}Cre}$*Tbx21*$^{FL/FL}$ (black circles) mice. Each circle represents an individual mouse; error bars indicate SEM; *p* values were calculated using Student's *t* test (* denotes *p* value < 0.05; ns – not significant). The data represent the combined results from 3 independent experiments.

Treg and CD4 effector T cells from *Tcra*$^{+/-}$ mice expressing a Foxp3 reporter and the DO11.10 TCRβ chain transgene so that TCR diversity is limited to a single functional TCRα chain locus (Feng et al., 2015). Indeed, TCR repertoires in CD44^{hi}CXCR3^{+} and CD44^{hi}CXCR3^{-} Treg cell populations were distinct—unlike TCR repertoires in the effector T cell populations—suggesting that preferential recognition of particular antigens by T-bet^{+} Treg cells may, in addition to their unique transcriptional program and migratory properties, be an essential determinant of their suppressor capacity (Figure 4.8).

Therefore, we sought to determine the effect of eliminating the T-bet^{+} Treg cell population in its entirety. Since Treg cell suppressor function requires continuous expression of the *Foxp3* gene we generated *Tbx21*$^{tdTomato\text{-}T2A\text{-}Cre}$ knock-in mice (Figure 4.9A) and performed the reverse experiment to deleting T-bet in Foxp3-expressing cells, i.e. ablating Foxp3 expression in T-bet-expressing Treg cells. Indeed, Cre-mediated loss of Foxp3 expression in T-bet^{+} Treg cells in male *Tbx21*$^{RFP\text{-}Cre/RFP\text{-}Cre}$*Foxp3*^{FL} (hereafter referred to as *Tbx21*$^{RFP\text{-}Cre}$*Foxp3*^{FL}) mice resulted in a failure to thrive reflected in a decreased weight gain, a variable, patchy loss of hair pigmentation, and marked immune infiltration and pathology in the lung (Figure 4.10A,B and Figure 4.9B). These mice exhibited pronounced lymphadenopathy and T cell activation in the spleen, lymph nodes, and lungs when compared to littermate controls (Figure 4.10C,D and Figure 4.9). While significantly depleted of CXCR3^{+} cells, neither total Treg cell numbers nor numbers of CD44^{hi}CD62L^{lo} effector Treg cells were diminished (Figure 4.10E and Figure 4.9H). Importantly, this indicates that deletion of *Foxp3* in some 'exT-bet^{+}' Treg cells that had only transiently expressed low levels of T-bet and Cre recombinase

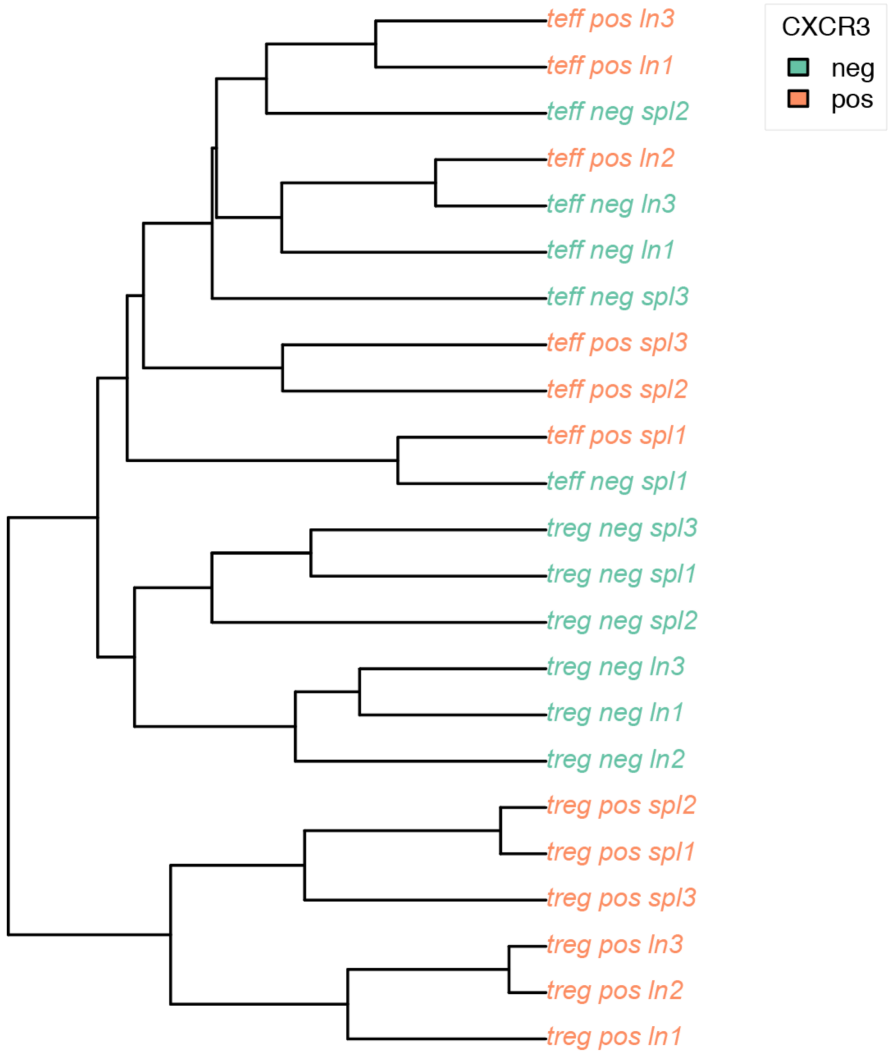

Figure 4.8. T-bet^{+} CD44^{hi}CXCR3^{+} Treg cells have a distinct TCR repertoire.
Dendrogram showing clustering of TCR sequences in CD44^{hi}CXCR3^{+} Treg (treg pos) and CD44^{hi}CXCR3^{-} Treg (treg neg) as well as CD44^{hi}CXCR3^{+} effector (teff pos) and CD44^{hi}CXCR3^{-} effector (teff neg) T cell populations sorted from spleens (spl) and axial/brachial/cervical/inguinal lymph nodes (ln) of DO11.10 TCRβ^{+} Tcra$^{+/-}$ Foxp3 reporter mice. Sample preparation and statistical analyses are described in the Methods section. Pearson correlation of clonotype frequencies for the shared TCR clones was used for the generation of the dendrogram.

Figure 4.9. Generation and analysis of *Tbx21*$^{RFP\text{-}Cre}$Foxp3^{FL} mice.
A, Targeting strategy for the *Tbx21* locus (above) and RFP expression in the indicated cell populations in spleens of homozygous *Tbx21*$^{RFP\text{-}Cre/RFP\text{-}Cre}$ mice (below). **B**, Representative patchy loss of hair pigmentation in 8-week old *Tbx21*$^{RFP\text{-}Cre}$*Foxp3*^{FL} mouse compared to a littermate male control. **C**, Representative flow cytometry analysis of the indicated populations in *Tbx21*$^{RFP\text{-}Cre}$*R26Y* mice. **D-E**, Percent CD44^{hi} of CD4^{+}Foxp3^{-}CD25^{-} cells (left) and percent CD44^{hi}RFP^{-} and CD44^{hi}RFP^{+} CD4^{+}CD25^{-} cells (right) in pooled axial/brachial/cervical/inguinal lymph nodes (**D**) and lungs (**E**) of the indicated mice. **F**, Percent CD44^{hi}CD62L^{lo} of CD8^{+} T cells in lymph nodes (left) and lungs (right) of the indicated mice. **G**, Cytokine production by CD4^{+}Foxp3^{-} and CD8^{+} T cells in lungs. **H**, Percent CXCR3^{+} of CD4^{+}Foxp3^{+} cells (left), and absolute numbers of CD4^{+}Foxp3^{+} (middle) and CD44^{hi}CD62L^{lo} Foxp3^{+} (right) cells in lymph nodes. **I**, Percent Foxp3^{-}CD25^{+} of CD4^{+} cells in spleen (left), lymph nodes (middle), and lung (right) of mice of the indicated genotypes. **J**, Representative flow cytometric analysis of cells gated on CD4^{+} TCRβ^{+} PBS-57-CD1d tetramer^{-} splenic cells, as quantified in (**I**). Numbers indicate the percent Foxp3^{-}CD25^{+}. **K**, Representative histograms showing expression of Treg cell signature molecules in CD4^{+}Foxp3^{-}CD25^{+} cells in spleens of *Tbx21*$^{RFP\text{-}Cre}$*Foxp3*^{WT} (open gray histogram), *Tbx21*$^{RFP\text{-}Cre}$*Foxp3*^{FL} (open red histogram), *Tbx21*$^{RFP\text{-}Cre}$*Foxp3*$^{WT/WT}$ (open blue histogram), and *Tbx21*$^{RFP\text{-}Cre}$*Foxp3*$^{FL/WT}$ (open black histogram) mice. CD4^{+}Foxp3^{+}CD25^{+} cells from a *Tbx21*$^{RFP\text{-}Cre}$*Foxp3*^{WT} (shaded gray histogram) mouse are shown as a point of reference. Each circle represents an individual mouse; the horizontal bars represent mean value; *p* values were calculated using Student's *t* test (***, **, and * denotes *p* values <0.001, 0.01, and 0.05, respectively; ns – not significant). The data represent the combined results from several independent experiments.

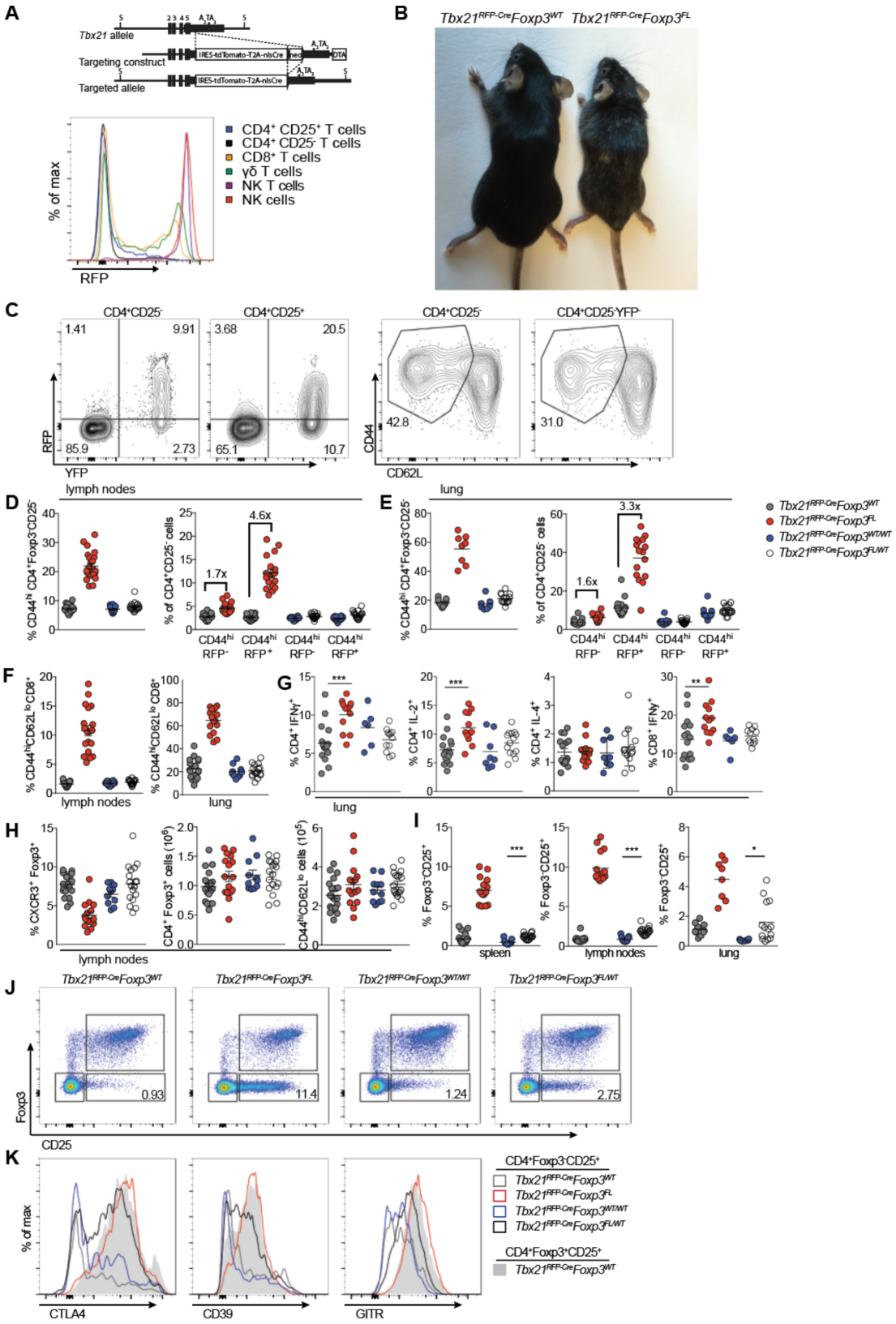
A
Tbx21 allele
Targeting construct
Targeted allele
IRES-tdTomato-T2A-nlsCre
DTA
CD4+ CD25+ T cells
CD4+ CD25- T cells
CD8+ T cells
γδ T cells
NK T cells
NK cells
% of max
RFP
B
Tbx21RFP-CreFoxp3WT
Tbx21RFP-CreFoxp3FL
C
CD4+CD25-
CD4+CD25+
CD4+CD25-YFP-
RFP
YFP
CD44
CD62L
1.41
9.91
85.9
2.73
3.68
20.5
65.1
10.7
42.8
31.0
D
lymph nodes
% CD44hi CD4+Foxp3-CD25-
% of CD4+CD25- cells
1.7x
4.6x
CD44hi RFP-
CD44hi RFP+
E
lung
1.6x
3.3x
Tbx21RFP-CreFoxp3WT
Tbx21RFP-CreFoxp3FL
Tbx21RFP-CreFoxp3WT/WT
Tbx21RFP-CreFoxp3FL/WT
F
% CD44hiCD62LloCD8+
lymph nodes
lung
G
% CD4+ IFNγ+
% CD4+ IL-2+
% CD4+ IL-4+
% CD8+ IFNγ+
H
% CXCR3+ Foxp3+
CD4+ Foxp3+ cells (10^6)
CD44hiCD62Llo cells (10^5)
I
% Foxp3-CD25+
spleen
lymph nodes
J
Foxp3
CD25
0.93
11.4
1.24
2.75
K
% of max
CTLA4
CD39
GITR
CD4+Foxp3-CD25+
CD4+Foxp3+CD25+

Figure 4.10. Foxp3 ablation in T-bet$^+$ Treg cells results in severe spontaneous T_H1 autoimmune disease.

A, Analysis of body weights of 8-10 week old *Tbx21$^{RFP\text{-}Cre}$Foxp3^{WT}* (gray circles), *Tbx21$^{RFP\text{-}Cre}$Foxp3^{FL}* (red circles), *Tbx21$^{RFP\text{-}Cre}$Foxp3$^{WT/WT}$* (blue circles), and *Tbx21$^{RFP\text{-}Cre}$Foxp3$^{FL/WT}$* (white circles) mice. **B**, Representative H&E staining (left) and histology scores (right) of lungs from the indicated mice, treated or not treated with antibiotics (ABX). *Tbx21$^{RFP\text{-}Cre}$Foxp3^{FL}* mice show moderate perivascular and peribronchiolar inflammation, mild respiratory epithelial hyperplasia and mucus metaplasia with hyalinization (arrows). Pulmonary arterioles are contracted with thickened media, reactive endothelia, and marginating leukocytes (arrowheads). Original magnification, 20x. **C**, Lymph node cell numbers in mutant and control mice. **D**, CD4$^+$Foxp3$^-$CD25$^-$ (left) and CD8$^+$ (right) T cell activation in spleens. **E**, Percent CXCR3$^+$ of Foxp3$^+$ (left), and absolute numbers of Foxp3$^+$ (middle) and CD44^{hi}CD62L^{lo} Foxp3$^+$ (right) T cells in spleens. **F**, Representative flow cytometric analysis of splenic cells in *Tbx21$^{RFP\text{-}Cre}$Foxp3^{WT}* (left) and *Tbx21$^{RFP\text{-}Cre}$Foxp3^{FL}* (right) mice, gated on fixed CD4$^+$ TCRβ$^+$ PBS-57-CD1d tetramer$^-$ (above) and live CD4$^+$ TCRβ$^+$ PBS-57-CD1d tetramer$^-$ CD25$^-$ (below) cells. Numbers indicate percentages of the indicated cell subsets. **G**, Quantification of percentages of splenic CD44^{hi}RFP$^-$ and CD44^{hi}RFP$^+$ CD4$^+$CD25$^-$ cells, as shown in (**F**, bottom). **H**, RFP expression (left) and cytokine production (right) in splenic CD8$^+$ T cells in *Tbx21$^{RFP\text{-}Cre}$Foxp3^{WT}* (gray histogram) and *Tbx21$^{RFP\text{-}Cre}$Foxp3^{FL}* (red histogram), *Tbx21$^{RFP\text{-}Cre}$Foxp3$^{WT/WT}$* (blue histogram) and *Tbx21$^{RFP\text{-}Cre}$Foxp3$^{FL/WT}$* (black histogram) mice. **I**, Cytokine production by splenic CD4$^+$Foxp3$^-$ T cells. Each circle represents an individual mouse; error bars indicate standard error of the mean (SEM); *p* values were calculated using Student's *t* test (***, **, and * denotes *p* values <0.001, 0.01, and 0.05, respectively; ns – not significant). The data represent the combined results from several independent experiments.

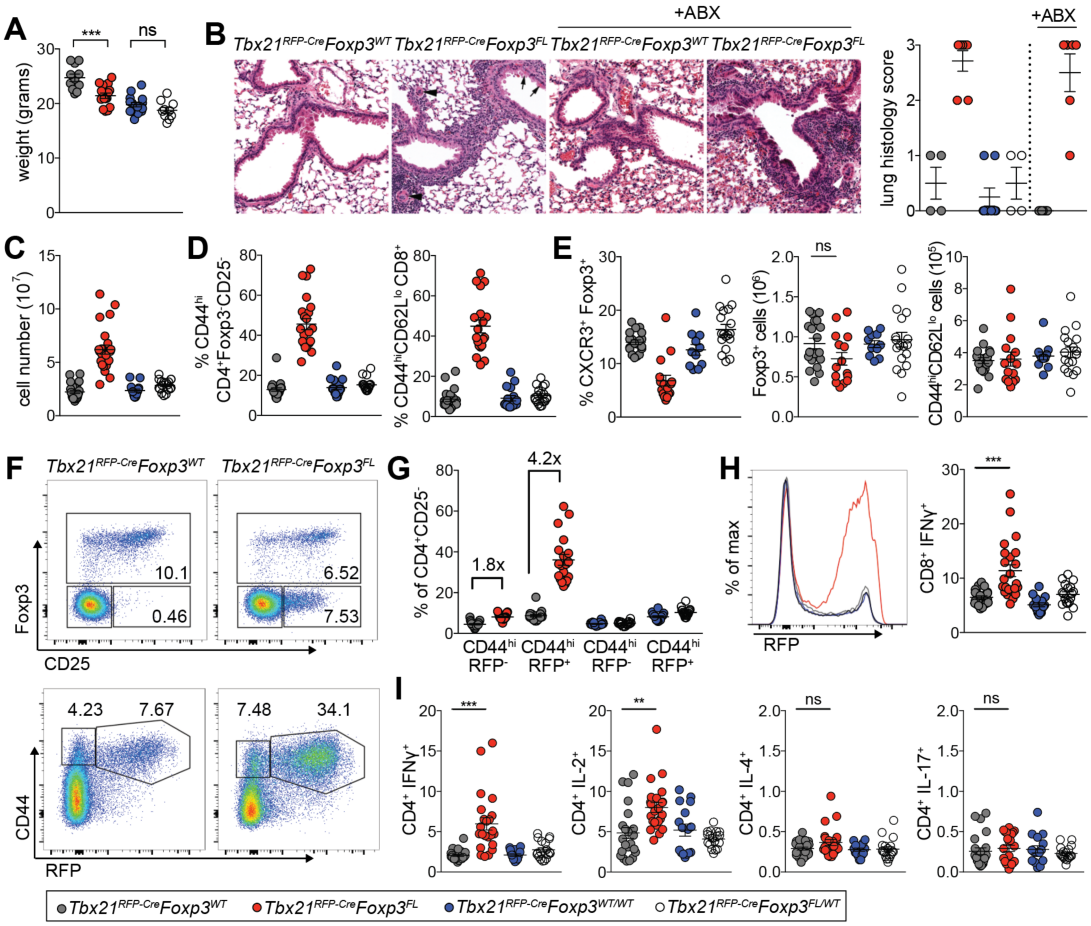
A
***
ns
weight (grams)
B
+ABX
Tbx21RFP-CreFoxp3WT Tbx21RFP-CreFoxp3FL Tbx21RFP-CreFoxp3WT Tbx21RFP-CreFoxp3FL
+ABX
lung histology score
C
cell number (10^7)
D
% CD44hi CD4+Foxp3-CD25-
% CD44hiCD62Llo CD8+
E
% CXCR3+ Foxp3+
ns
Foxp3+ cells (10^6)
CD44hiCD62Llo cells (10^6)
F
Tbx21RFP-CreFoxp3WT
Tbx21RFP-CreFoxp3FL
Foxp3
CD25
10.1
0.46
6.52
7.53
CD44
RFP
4.23
7.67
7.48
34.1
G
% of CD4+CD25-
1.8x
4.2x
CD44hi RFP-
CD44hi RFP+
CD44hi RFP-
CD44hi RFP+
H
% of max
RFP
***
CD8+ IFNγ+
I
***
CD4+ IFNγ+
**
CD4+ IL-2+
ns
CD4+ IL-4+
ns
CD4+ IL-17+
Tbx21RFP-CreFoxp3WT
Tbx21RFP-CreFoxp3FL
Tbx21RFP-CreFoxp3WT/WT
Tbx21RFP-CreFoxp3FL/WT

(Figure 4.3) did not prevent activation and expansion of CD44^{hi} effector Treg cells that did not express T-bet. Indeed, analysis of CD4^{+}CD25^{+} cells in *Tbx21$^{RFP\text{-}Cre}$R26Y* mice indicated that—even in the absence of inflammation that likely promoted expansion of T-bet^{-} CD44^{hi}CD62L^{lo} Treg cells in *Tbx21$^{RFP\text{-}Cre}$Foxp3^{FL}* mice—significant percentages of CD44^{hi}CD62L^{lo} Treg cells had not undergone Cre-mediated recombination (Figure 4.9C). We confirmed by intracellular staining that residual CXCR3^{+} Treg cells in *Tbx21$^{RFP\text{-}Cre}$Foxp3^{FL}* mice expressed T-bet (data not shown), indicating that even some T-bet^{+} Treg cells, likely T-bet^{lo} cells—a significant percentage of which remain YFP^{-} in *Tbx21$^{RFP\text{-}Cre}$R26Y* mice (Figure 4.9C)—escape Cre-mediated recombination. These results suggested that immune activation could not be attributed to decreased numbers of Treg cells, or even to wholesale loss of effector-like Treg cells.

Foxp3^{-} ex-Treg cells expressing high levels of Treg cell signature genes coding for a number of molecules including CD25, CD39, CTLA4, and GITR were readily found in spleens and lymph nodes of male *Tbx21$^{RFP\text{-}Cre}$Foxp3^{FL}* (and to a lesser extent female *Tbx21$^{RFP\text{-}Cre}$Foxp3$^{FL/WT}$*) mice, confirming the essential role of continuous Foxp3 expression in Treg cells for suppressive function (Figure 4.10F and Figure 4.9I-K) (Gavin et al., 2007; Lahl et al., 2009; Williams and Rudensky, 2007). The fact that there was no detectable autoimmunity in female *Tbx21$^{RFP\text{-}Cre}$Foxp3$^{FL/WT}$* mice—in which only half of T-bet^{+} Treg cells lose Foxp3 expression due to X-inactivation—suggested that ex-Treg cells were unable to cause autoimmunity in a strictly cell-intrinsic manner as they could be controlled by a competent population of T-bet^{+} Treg cells (in the same way that 'wannabe' Foxp3^{KO} Treg cells in female *Foxp3$^{WT/KO}$* mice are effectively controlled by Foxp3^{+} Treg cells present in the same mice

(Figure 4.10). However, it is additionally possible that ex-Treg cells may play some role in the observed autoimmune activation in *Tbx21*$^{RFP\text{-}Cre}$*Foxp3*^{FL} mice lacking T-bet-expressing Treg cells.

Indicative of T_H1-type inflammation, the majority of expanded, activated CD44^{hi} CD4$^+$CD25$^-$ and CD8$^+$ T cells in the spleen, lymph nodes, and lung of *Tbx21*$^{RFP\text{-}Cre}$*Foxp3*^{FL} mice expressed T-bet (RFP) (Figure 4.10F-H and Figure 4.9). Additionally, IFNg production by both CD4 and CD8 T cells and IL-2, but neither IL-4 nor IL-17 production by CD4 T cells were increased in spleens and lungs compared to controls (Figure 4.10H,I and Figure 4.9). To determine whether T_H1 inflammation was driven by microbiota, *Tbx21*$^{RFP\text{-}Cre}$*Foxp3*^{FL} mice were treated from the time of weaning with a broad spectrum cocktail of antibiotics and analyzed at two months of age. Antibiotic treatment did not mitigate weight loss, systemic immune activation, or lung pathology in *Tbx21*$^{RFP\text{-}Cre}$*Foxp3*^{FL} mice compared to antibiotic treated *Tbx21*$^{RFP\text{-}Cre}$*Foxp3*^{WT} controls and untreated experimental and control groups (Figure 4.10B and data not shown). This result suggested that most likely “self”, dietary, and other environmental rather than microbial antigens were the drivers of T_H1 inflammation and disease upon the loss of function of T-bet$^+$ Treg cells.

Although Treg cells in *Tbx21*$^{RFP\text{-}Cre}$*Foxp3*^{FL} mice efficiently controlled T_H2 and T_H17 cytokine production at steady state, basal production of these cytokines is relatively low in C57BL/6 mice; therefore, we considered whether induction of a robust “non-T_H1” immune response in *Tbx21*$^{RFP\text{-}Cre}$*Foxp3*^{FL} mice might reveal a function for T-bet$^+$ Treg cells in control of these responses. Accordingly, we challenged *Tbx21*$^{RFP\text{-}Cre}$*Foxp3*^{FL} and littermate controls with *Nippostrongylus brasiliensis* and assessed immune activation on day 9. We found that the T_H2 response—as assessed by eosinophilia in the lung, and

percentages of GATA3$^+$ and IL-4, -13, and -5-producing CD4$^+$ T cells in spleen and lungs—was not increased and remained essentially indistinguishable in *Tbx21*$^{RFP\text{-}Cre}$*Foxp3*^{FL} compared to control *Tbx21*$^{RFP\text{-}Cre}$*Foxp3*^{WT} mice (Figure 4.11). This is in contrast to increased TH2 responses observed upon general Treg cell depletion in helminth-infected mice (Blankenhaus et al., 2014; Sawant et al., 2014; Smith et al., 2016). Thus, T-bet$^+$ Treg cells appear to be largely dispensable for control of T_H2 immunity, consistent with the notion that T-bet$^+$ Treg cells are preferentially—if not selectively—involved in control of T_H1 responses.

Lastly, to determine whether punctual ablation of T-bet$^+$ Treg cells in adult mice would similarly unleash T_H1-type inflammation, we generated chimeric mice by reconstituting irradiated T cell-deficient *Tcrb*^{KO}*Tcrd*^{KO} mice with a 1:1 mix of either CD45.1$^+$ *Foxp3*^{WT} or *Foxp3*^{KO} with CD45.2$^+$ *Tbx21*$^{RFP\text{-}Cre/WT}$*Rosa26*^{iDTR} hematopoietic precursor cells (Figure 4.12). All T-bet expressing hematopoietic cells originating from *Tbx21*$^{RFP\text{-}Cre/WT}$*Rosa26*^{iDTR} precursors expressed diphtheria toxin receptor (DTR) due to Cre-mediated excision of a loxP site-flanked STOP cassette in front of the simian DTR coding sequence inserted into the *Rosa26* locus (Buch et al., 2005). Thus, in *Foxp3*^{KO} + *Tbx21*$^{RFP\text{-}Cre/WT}$*Rosa26*^{iDTR} -> *Tcrb*^{KO}*Tcrd*^{KO} mixed chimeras all T-bet$^+$ Treg cells expressed DTR and were, therefore, susceptible to diphtheria toxin (DT)-mediated ablation, whereas the rest of T-bet expressing cell types and subsets represented a 1:1 mix of DTR-expressing and non-expressing cells. Two weeks of daily DT administration resulted in weight loss, profound T cell activation, and a selective increase in IFNγ production by CD4 and CD8 T cells in *Foxp3*^{KO} + *Tbx21*$^{RFP\text{-}Cre/WT}$*Rosa26*^{iDTR} -> *Tcrb*^{KO}*Tcrd*^{KO} chimeric mice

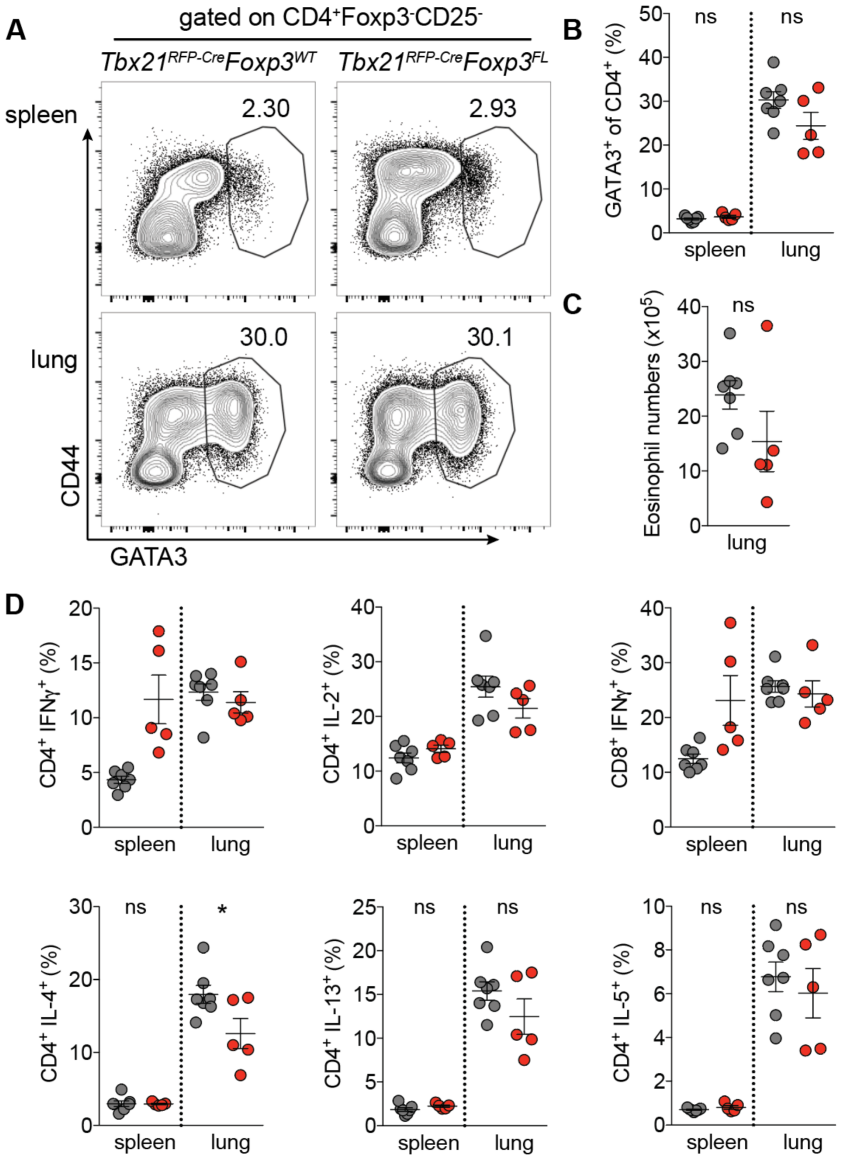

Figure 4.11. The T_H2 response to *N. brasiliensis* is not exacerbated in *Tbx21*$^{RFP\text{-}Cre}$*Foxp3*^{FL} mice.

Tbx21$^{RFP\text{-}Cre}$*Foxp3*^{FL} and control *Tbx21*$^{RFP\text{-}Cre}$*Foxp3*^{WT} mice were infected with Nb and analyzed on day 9 post challenge. **A**, Representative flow cytometry plots showing GATA3 expression in CD4$^+$Foxp3$^-$ T cells in spleens (above) and lungs (below) in *Tbx21*$^{RFP\text{-}Cre}$*Foxp3*^{WT} (left) and *Tbx21*$^{RFP\text{-}Cre}$*Foxp3*^{FL} (right) mice. **B**, Quantification of data in (**A**). **C**, Numbers of eosinophils in lungs of the indicated mice. **D**, Cytokine production by CD4$^+$Foxp3$^-$ T cells in spleens and lungs of the indicated mice. Data shows a single experiment with at least 5 mice per group. Each circle represents an individual mouse; the horizontal bars represent mean value; *p* values were calculated using Student's *t* test (* denotes *p* values < 0.05; ns – not significant).

Figure 4.12. Acute ablation of T-bet$^+$ Treg cells in adult mice results in T_H1 immune activation.
Lethally irradiated *Tcrb*$^{-/-}$*Tcrd*$^{-/-}$ mice were reconstituted with a 1:1 mix of *CD45.2*$^+$*Tbx21*$^{RFP\text{-}Cre/WT}$*Rosa26*^{iDTR} T-cell depleted bone marrow cells with either *CD45.1*$^+$*Foxp3*^{KO} or *CD45.1*$^+$*Foxp3*^{WT} T-cell depleted bone marrow cells and rested for three months. Mice were injected i.p. with 0.5µg diphtheria toxin (DT) on day 0, then treated daily with 0.1µg DT for 14 days before analysis. **A**, Weight loss in *Tbx21*$^{RFP\text{-}Cre/WT}$*Rosa26*^{iDTR}*:Foxp3*^{KO}- vs. *Tbx21*$^{RFP\text{-}Cre/WT}$*Rosa26*^{iDTR}*:Foxp3*^{WT}-reconstituted mice. **B**, Representative plots, gated on splenic CD4$^+$ TCRβ$^+$ cells (above) and CD4$^+$ TCRβ$^+$ Foxp3$^+$ cells (below) in *Tcrb*$^{-/-}$*Tcrd*$^{-/-}$ mice reconstituted with the indicated bone marrow cells. **C**, Representative flow cytometry analysis showing CD44 and CD62L expression in CD45.1$^+$ and CD45.2$^+$ CD4$^+$Foxp3$^+$ cell populations in the indicated mice. **D**, CD4$^+$ and CD8$^+$ T cell activation and cytokine production in *Tcrb*$^{-/-}$*Tcrd*$^{-/-}$ mice reconstituted with the indicated bone marrow cells. Each circle represents an individual mouse; error bars indicate SEM; *p* values were calculated using Student's *t* test (ns – not significant). The data is representative of 2 independent experiments with at least 6 mice per group each.

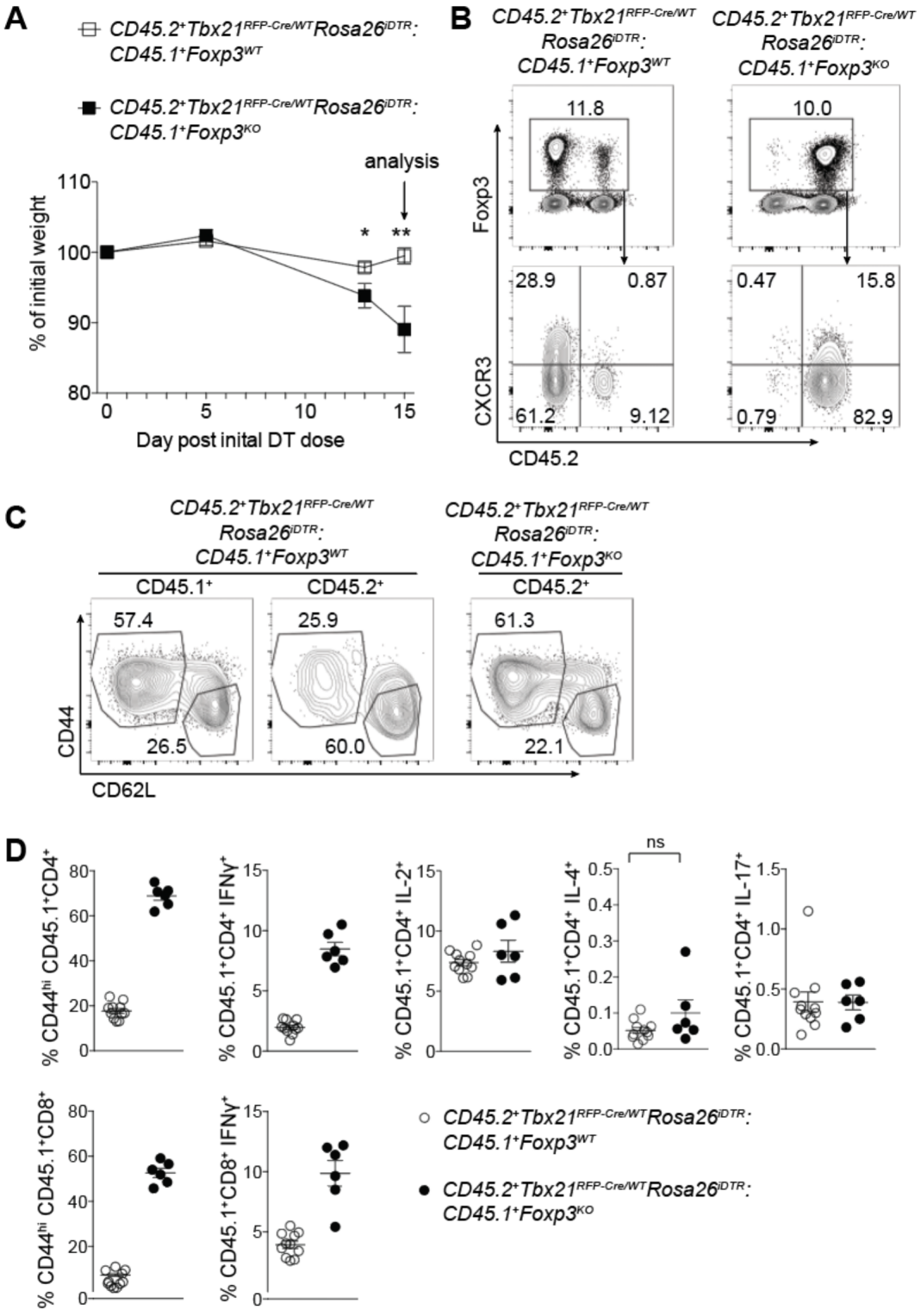
A
CD45.2+Tbx21RFP-Cre/WTRosa26iDTR:
CD45.1+Foxp3WT
CD45.2+Tbx21RFP-Cre/WTRosa26iDTR:
CD45.1+Foxp3KO
analysis
% of initial weight
Day post inital DT dose
B
CD45.2+Tbx21RFP-Cre/WT
Rosa26iDTR:
CD45.1+Foxp3WT
CD45.2+Tbx21RFP-Cre/WT
Rosa26iDTR:
CD45.1+Foxp3KO
11.8
10.0
Foxp3
28.9
0.87
0.47
15.8
CXCR3
61.2
9.12
0.79
82.9
CD45.2
C
CD45.2+Tbx21RFP-Cre/WT
Rosa26iDTR:
CD45.1+Foxp3WT
CD45.2+Tbx21RFP-Cre/WT
Rosa26iDTR:
CD45.1+Foxp3KO
CD45.1+
CD45.2+
CD45.2+
57.4
25.9
61.3
CD44
26.5
60.0
22.1
CD62L
D
% CD44hi CD45.1+CD4+
% CD45.1+CD4+ IFNγ+
% CD45.1+CD4+ IL-2+
ns
% CD45.1+CD4+ IL-4+
% CD45.1+CD4+ IL-17+
% CD44hi CD45.1+CD8+
% CD45.1+CD8+ IFNγ+
CD45.2+Tbx21RFP-Cre/WTRosa26iDTR:
CD45.1+Foxp3WT
CD45.2+Tbx21RFP-Cre/WTRosa26iDTR:
CD45.1+Foxp3KO

ablated of T-bet^{+} Treg cells compared to control *Foxp3^{WT}* + *Tbx21$^{RFP\text{-}Cre/WT}$Rosa26^{iDTR}* -> *Tcrb^{KO}Tcrd^{KO}* mice (Figure 4.12).

Despite a competitive disadvantage of CD45.2^{+} DT-depleted Treg cells in *Foxp3^{WT}* + *Tbx21$^{RFP\text{-}Cre/WT}$Rosa26^{iDTR}* -> *Tcrb^{KO}Tcrd^{KO}* mice (Figure 4.12B), Treg cells in *Foxp3^{KO}* + *Tbx21$^{RFP\text{-}Cre/WT}$Rosa26^{iDTR}* -> *Tcrb^{KO}Tcrd^{KO}* mice as a percent of total CD4^{+} T cells were only modestly decreased (from 13±0.53 to 11±0.82, p=0.022) compared to in control mice (Figure 4.12B). Consistent with a highly activated and proliferative state, Treg cells in experimental mice had undiminished percentages of CD44^{hi}CD62L^{lo} and increased percentages of Ki67^{+} cells compared to Treg cells in control animals (Figure 4.12C data not shown), indicating that in these mice as in *Tbx21$^{RFP\text{-}Cre}$Foxp3^{FL}* mice a nonselective decrease in effector Treg cells cannot account for the observed immune activation. Indeed, even in *Foxp3^{WT}* + *Tbx21$^{RFP\text{-}Cre/WT}$Rosa26^{iDTR}* -> *Tcrb^{KO}Tcrd^{KO}* mice, a substantial fraction of CD45.2^{+} CD44^{hi}CD62L^{lo} Treg cells which had not expressed T-bet and thus had not been depleted by DT were readily apparent (Figure 4.12C). Importantly, this experimental model did not generate the ex-Treg cells that were present in *Tbx21$^{RFP\text{-}Cre}$Foxp3^{FL} mice*, providing additional evidence that these cells were not the sole drivers of pathology in the absence of T-bet^{+} Treg cells. We cannot rule out the possibility that increased fractional loss of Treg cells early after DT treatment of *Foxp3^{KO}* + *Tbx21$^{RFP\text{-}Cre/WT}$Rosa26^{iDTR}* -> *Tcrb^{KO}Tcrd^{KO}* compared to in *Foxp3^{WT}* + *Tbx21$^{RFP\text{-}Cre/WT}$Rosa26^{iDTR}* -> *Tcrb^{KO}Tcrd^{KO}* mice may play some role in the observed immune activation in experimental mice. However, the fact that there are no signs of T_H2 or T_H17 activation in these mice (Figure 4.12D) is consistent with both our data from *Tbx21$^{RFP\text{-}Cre}$Foxp3^{FL}* mice and with the notion that T-bet^{+} Treg cells play a particular role specifically in the

control over T_H1 autoimmunity. Conversely, non-specific partial depletion of Treg cells in *Foxp3*^{DTR} mice, ablation of the TCR on Treg cells which disproportionally affects CD44^{hi}CD62L^{lo} Treg cells, or specific manipulation and depletion of the entire CD44^{hi}CD62L^{lo} effector Treg cell population all result in non-selective increases in T_H2 and T_H17, as well as T_H1, activation (Levine et al., 2014; Luo et al., 2016). Finally, it was noteworthy that weight loss was not observed in *Tcrb*^{KO} + *Tbx21*$^{RFP\text{-}Cre/WT}$*Rosa26*^{iDTR} -> *Tcrb*^{KO}*Tcrd*^{KO} mixed chimeras, in which all T-bet$^+$ TCRαβ$^+$ cells were simultaneously ablated along with T-bet$^+$ Treg cells (Figure 4.13). The latter observation demonstrated that T-bet-expressing effector αβT cells drive disease in the absence of T-bet$^+$ Treg cells consistent with a prominent role of the latter in control of T_H1 responses.

Discussion

In this study, we investigated the apparent heterogeneity of Treg cells—namely, whether it results from Treg cell differentiation into different states with potentially distinct functions or merely reflects readily reversible 'plastic' states of activation within a homogenous effector Treg cell pool. Our studies using a novel *Tbx21* fate mapping allele revealed remarkable stability of T-bet expression in Treg cells acquired upon their differentiation after passing through an unstable intermediate stage. The observed resilience of T-bet expression in Treg as well as in effector CD4 T cells under T_H2 polarizing conditions argues against a notion of plasticity of Treg cells and their effector counterparts.

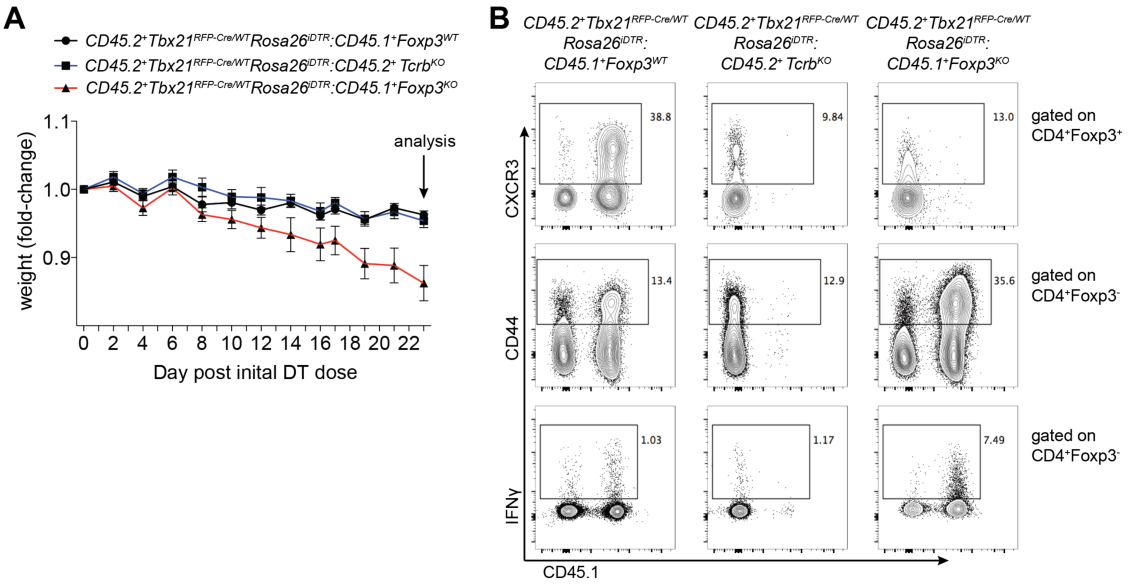

Figure 4.13. Wasting disease observed upon T-bet$^+$ Treg cell ablation is driven by T-bet-expressing effector αβ T cells.
Lethally irradiated *Tcrb*$^{-/-}$*Tcrd*$^{-/-}$ mice were reconstituted with a 1:1 mix of *CD45.2*$^+$*Tbx21*$^{RFP\text{-}Cre/WT}$*Rosa26*^{iDTR} T-cell depleted bone marrow cells with either *CD45.1*$^+$*Foxp3*^{KO}, *CD45.1*$^+$*Foxp3*^{WT}, or *CD45.2*$^+$*Tcrb*^{KO} T-cell depleted bone marrow cells and rested for three months. Mice were injected i.p. with 0.5µg diphtheria toxin (DT) on day 0, then treated daily with 0.1µg DT for 22 days before analysis. **A**, Weight loss in *Tbx21*$^{RFP\text{-}Cre/WT}$*Rosa26*^{iDTR}*:Foxp3*^{KO} (red line) vs. *Tbx21*$^{RFP\text{-}Cre/WT}$*Rosa26*^{iDTR}*:Foxp3*^{WT} (black line) vs. *Tbx21*$^{RFP\text{-}Cre/WT}$*Rosa26*^{iDTR}*:Tcrb*^{KO} (blue line) reconstituted mice. **B**, Representative flow cytometry plots of CXCR3 expression in TCRβ$^+$ CD4$^+$ Foxp3$^+$ cells (top row) and CD44 (middle row) and IFNg (bottom row) expression in TCRβ$^+$ CD4$^+$ Foxp3$^-$ cells in *Tcrb*$^{-/-}$*Tcrd*$^{-/-}$ mice reconstituted with the indicated bone marrow cells. The data are representative of 1 experiment with at least 6 mice per group.

Our fate-mapping studies during *Listeria monocytogenes* and LCMV challenge showed that bacterial or viral infections can serve as other independent sources for the generation of T-bet-expressing Treg cells from a distinct pool of precursor T-bet$^-$ Treg cells. Fate-mapped T-bet-expressing Treg cells generated during infection maintained T-bet expression following pathogen clearance. Significantly, these cells were preferentially activated during reinfection, as opposed to at steady state, whereas steady state-generated T-bet$^+$ Treg cells appeared to be preferentially activated at steady state, as opposed to infection. These results were indicative of a further layer of heterogeneity within the T-bet$^+$ Treg cell population.

The continuous peripheral generation of T-bet$^+$ Treg cells resulting in stability of T-bet^{hi} Treg cells implied a potentially specific function for T-bet$^+$ Treg cells in immunological tolerance. Indeed, we found that both elimination of steady state T-bet$^+$ Treg cells and their loss of function upon targeted Foxp3 ablation resulted in a selective failure to restrain pronounced T_H1-type T cell activation and associated severe autoimmune pathology. In addition to suppressing steady state T_H2 and T_H17 autoimmune responses, mice depleted of T-bet$^+$ Treg cells also efficiently regulated T_H2 responses to *N. brasiliensis*, further suggesting that T-bet$^+$ Treg cell function may be restricted to T_H1 responses. Although we cannot formally exclude the possibility that elimination of some 'exT-bet'-expressing Treg cells in *Tbx21*$^{RFP\text{-}Cre}$*Foxp3*^{FL} and *Foxp3*^{KO} + *Tbx21*$^{RFP\text{-}Cre/WT}$*Rosa26*^{iDTR} -> *Tcrb*^{KO}*Tcrd*^{KO} mice (due to transient Cre expression) contributed to the observed T_H1 immune activation, the lack of exacerbated T_H2 and T_H17 responses both at steady state and following helminth infection in these mice argue strongly against a general deficiency in the Treg cell (or specifically effector Treg cell) compartment—which results in

non-specific T_H1, T_H2, and T_H17 inflammation—and instead suggests that the Treg cell pool depleted of T-bet$^+$ cells can efficiently control T_H2 and T_H17 but not T_H1 responses.

Notably, we found that T-bet, by itself, contributed only modestly to the ability of T-bet-expressing Treg cells to control T_H1 responses and—consistent with previous reports—was dispensable for preventing disease. As STAT1 activation precedes and is required for T-bet expression in Treg cells induced upon IFNg or IL-27 signaling in different contexts and in different anatomical sites (Hall et al., 2012; Koch et al., 2012; Koch et al., 2009), it is likely that STAT1 and T-bet jointly contribute to some degree to T-bet$^+$ Treg cell function. At the same time, it is possible that T-bet, in combination with STAT1, might continuously enforce its own expression, resulting in the stable T-bet$^+$ phenotype.

A recent study showed that IL-27 producing dendritic cells, which have been exposed to IFNg stimulation, are capable of inducing T-bet expression in Treg cells (Lee et al., 2015). It seems reasonable to speculate that presentation of self-antigens by these dendritic cells induces T-bet and imparts the lasting T-bet expression in T-bet^{hi} Treg cells at steady state. Indeed, our TCR sequencing results suggest that T-bet$^+$ Treg cells possess a distinct TCR repertoire. This observation together with our observations that a paucity of commensal microbiota resulting from treatment of mice with a cocktail of broad-spectrum antibiotics failed to diminish numbers of these cells are consistent with an idea that under physiologic conditions T-bet$^+$ Treg cells are likely continuously generated in response to self, rather than microbial, antigens. We suggest that in addition to T-bet-dependent CXCR3 expression, distinct TCR specificities of T-bet$^+$ Treg cells may play an important role in

accumulation and activation-dependent suppressor function of T-bet$^+$ Treg cells at sites of T_H1 inflammation.

TCR specificity may account in large part for the observed heterogeneity within the Treg cell population. In this regard, new generation of T-bet-expressing Treg cells in response to *Lm* infection—rather than expansion of a pre-existent T-bet$^+$ cell population—parallels differentiation of CD4 T cells into T_H1 effectors, and was consistent with an antigen-dependent generation. Furthermore, contraction of *Lm*-experienced Treg cells following resolution of the infection and preferential re-expansion of these cells following reinfection, albeit moderate in comparison to their effector counterparts, resembled antigen-specific effector CD4 T cell recall responses. In this context, it is notable that we have observed T-bet$^+$ Treg cell differentiation in response to *Lm* as well as LCMV infections in which Treg cells have not been shown to recognize known or surrogate pathogen-derived antigens (Ertelt et al., 2009; Shafiani et al., 2013; Srivastava et al., 2014). Thus, it is possible that *de novo* generation of T-bet$^+$ Treg cells during infection was potentially due to recognition of "pathogen-activated" self-antigens or steady state antigens differentially presented during infection. The former likely supported the observed acquisition of T-bet expression by resting ("naïve") T-bet$^-$ Treg cells whereas the latter may have promoted T-bet induction in activated CD44^{hi} T-bet$^-$ precursors.

In conclusion, our study suggests that heterogeneity of Treg cells may be a critical feature of immunological tolerance. Peripheral Treg cells can differentiate into a highly stable T-bet-expressing population independently contributed to by acquisition of T-bet expression at steady state and during infectious challenge. Our results suggest that under physiologic conditions

immunological tolerance may be maintained by polarized differentiation of Treg cells into an “effector-like” state with particular function concomitant with differentiation of polarized effector CD4 T cells. Such a mechanism may enable the adaptive immune system to coordinate potency of anti-inflammatory and inflammatory responses to maintain a necessary balance.

Acknowledgements

We thank N. Arpaia and members of the Rudensky lab for critical discussions, and I. Leiner and members of E. Pamer’s lab for helpful advice regarding *Lm* infections. We thank J. Sun for providing *Lm* stocks, and A.H. Bravo, S.E. Lee, and M.B. Faire for experimental support. This work was supported by an NIH Medical Scientist Training Program grant T32GM07739 to the Weill Cornell/Rockefeller/Sloan-Kettering Tri-Institutional MD-PhD Program (A.G.L); the Frank Lappin Horsfall Jr. Student Fellowship (A.G.L); NIH grant R37AI034206 (A.Y.R.), the Ludwig Center at Memorial Sloan Kettering Cancer Center, and the Hilton-Ludwig Cancer Prevention Initiative (Conrad N. Hilton Foundation and Ludwig Cancer Research) (A.Y.R.); and the NIH/NCI Cancer Center Support Grant P30 CA008748. A.Y.R. is an investigator with the Howard Hughes Medical Institute.

Materials and Methods

Animals

Tbx21$^{tdTomato\text{-}T2A\text{-}CreERT2}$ mice were generated upon insertion of the corresponding targeting construct into the *Tbx21* locus by homologous recombination in embryonic stem cells (ESCs) on the C57BL/6 background; the targeting construct was generated by inserting sequence containing Exons

2-5 of the *Tbx21* gene from BAC RP23-237M14 (BACPAC Resources Center) into a plasmid backbone containing a PGK promoter driving expression of diphtheria toxin A subunit (DTA) followed by BGHpA sequence (modified PL452 plasmid). A SalI restriction enzyme site was simultaneously engineered into the *Tbx21* 3'UTR between the stop codon and the polyadenylation site. The Clontech Infusion HD Cloning system was used to generate in the pUC19 plasmid backbone sequence containing (in order from 5' to 3') encephalomyocarditis virus IRES; tandem dimer (td) Tomato; T2A self-cleaving peptide from Thoseaasigna virus; Cre recombinase fused to the estrogen receptor ligand binding domain (ER); followed by a frt site-flanked PGK-Neomycin resistance gene (NEO)-BGHpA cassette. The IRES-tdTomato-T2A-CreERT2-frt-NEO-BGHpA-frt sequence was PCR-amplified and inserted into the SalI site in the *Tbx21* 3'UTR in the modified PL452 backbone. The resulting plasmid was linearized with the restriction enzyme NotI prior to electroporation into ESCs. *Tbx21*$^{tdTomato\text{-}T2A\text{-}Cre}$ mice were generated similarly, with Cre recombinase containing a nuclear localization sequence replacing the CreERT2 sequence. *Tbx21*$^{tdTomato\text{-}T2A\text{-}CreERT2}$ and *Tbx21*$^{tdTomato\text{-}T2A\text{-}Cre}$ mice were bred to FLPeR mice to excise the NEO cassette and backcrossed to C57BL/6 mice to remove the FLPeR allele.

Foxp3$^{Thy1.1}$, *R26Y*, *Foxp3*^{FL}, *Foxp3*^{KO}, *Rorc*^{GFP}, *Foxp3*$^{YFP\text{-}Cre}$, *IL-10*^{eGFP}, and *Tbx21*^{FL} mice have been previously described (Eberl et al., 2004; Fontenot et al., 2003; Intlekofer et al., 2008; Kamanaka et al., 2006; Liston et al., 2008; Rubtsov et al., 2008; Srinivas et al., 2001). *CD45.1*, *Rosa26*^{iDTR}, and *Tcrb*^{KO} mice were purchased from Jackson Laboratories. Generation and treatments of mice were performed under protocol 08-10-023 approved by the Sloan

Kettering Institute (SKI) Institutional Animal Care and Use Committee. All mouse strains were maintained in the SKI animal facility in specific pathogen free (SPF) conditions in accordance with institutional guidelines.

For tamoxifen administration, 40 mg tamoxifen dissolved in 100 µl ethanol and subsequently in 900 mL olive oil (Sigma-Aldrich) were sonicated 4 × 30 seconds in a Bioruptor Twin (Diagenode). Mice were orally gavaged with 200µl tamoxifen emulsion per treatment. For diphtheria toxin (DT) injections, DT (Sigma-Aldrich) was dissolved in PBS and 200 µl of indicated doses were injected i.p per mouse. For antibiotic treatment, 0.5 g Ampicillin, 0.5 g Kanamycin, 0.4 g Vancomycin, 0.5 g Metronidazole, and 7 packets of Splenda^{TM} sweetener were dissolved in 500mL of water and filter sterilized. Mice were weaned onto antibiotic-treated water, which was changed once a week until the time of analysis.

Isolation of cells

Spleens and lymph nodes were dissociated using ground glass slides and filtered. Red blood cells in spleens were lysed before analysis. For analysis of YFP-labeled CD4 T cells in *Tbx21*$^{RFP\text{-}CreERT2}$ mice, CD4 T cells in spleens and lymph nodes were enriched using the Dynabeads CD4 Positive Isolation Kit (Invitrogen). To isolate lymphocytes from tissues, mice were euthanized and immediately perfused with 20 mL PBS. Small and large intestines were removed, flushed with PBS, Peyer's patches were removed, and residual fat and connective tissue was removed. Intestines were opened lengthwise and cut into 0.5 cm-long pieces that were further washed by vortexing in PBS. Samples were incubated in PBS supplemented with 5% fetal calf serum, 1% L-

glutamine, 1% penicillin-streptomycin, 10 mM HEPES, 1 mM dithiothreitol, and 1 mM EDTA for 15 minutes to dissociate intraepithelial lymphocytes, which were discarded. Samples were washed and incubated in digest solution (RPMI supplemented with 5% fetal calf serum, 1% L-glutamine, 1% penicillin-streptomycin, 10 mM HEPES, 1 mg/mL collagenase, and 1 U/mL DNase I) for 10 minutes. Cells were collected through a 100-µm strainer, and the residual samples were incubated in digest solution again for 10 minutes before filtering through 100-µm strainers and combining with previously collected cells. Cells were resuspended in 35% Percoll to eliminate debis before resuspension in staining buffer. To isolate lymphocytes from livers and lungs, tissues were physically dissociated using scissors and incubated for 50-60 minutes in digest solution before being filtered through 100-µm strainers. Lungs samples were resuspended in 35% Percoll to eliminate debris before resuspension in staining buffer. Lymphocytes from liver samples were resuspended in 44% Percoll, underlaid with 67% Percoll, and spun at 1000xg for 7.5 minutes at room temperature. Cells were collected from the interface of the Percoll layers and washed before resuspension in staining buffer.

Nippostrongylus brasiliensis infection

Nippostrongylus brasiliensis (*Nb*) was maintained by passage in 9 to 10 week-old Wistar rats as previously described (Camberis et al., 2003). Briefly, rats were injected subcutaneously (s.c.) with 7000 L3 *Nb* and stool was collected on days 6-9 post infection. Fecal pellets were mixed with 5x8 bone charcoal and incubated on moisten filter paper in petri dishes at 26°C for 7 days. L3 larvae were recovered from the edge of the filter paper and the perimeter of the plates and extensively washed with PBS to eliminate contaminants before

infection. Mice infections were carried out using a 23G needle at a concentration of 500 L3 *Nb* in 200 µL.

Listeria monocytogenes infection

For *Listeria monocytogenes* (*Lm*) infections, frozen stocks were thawed, resuspended in Brain-Heart Infusion media, and grown at 37°C to an OD_{600} of 0.1. For primary infections, mice were injected via lateral tail vein with 5–10x10^3 colony-forming units (cfu) of *Lm* diluted in 200 µL PBS. For secondary infection, mice were injected via lateral tail vein with 10^5 cfu of *Lm* in 200 µL PBS.

Cell transfer experiments

For cell transfer experiments, pooled spleens and lymph nodes were enriched for CD4 T cells using the Dynabeads CD4 Positive Isolation Kit. Cells were FACS-sorted on an Aria II cell sorter (BD Bioscience), washed 3 times in PBS, resuspended in 200 µL PBS, and transferred into recipients via retro-orbital injection.

Generation of bone marrow chimeric mice

Tcrb$^{-/-}$*Tcrd*$^{-/-}$ recipient mice were lethally irradiated with 650 Gy. The following day, bone marrow was isolated from femurs of donor mice and depleted of T cells and RBCs via staining with biotinylated anti-Thy1.2 and anti-Ter119 antibodies followed by magnetic bead negative selection. 5x10^6 total T cell-depleted bone marrow cells were transferred into recipient mice via retro-orbital injection.

Flow cytometric analysis

Cells were stained with LIVE/DEAD Fixable Yellow Dead Cell Stain (Molecular Probes) and the following antibodies purchased from eBioscience, BioLegend, BD Biosciences, Tonbo, or obtained from the NIH tetramer core facility: anti-CD4 (RM4-5), anti-CD8a (5H10), anti-TCRβ (H57-597), PBS-57-loaded mCD1d tetramer, anti-Thy1.1 (HIS51), anti-CD44 (IM7), anti-CD62L (MEL-14), anti-CXCR3 (CXCR3-173), anti-CD25 (PC61), anti-CTLA-4 (UC10-4B9), anti-GITR (DTA-1), anti-CD39 (24-DMS1), anti-Foxp3 (FJK-16s), anti-T-bet (4B10), anti-RORγt (B2D), anti-Gata-3 (TWAJ), anti- IFNg (XMG1.2), anti-IL-4 (11B11), anti-IL-17A (17B7), and anti-IL-2 (JES6-5H4). Flow cytometric analysis was performed using an LSRII flow cytometer (BD Bioscience) and FlowJo software (Tree Star). Intracellular staining was performed using eBioscience Fixation Permeabilization buffers. For cytokine staining lymphocytes were stimulated with soluble anti-CD3 clone 2C11 (5µg/ml) and anti-CD28 clone 37.51 (5µg/ml) in the presence of 1µg/mL brefeldin A for 5 hours at 37°C, 5% CO^2.

RNA-seq analysis

Pooled spleens and lymph nodes were enriched for CD4 T cells using the Dynabeads CD4 Positive Isolation Kit. $CD4^+Thy1.1^+$ cells were FACS-sorted on an Aria II cell sorter (BD Bioscience) into 4 populations ($CD62L^{hi}CD44^{lo}RFP^-$, $CD44^{hi}RFP^-$, $CD44^{hi}RFP^{lo}CXCR3^-$, and $CD44^{hi}RFP^{hi}CXCR3^+$ cells) and resuspended in Trizol. Three replicates of each cell subset were generated. RNA-sequencing reads were aligned to the reference mouse genome GRCm38 using the Burrows-Wheeler Aligner (BWA) (Li and Durbin, 2010) and local realignment was performed using the Genome

Analysis Toolkit (GATK) (McKenna et al., 2010). For each sample, raw count of reads per gene was measured using R, and DESeq2 R package (Love et al., 2014) was used to perform differential gene expression among different conditions. A cutoff of 0.05 was set on the obtained *p* values (that were adjusted using Benjamini-Hochberg multiple testing correction) to get the significant genes of each comparison.

TCR sequencing and data analysis

Briefly, following isolation of $CD4^+$ T cells from spleens and lymph nodes of DO11.10 TCRβ transgenic *Tcra*$^{+/-}$ *Foxp3*^{DTReGFP} mice using the Dynabeads CD4 Positive Isolation Kit (Invitrogen), $CD44^{hi}CXCR3^-$ and $CD44^{hi}CXCR3^+$ eGFP(Foxp3)$^+$ Treg and $eGFP^-$ effector CD4 T cells were FACS sorted and stored in Trizol. TCR sequencing and data analysis were performed as previously described (Feng et al., 2015). Pearson correlation of clonotype frequencies for the shared TCR clones was used for the generation of the dendrogram.

Statistical analysis

All statistical analyses (excluding RNA-seq and TCR sequence analyses, described above) were performed using GraphPad Prism 6 software. Differences between individual groups were analyzed for statistical significance using the unpaired or paired two-tailed Student's t-test. *, $p \geq 0.05$; **, $p \geq 0.01$; ***, $p \geq 0.001$; ns, not significant.

References

Blankenhaus, B., Reitz, M., Brenz, Y., Eschbach, M.L., Hartmann, W., Haben, I., Sparwasser, T., Huehn, J., Kuhl, A., Feyerabend, T.B.*, et al.* (2014). Foxp3(+) regulatory T cells delay expulsion of intestinal nematodes by suppression of IL-9-driven mast cell activation in BALB/c but not in C57BL/6 mice. PLoS pathogens *10*, e1003913.

Buch, T., Heppner, F.L., Tertilt, C., Heinen, T.J., Kremer, M., Wunderlich, F.T., Jung, S., and Waisman, A. (2005). A Cre-inducible diphtheria toxin receptor mediates cell lineage ablation after toxin administration. Nature methods *2*, 419-426.

Camberis, M., Le Gros, G., and Urban, J., Jr. (2003). Animal model of Nippostrongylus brasiliensis and Heligmosomoides polygyrus. Current protocols in immunology / edited by John E. Coligan ... [et al.] *Chapter 19*, Unit 19 12.

Colbeck, E.J., Hindley, J.P., Smart, K., Jones, E., Bloom, A., Bridgeman, H., McPherson, R.C., Turner, D.G., Ladell, K., Price, D.A.*, et al.* (2015). Eliminating roles for T-bet and IL-2 but revealing superior activation and proliferation as mechanisms underpinning dominance of regulatory T cells in tumors. Oncotarget *6*, 24649-24659.

Eberl, G., Marmon, S., Sunshine, M.J., Rennert, P.D., Choi, Y., and Littman, D.R. (2004). An essential function for the nuclear receptor RORgamma(t) in the generation of fetal lymphoid tissue inducer cells. Nature immunology *5*, 64-73.

Ertelt, J.M., Rowe, J.H., Johanns, T.M., Lai, J.C., McLachlan, J.B., and Way, S.S. (2009). Selective priming and expansion of antigen-specific Foxp3- CD4+ T cells during Listeria monocytogenes infection. Journal of immunology *182*, 3032-3038.

Feng, Y., Arvey, A., Chinen, T., van der Veeken, J., Gasteiger, G., and Rudensky, A.Y. (2014). Control of the inheritance of regulatory T cell identity by a cis element in the Foxp3 locus. Cell *158*, 749-763.

Feng, Y., van der Veeken, J., Shugay, M., Putintseva, E.V., Osmanbeyoglu, H.U., Dikiy, S., Hoyos, B.E., Moltedo, B., Hemmers, S., Treuting, P.*, et al.* (2015). A mechanism for expansion of regulatory T-cell repertoire and its role in self-tolerance. Nature *528*, 132-136.

Fontenot, J.D., Gavin, M.A., and Rudensky, A.Y. (2003). Foxp3 programs the development and function of CD4+CD25+ regulatory T cells. Nature immunology *4*, 330-336.

Gavin, M.A., Rasmussen, J.P., Fontenot, J.D., Vasta, V., Manganiello, V.C., Beavo, J.A., and Rudensky, A.Y. (2007). Foxp3-dependent programme of regulatory T-cell differentiation. Nature *445*, 771-775.

Hall, A.O., Beiting, D.P., Tato, C., John, B., Oldenhove, G., Lombana, C.G., Pritchard, G.H., Silver, J.S., Bouladoux, N., Stumhofer, J.S.*, et al.* (2012). The cytokines interleukin 27 and interferon-gamma promote distinct Treg cell populations required to limit infection-induced pathology. Immunity *37*, 511-523.

Hori, S., Nomura, T., and Sakaguchi, S. (2003). Control of regulatory T cell development by the transcription factor Foxp3. Science *299*, 1057-1061.

Hwang, E.S., Szabo, S.J., Schwartzberg, P.L., and Glimcher, L.H. (2005). T helper cell fate specified by kinase-mediated interaction of T-bet with GATA-3. Science *307*, 430-433.

Intlekofer, A.M., Banerjee, A., Takemoto, N., Gordon, S.M., Dejong, C.S., Shin, H., Hunter, C.A., Wherry, E.J., Lindsten, T., and Reiner, S.L. (2008). Anomalous type 17 response to viral infection by CD8+ T cells lacking T-bet and eomesodermin. Science *321*, 408-411.

Kamanaka, M., Kim, S.T., Wan, Y.Y., Sutterwala, F.S., Lara-Tejero, M., Galan, J.E., Harhaj, E., and Flavell, R.A. (2006). Expression of interleukin-10 in intestinal lymphocytes detected by an interleukin-10 reporter knockin tiger mouse. Immunity *25*, 941-952.

Khattri, R., Cox, T., Yasayko, S.A., and Ramsdell, F. (2003). An essential role for Scurfin in CD4+CD25+ T regulatory cells. Nature immunology *4*, 337-342.

Kim, K.S., Hong, S.W., Han, D., Yi, J., Jung, J., Yang, B.G., Lee, J.Y., Lee, M., and Surh, C.D. (2016). Dietary antigens limit mucosal immunity by inducing regulatory T cells in the small intestine. Science *351*, 858-863.

Koch, M.A., Thomas, K.R., Perdue, N.R., Smigiel, K.S., Srivastava, S., and Campbell, D.J. (2012). T-bet(+) Treg cells undergo abortive Th1 cell differentiation due to impaired expression of IL-12 receptor beta2. Immunity *37*, 501-510.

Koch, M.A., Tucker-Heard, G., Perdue, N.R., Killebrew, J.R., Urdahl, K.B., and Campbell, D.J. (2009). The transcription factor T-bet controls regulatory T cell homeostasis and function during type 1 inflammation. Nature immunology *10*, 595-602.

Lahl, K., Mayer, C.T., Bopp, T., Huehn, J., Loddenkemper, C., Eberl, G., Wirnsberger, G., Dornmair, K., Geffers, R., Schmitt, E.*, et al.* (2009). Nonfunctional regulatory T cells and defective control of Th2 cytokine production in natural scurfy mutant mice. Journal of immunology *183*, 5662-5672.

Lee, H.M., Fleige, A., Forman, R., Cho, S., Khan, A.A., Lin, L.L., Nguyen, D.T., O'Hara-Hall, A., Yin, Z., Hunter, C.A.*, et al.* (2015). IFNgamma signaling endows DCs with the capacity to control type I inflammation during parasitic infection through promoting T-bet+ regulatory T cells. PLoS pathogens *11*, e1004635.

Levine, A.G., Arvey, A., Jin, W., and Rudensky, A.Y. (2014). Continuous requirement for the TCR in regulatory T cell function. Nature immunology *15*, 1070-1078.

Li, H., and Durbin, R. (2010). Fast and accurate long-read alignment with Burrows-Wheeler transform. Bioinformatics *26*, 589-595.

Liston, A., and Gray, D.H. (2014). Homeostatic control of regulatory T cell diversity. Nature reviews. Immunology *14*, 154-165.

Liston, A., Nutsch, K.M., Farr, A.G., Lund, J.M., Rasmussen, J.P., Koni, P.A., and Rudensky, A.Y. (2008). Differentiation of regulatory Foxp3+ T cells in the thymic cortex. Proceedings of the National Academy of Sciences of the United States of America *105*, 11903-11908.

Love, M.I., Huber, W., and Anders, S. (2014). Moderated estimation of fold change and dispersion for RNA-seq data with DESeq2. Genome biology *15*, 550.

Luo, C.T., Liao, W., Dadi, S., Toure, A., and Li, M.O. (2016). Graded Foxo1 activity in Treg cells differentiates tumour immunity from spontaneous autoimmunity. Nature *529*, 532-536.

McKenna, A., Hanna, M., Banks, E., Sivachenko, A., Cibulskis, K., Kernytsky, A., Garimella, K., Altshuler, D., Gabriel, S., Daly, M., and DePristo, M.A.

(2010). The Genome Analysis Toolkit: a MapReduce framework for analyzing next-generation DNA sequencing data. Genome research *20*, 1297-1303.

McPherson, R.C., Turner, D.G., Mair, I., O'Connor, R.A., and Anderton, S.M. (2015). T-bet Expression by Foxp3(+) T Regulatory Cells is Not Essential for Their Suppressive Function in CNS Autoimmune Disease or Colitis. Frontiers in immunology *6*, 69.

Ohnmacht, C., Park, J.H., Cording, S., Wing, J.B., Atarashi, K., Obata, Y., Gaboriau-Routhiau, V., Marques, R., Dulauroy, S., Fedoseeva, M.*, et al.* (2015). MUCOSAL IMMUNOLOGY. The microbiota regulates type 2 immunity through RORgammat(+) T cells. Science *349*, 989-993.

Rubtsov, Y.P., Niec, R.E., Josefowicz, S., Li, L., Darce, J., Mathis, D., Benoist, C., and Rudensky, A.Y. (2010). Stability of the regulatory T cell lineage in vivo. Science *329*, 1667-1671.

Rubtsov, Y.P., Rasmussen, J.P., Chi, E.Y., Fontenot, J., Castelli, L., Ye, X., Treuting, P., Siewe, L., Roers, A., Henderson, W.R., Jr.*, et al.* (2008). Regulatory T cell-derived interleukin-10 limits inflammation at environmental interfaces. Immunity *28*, 546-558.

Rudra, D., deRoos, P., Chaudhry, A., Niec, R.E., Arvey, A., Samstein, R.M., Leslie, C., Shaffer, S.A., Goodlett, D.R., and Rudensky, A.Y. (2012). Transcription factor Foxp3 and its protein partners form a complex regulatory network. Nature immunology *13*, 1010-1019.

Sawant, D.V., Gravano, D.M., Vogel, P., Giacomin, P., Artis, D., and Vignali, D.A. (2014). Regulatory T cells limit induction of protective immunity and promote immune pathology following intestinal helminth infection. Journal of immunology *192*, 2904-2912.

Sefik, E., Geva-Zatorsky, N., Oh, S., Konnikova, L., Zemmour, D., McGuire, A.M., Burzyn, D., Ortiz-Lopez, A., Lobera, M., Yang, J.*, et al.* (2015). MUCOSAL IMMUNOLOGY. Individual intestinal symbionts induce a distinct population of RORgamma(+) regulatory T cells. Science *349*, 993-997.

Shafiani, S., Dinh, C., Ertelt, J.M., Moguche, A.O., Siddiqui, I., Smigiel, K.S., Sharma, P., Campbell, D.J., Way, S.S., and Urdahl, K.B. (2013). Pathogen-specific Treg cells expand early during mycobacterium tuberculosis infection but are later eliminated in response to Interleukin-12. Immunity *38*, 1261-1270.

Smith, K.A., Filbey, K.J., Reynolds, L.A., Hewitson, J.P., Harcus, Y., Boon, L., Sparwasser, T., Hammerling, G., and Maizels, R.M. (2016). Low-level regulatory T-cell activity is essential for functional type-2 effector immunity to expel gastrointestinal helminths. Mucosal immunology *9*, 428-443.
Srinivas, S., Watanabe, T., Lin, C.S., William, C.M., Tanabe, Y., Jessell, T.M., and Costantini, F. (2001). Cre reporter strains produced by targeted insertion of EYFP and ECFP into the ROSA26 locus. BMC developmental biology *1*, 4.

Srivastava, S., Koch, M.A., Pepper, M., and Campbell, D.J. (2014). Type I interferons directly inhibit regulatory T cells to allow optimal antiviral T cell responses during acute LCMV infection. The Journal of experimental medicine *211*, 961-974.

Tian, L., Humblet-Baron, S., and Liston, A. (2012). Immune tolerance: are regulatory T cell subsets needed to explain suppression of autoimmunity? BioEssays : news and reviews in molecular, cellular and developmental biology *34*, 569-575.

Vahl, J.C., Drees, C., Heger, K., Heink, S., Fischer, J.C., Nedjic, J., Ohkura, N., Morikawa, H., Poeck, H., Schallenberg, S.*, et al.* (2014). Continuous T cell receptor signals maintain a functional regulatory T cell pool. Immunity *41*, 722-736.

Williams, L.M., and Rudensky, A.Y. (2007). Maintenance of the Foxp3-dependent developmental program in mature regulatory T cells requires continued expression of Foxp3. Nature immunology *8*, 277-284.

Wohlfert, E.A., Grainger, J.R., Bouladoux, N., Konkel, J.E., Oldenhove, G., Ribeiro, C.H., Hall, J.A., Yagi, R., Naik, S., Bhairavabhotla, R.*, et al.* (2011). GATA3 controls Foxp3(+) regulatory T cell fate during inflammation in mice. The Journal of clinical investigation *121*, 4503-4515.

Yu, F., Sharma, S., Edwards, J., Feigenbaum, L., and Zhu, J. (2015). Dynamic expression of transcription factors T-bet and GATA-3 by regulatory T cells maintains immunotolerance. Nature immunology *16*, 197-206.

Zhou, L., Lopes, J.E., Chong, M.M., Ivanov, II, Min, R., Victora, G.D., Shen, Y., Du, J., Rubtsov, Y.P., Rudensky, A.Y.*, et al.* (2008). TGF-beta-induced Foxp3 inhibits T(H)17 cell differentiation by antagonizing RORgammat function. Nature *453*, 236-240.

Zhu, J., Yamane, H., and Paul, W.E. (2010). Differentiation of effector CD4 T cell populations (*). Annual review of immunology *28*, 445-489.

CHAPTER 5
CONCLUSION

In our studies, we have attempted to address how Treg cells generated in the thymus mature in the periphery and suppress autoimmune responses. Our results suggest that Treg cell maturation and function is elicited and organized in a manner similar to that of conventional effector $CD4^+$ T cells.

Akin to effector $CD4^+$ T cells, Treg cells emerge from the thymus as naïve $CD44^{lo}CD62L^{hi}$ cells and subsequently undergo effector differentiation into $CD44^{hi}CD62L^{lo}$ cells in the periphery through a TCR-dependent process, which in Treg cells is likely driven by self-antigen recognition. Following peripheral maturation into a Treg cell population consisting of effector as well as naïve cells, Treg cells continue to require the TCR for suppression of autoimmunity, much as effector $CD4^+$ T cells require TCR engagement for cytokine production and elaboration of effector functions against invading pathogens. Consequently, inducible deletion of the TCR in Treg cells in adult mice resulted in rapid autoimmune activation. Although in our experiments it was not possible to discriminate between the TCR-dependent functions of effector versus naïve Treg cells, our finding that loss of the TCR dramatically affected gene expression specifically in the effector Treg cell subset suggested that a significant portion of suppressive function may be confined to the effector Treg cell pool at steady state. However, it is also likely that naïve Treg cells may inhibit certain aspects of autoimmunity in a TCR-dependent manner, such as priming of analogously naïve yet autoreactive $CD4^+$ T cells.

In regards to Treg cell TCR specificity, our experiments switching the endogenous Treg cell TCR repertoire for predominantly a single specificity

suggested that, to an extent, TCR-dependent function could be maintained in the absence of diverse and developmentally established specificities. However, suppression by such a monoclonal Treg cell compartment was also notably limited, indicating the importance of specificity and diversity for comprehensive control of spontaneously induced autoimmunity and inflammation by Treg cells.

We also found that, like some conventional $CD44^{hi}$ $CD4^+$ T cells that stably express the T_H1 specifying transcription factor T-bet and produce IFNγ at steady state, a portion of regulatory T cells likewise stably expressed high amounts of T-bet. Both effector $CD4^+$ and Treg cell compartments underwent a continuous process of differentiation at steady state whereby some percentage of T-bet^- cells gradually up-regulated T-bet to ultimately achieve high and stable expression of the transcription factor, which was not lost even in strongly T_H2 polarizing conditions resulting from helminthic infection. Just as conventional $CD4^+$ T cells responded to intracellular bacterial and viral infections by differentiating into $CD44^{hi}$ effectors that expressed T-bet, both *Listeria monocytogenes* and *LMCV* infections induced T-bet expression in a subset of Treg cells. Moreover, re-expansion of *Listera*-induced T-bet^+ effector $CD4^+$ T cells during re-challenge was accompanied by a concomitant re-expansion of *Listeria*-induced Treg cells, demonstrating in this instance a T-bet^+ Treg cell recall response mirroring that of effector cells.

These results suggested that T-bet^+ Treg cells induced at steady state might regulate T-bet^+ effector $CD4^+$ T cells induced at steady state, while T-bet^+ Treg cells induced by pathogenic challenge might regulate T-bet^+ effector $CD4^+$ T cells induced by that same pathogen. Indeed, we found that wholesale elimination of T-bet^+ Treg cells—but not of T-bet itself—at steady

state unleashed a selectively T_H1 autoimmunity that was driven by T-bet$^+$ αβ T cells. Together, these results indicate that immunological tolerance may be maintained through a TCR-dependent process of parallel differentiation of Treg cells into polarized effector states concomitant with differentiation of conventional CD4$^+$ T cells into polarized effectors, occurring both at steady state and during infectious episodes. Such a mechanism may enable the adaptive immune system to coordinate potency of anti-inflammatory and inflammatory responses to maintain a necessary balance.